STEM CELL DIFFERENTIATION ON STRETCHABLE CONDUCTING SUBSTRATES

A Thesis

Submitted for the degree of

MASTER OF SCIENCE

(Engineering by research)

By

Nishit Srivastava

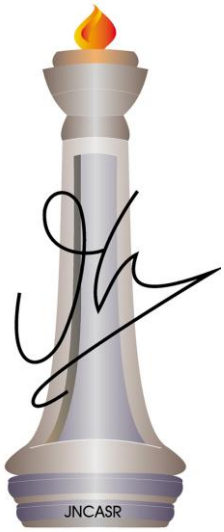

CHEMISTRY AND PHYSICS OF MATERIALS UNIT

JAWAHARLAL NEHRU CENTRE FOR ADVANCED SCIENTIFIC RESEARCH

(A DEEMED UNIVERSITY)

Bangalore – 560 064

To my parents……

DECLARATION

I hereby declare that the matter embodied in the thesis entitled "**STEM CELL DIFFERENTIATION ON STRETCHABLE CONDUCTING SUBSTRATES**" is the result carried out by me at the Molecular Electronics Laboratory, Jawaharlal Nehru Centre for Advanced Scientific Research, Bangalore, India under the supervision of Prof. K. S. Narayan and has not been submitted elsewhere for the award of any degree or diploma.

In keeping with the general practice in reporting scientific observations, due acknowledgement has been made whenever the work described is based on the findings of other investigators.

Nishit Srivastava

JAWAHARLAL NEHRU CENTRE FOR ADVANCED SCIENTIFIC RESEARCH

Jakkur, Bangalore 560064, India

K. S. NARAYAN
Professor
PHONE: 91 80 22082822
FAX: 91 80 22082766
e-mail: narayan@jncasr.ac.in

August 23rd, 2012

CERTIFICATE

I hereby certify that the matter embodied in this thesis entitled "**STEM CELL DIFFERENTIATION ON STRETCHABLE CONDUCTING SUBSTRATES**" has been carried out by Mr. NishitSrivastava at the Molecular Electronics Laboratory, Chemistry and Physics of Materials Unit, Jawaharlal Nehru Centre for Advanced Scientific Research, Bangalore, India under my supervision and it has not been submitted elsewhere for the award of any degree or diploma.

Prof. K. S. Narayan

ACKNOWLEDGEMENT

I am deeply indebted to ***Prof. K. S. Narayan***, my research supervisor for introducing me to an interesting and challenging research problem. I am grateful for his invaluable guidance, constant support and encouragement throughout my masters' research work. His approach of applying fundamental knowledge of various subjects has shaped my perspective to think about a research problem. I am also thankful to his family members for their hospitality and support.

I offer my gratitude to Prof. MRS Rao, President JNCASR for his valuable input, encouragement and monetary support for my research work. He has always been a source of inspiration for me.

I am thankful to *Dr. Jackson James* of Rajiv Gandhi centre for Biotechnology, for providing me an opportunity to work in his lab. I am especially thankful for all the discussions and help during the experiments.

I thank all CPMU, MBGU, NCU and IISc faculties for coursework and wonderful discussions. The coursework paved way to understand this beautiful field of science in much more detail and increased the inquisitiveness to learn something new. I would like to thank Prof. UdaykumarRanga for the valuable discussion and critical inputs.

I acknowledge my lab members- past and present: Dr. Monojit, Dr. Sabayasachi, Dr. Srinidhi, Dr. Kishore, Anshuman, Vini, Satya, Ravi, Prashant,Ashar, Vijay, Madhu and Swathi for valuable scientific discussions and help on understanding the experimental techniques. My special thanks to Vijay for helping me out in the experiments and introducing me to the "stretchable" world of SEBS.

I would also thank the members of Neural stem cell biology lab, RGCB especially Divya for providing me a wonderful atmosphere to work and giving me a chance to learn many experimental techniques. The discussions went a long way in shaping this work and were critical in its outcome.

No journey is complete without the fellow travelers and I would like to thank all my friends in JNCASR and IIScespecially Ankit, Mohit, Amrit, Pawan, Chidambar, Shalini, Simi for supporting me through various crests and troughs of my JNC life.The discussions (scientific and non-scientific) were both refreshing and knowledgeable and provided food for thought and get-away from the regular chores.

I would also thank all my friends especially those in Bangalore for the constant support and encouragement which helped me in the gloomy and surreal days.

I would like to thank Suma for the help with the confocal microscope imaging. I also thank other Technical, Academic, Administrative, Complab staff and JNC doctors for their help during my stay here. I would like to thank everyone who helped in my work and during my stay at JNC.

Last but not the least, I would thank my parents for their love, care, motivation and constant moral support. Nothing in this world would be possible without them and I am always indebted to them for being there for me, enabling me to be who I am and wherever I am. I will always try to make you proud at every step of my life.

SYNOPSIS

Stretchable conducting polymer (CP) substrates offer an alternate substrate for neuronal growth which can be used for the development of neuroprosthetic devices. Promotingneuronal growth on the conducting polymer electrodes enables intricate contact at the cell-electrode interfaceproviding long term cellular activation and functional recordings.Electrically conducting polymer on a soft elastomeric scaffold provides a conducive support for the differentiation of stem cells. These substrates can be used for the implantation in the injured tissue areas providing mechanical support and spatially arranged cues for the regenerating neurons. Stem cell differentiation is affected by a myriad of factors like stiffness, topography and biochemical factors and it would be interesting to see if CP can provide guidance cues for the differentiation of cells which can be assimilated within their developmental program.

In this work, the role of conductivity and microstructure of the conducting polymer surface for stem cell differentiation and proliferationare emphasized.The conductivity of the CP coated elastomeric substrate was precisely controlled by the application of strain. Randomly distributed spherical PEDOT domains transform into ellipsoidal domains within the polyanionic PSS matrix. The surface potential distribution of the CP substrate changes significantly suggesting a control of the distribution of these surface potentials at nanometer length scales by straining. Application of strain also results in the increase of stiffness of the substrates due to strain hardening of the underlying elastomer. Nanotopographical features and surface roughness is also modulated by the application of strain on these substrates.

In Chapter 3, results from the differentiation of embryonic stem cells (ES) into neurons on the CP substratesare discussed. The viability of the substrates for neuronal stem cell differentiation was assessed by GFP tagged ES cells which clearly showed that the substrates are conducive for the development of neurons. ES cells were differentiated on conducting CP substrates as well as non-conducting elastomeric substrates and post differentiation, they were immunostained with specific neuronal marker β-III tubulin to identify the immature neurons.

Strained CP and elastomeric substrates were hence used to study the influence of the substrate on the neuronal differentiation and it was observed that the conducting substrates affect the cell spreading which is signified in the formation of cellular aggregates. The tendency of cells to remain within the aggregates was accentuated on highly strained CP substrates. Neuronal differentiation was markedly reduced on these strained CP substrates with most neurons differentiating within the aggregates thus leading to a decrease in neurite length. In comparison, the neurons differentiated and spread well on the elastomeric substrates and these strained substrates promoted this cellular behavior. The z-stack confocal imaging of these aggregates showed neuronal differentiation at all the strata with more prominent neuronal networks at the aggregate-polymer interface.

The choice of spatial location on the strained substrate can possibly be explained by the formation of topographical features. Delamination of the CP films take place on straining the CP-coated elastomeric substrates which result in the formation of slip defects orthogonal to the strain direction. It can then be interpreted that these defects could lead to ‘defect patterning’ of cells with cellular aggregates aligning along these defects on highly strained CP substrates.

In Chapter four, the changes in the neuronal differentiation and spreading are investigated further and possible role of CP substratesare discussed. Actin cytoskeletal arrangement of differentiated neurons was assessed by phalloidin immunostaining and disruption of actin fiber arrangement was observed on CP substrates. In comparison, the neurons on non-conducting elastomer and glass coverslips exhibited well-arranged actin fibers. This showed that the changes in the cytoskeletal arrangement played a major role in modulating the stem cell activity. The cytoskeletal assembly of cells is affected by the PEDOT domain alignment and slip defects in CP layer on highly strained substrates. The variation in the surface potential modulates the extra-cellular matrix proteins adsorbed on the substrate which affects the initial cell adhesion events. The cellular spreading and aggregate formation of cells is affected by the underlying macroscopic film quality and the highly strained CP substrates perturb these cellular functions. Non-conducting elastomers, on the other hand, are devoid of these changes in the surface potential and present a neutral surface where cells adhere and spread evenly throughout and straining the substrates lead to a decrease in surface roughness which might alleviate the neuronal differentiation and spreading.

Table of Contents

List of Figures

List of tables

Notations/Abbreviations

ABBREVIATIONS	DETAILS
PDMS	Polydimethylsiloxane
ECM	Extra-cellular matrix
SEM	Scanning electron microscope
PTFE	Poly(tetraflouroethylene)
FBGC	Foreign body giant cells
DHEA	Dehydroepiandrosterone
MSC	Mesenchymal stem cells
LCST	Lower critical solution temperature
PE	Polyethylene
PP	Polypropylene
PET	Poly(ethylene terephthalate)
PMMA	Poly(methyl methacrylate)
PVC	Poly(vinyl chloride)
PLGA	Poly(lactic-glycolic acid)
PHMA	Poly(hydroxyl methacrylate)
PEG	Poly(ethylene glycol)

CP	Conducting polymers
SBS	Styrene-butadiene-styrene
PC12	Pheochromocytoma cells
SEBS	Styrene ethylene butylene styrene
PHEMA	Poly(hydroxyethyl methacrylate)
PVA	Poly(vinyl alcohol)
PEO	Poly(ethylene oxide)
PNIPAAm	Poly(N-isopropylacrylamide)
HA	hyaluronic acid
GAGS	glycosaminoglycan
RGD	Arginine-Glycine-Aspartic acid
IKVAV	Isoleucine-Lysine-Valine-Alanine-Valine
YIGSR	Tyrosine-Isoleucine-Glycine-Serine-Arginine
GHK	Glycine-Histidine-Lysine
RGDS	Arginine-Glycine-Aspartic acid-Serine
TGF-β	Transforming growth factor beta
BMP-2	Bone morphogenic protein-2
DNA	Deoxyribonucleic acid
ES	Embryonic stem cells
ICM	Inner cell mass

LIF	Leukemia inhibitory factor
hES	Human embryonic stem cells
CNS	Central nervous system
SVZ	Subventricular zone
RMS	Rostral migratory stream
HSC	Hematopoietic stem cell
CSPG	Chondroitin sulfate proteoglycans
MAP-2	Microtubule-associated protein 2
PEDOT	Poly(3,4-ethylenedioxythiophene)
PSS	Poly(styrene sulfonate)
PPy	Polypyrrole
DRG	Dorsal root ganglia
bFGF	Basic fibroblast growth factor
PLL	Poly-L-lysine
IPA	Isopropyl alcohol
TCE	Trichloroethylene
KPM	Kelvin probe microscope
AFM	Atomic force microscope
ES-NP	Embryonic stem cell derived neural progenitors
SDIA	Stromal cell derived inducing activity

EB	Embryoid bodies
RA	Retinoic acid
PSA-NCAM	Polysialylated neural cell adhesion molecule
ESGM	Embryonic stem cell growth medium
MEF	Mouse embryonic fibroblast
PBS	Phosphate buffer saline
EDTA	Ethylenediaminetetraacetic acid
DMSO	Dimethyl sulphoxide
FGF2	Fibroblast growth factor 2
EGF	Epidermal growth factor
PLLA	Poly(L-lactic acid)
GFP	Green fluorescent protein
DAPI	4',6-diamidino-2-phenylindole
FITC	Fluorescein isothiocyanate
GFAP	Glial fibrillary acidic protein
FA	Focal adhesion complex
NA	Nascent adhesions
FAK	Focal adhesion kinase

CHAPTER 1

GENERAL INTRODUCTION

1.1 Introduction

It is well-known that cells can adapt and grow in different biochemical conditions. The study of cell-substrate interaction is an important research area which has implications both in basic cell and molecular biology studies and in the field of biomaterials. *in vitro* studies of physiological properties of cell have shown that they can integrate and respond to a variety of biological, chemical and physical information provided to them by the extra-cellular matrix. The availability of synthetic-soft polymer substrates which mechanically mimic the *invivo* conditions has thrown open the field of tissue engineering.

The effect of biological and chemical cues on cell behavior and growth has been widely studied. The protocol for cell culture of different cell types is well-established and routinely used. The property of cells residing in their native tissue environment *in vivo* is occasionally different from the *in vitro* cultured cells. This shows the influence of mechanical environment and the extra-cellular matrix (ECM) on cell growth and proliferation. Pioneering work in this field by Discher et al. show that the variety of cell types is affected by the stiffness of the underlying substrate [4]. Movement and spreading of fibroblasts is affected by the change in elasticity of the polyacrylamide gels [5-6]. The peripheral nervous system cells and PC12 cells show variable neurite extensionand branching on mechanically tunable matrices and

culturesubstrates[7-10]. The role of substrate and ECM mechanical properties has also been observed in the behavior of tumor cell lines andtumor progression[11].

The most common attachment site for a mammaliancell *in vitro* is another similar cell or the extracellularmatrix, composed of synthetic polymeric materials having an elastic moduli in the range of 10 to 10,000 Pa[12]. Forces generated by cytoskeletalmotors applied to membrane attachment sites deform materials within this stiffness range but cannotmove an attachment site on a rigid surface. Consequently,cell morphology and functions strongly depend on substrate stiffness under conditions wherechemical signals are constant. Cells on soft, lightly cross-linked gels(E~ 1 kPa) show diffuse and dynamic adhesioncomplexes. In contrast, stiff, highly cross-linkedgels (E~ 30 to 100 kPa) show cellswith stable focal adhesions, typical of thoseseen in cells attached toglass. Similarly, rigidificationof cell-derived3-D matrices alter the matrixadhesions which get replacedby large, non-fibrillar focaladhesions similar to those found on 2-Dfibronectin substrates. Tyrosinephosphorylation of multipleproteins (includingpaxillin) appearto be broadlyenhanced in cells onstiffer gel substrates confirming its role in signaling and stiffness sensing. It has been seen that pharmacologicallyinduced, nonspecifichyperphosphorylation of these residues drive focal adhesion formationon soft materials.Inhibition of acto-myosincontractions, in contrast,largely eliminates prominentfocal adhesions,while stimulation ofcontractility drives integrinaggregation intoadhesions[4].

Stem cells are biological cells found in all multicellular organisms which can divide through mitosis and differentiate into variety of cell types. They divide asymmetrically to form a stem cell and a differentiated cell, thus replenishing their population. These cells provide excellent model system to study developmental biology and their differentiation into specific adult cells has enormous potential in the field of regenerative medicine. The role of ECM is evident in the modulation of stem cell differentiation. Mesenchymal stem cell (MSC) lineage is influenced by the stiffness of substrate; softer substrates induce neuronal growth while stiffer ones promote osetocyte culture [13]. Differentiation of neuronal progenitor cells increases on softer substrates with Young's modulus similar to the native brain tissue. These substrates are non-adhesive to astrocytes and promote neuronal differentiation only [14]. Embryonic stem cell differentiation and self-renewal is also affected by the surface property of various polymers. Thus, the properties of polymers can help us in directing the stem cell differentiation into a desired

lineage which is quite useful in the area of tissue engineering and regenerative medicine. In this chapter, the properties and application of various polymers in biomedical engineering is discussed which is followed by the discussion about the properties of stem cells, various factors which affect their differentiation especially into the neuronal lineage making them a prime target for disease therapies.

1.2 Properties of polymeric biomaterials

Polymers have found applications in virtually every discipline of medicine ranging from *in vitro* cell culture scaffolds to intricately designed implants. Each biotechnological application has its own highly specialized requirements hence a range of diverse materials with good biocompatibility but different chemical and physico-mechanical properties are desirable.

The wide variety of natural polymers relevant to the field of biomaterials includes plant materials such as cellulose, sodium alginate, natural rubber, animal materials such as hyaluronic acid, heparin, collagen, glucosaminoglycans (GAGs) and keratin. Although these polymers are important and have widespread applications, they are sometimes masked by synthetic polymers which are available today. Synthetic polymeric biomaterials include hydrophobic materials such as silicone rubber, polyethylene (PE), polypropylene (PP), poly(ethylene terephthalate) (PET), poly(tetrafluoroethylene) (PTFE) and poly(methyl methacrylate) (PMMA). They also consist of more polar materials such as poly(vinyl chloride) (PVC), poly(lactic-glycolic acid) (PLGA), nylons, water swelling materials such as poly(hydroxyl methacrylate) (PHMA) and water soluble materials such as poly(ethylene glycol) (PEG).

Conducting polymers (CP) are another class of synthetic polymers which have interesting optical as well as electronic properties. These polymers exhibit high conductivity (upto one-tenth of Cu^{2+} ions) and show electroluminescence. The impact of the field of conducting polymers on science in general was recognized by the award of Nobel Prize for chemistry in 2000 to the discoverers of the conducting polymers. These polymers are used as antistatic coatings in photographic films, photovoltaic devices, light emitting diodes and organic field-

effect transistors. These polymers also find increasing relevance in the field of biomedical engineering for designing neuro-prosthetic devices, cochlear implants which are based on electrical stimulation and electro-mechanical devices such as biosensors. Numerous cell culture studies on these polymers show their ability to support variety of cell types, especially neuronal populations for a long period of time.

Both natural and synthetic polymers are long chain molecules that consist of a large number of small repeating units. In synthetic polymers, the chemistry of the repeat units differs from the small molecules (monomers) due to a loss of unsaturation or elimination of small molecule such as water. The properties of these long chain polymers are much different and complex than their monomeric components.

The characteristics of the polymers, which define its potential use for biomedical applications, are dependent on the following properties:-

- Molecular weight- Linear polymers used for biomedical applications generally have $M_n$in the range of 25,000 to 100,000 and M_w in the range of 50,000 to 300,000. Molecular weight of the polymer defines the physical property of the materials especially melting point and boiling point. Higher or lower molecular weight of the polymers may be necessary depending upon the ability of the polymer chains to crystallize or exhibit secondary interactions such as hydrogen bonding. These secondary interactions may affect the protein adsorption on their surface which in turn modulates the cell adhesion.

- Tacticity- This refers to the conformational arrangement of the substituents around the extended polymer chain (fig.1.1). Chains in which all substituents are located on the same side of the zig-zag plane are isotactic, whereas syndiotactic chains have constituents alternating from side to side. In atactitc arrangement, the substituent groups appear at random on either side of the extended chain backbone. Tacticity affects the crystallinity of the polymers which is required for the proper conformational arrangement and affects the attachment of ligands to the surface. Atactic polymers do not crystallize while syndiotactic and isotactic does. For ex. Polyethylene is an isotactic

polymer which crystallizes to a higher order structure characterized by folded chain lamellar growth which aids the formation of spherulites[15].

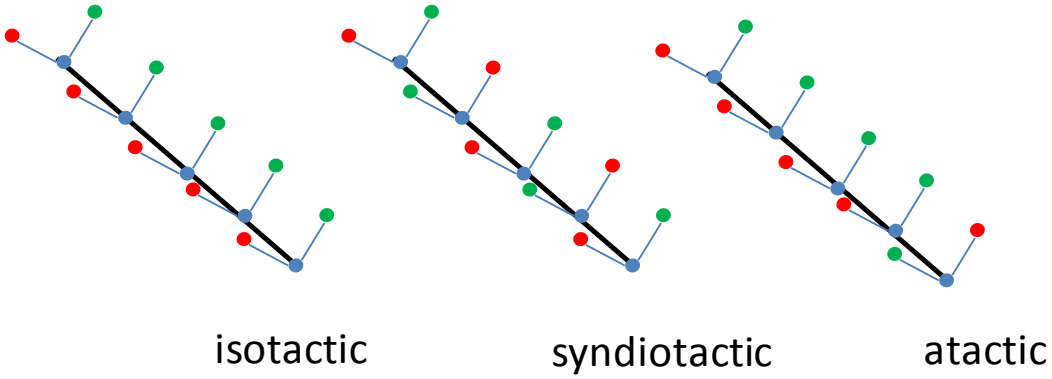

Fig. 1.1- Tacticity of polymers.

- Mechanical properties- The mechanical property of a polymer is an important consideration for its application in human body as an implant or for cell culture purposes. Scar formation is observed in the implanted area of the body due to mechanical mismatch between the polymer and native tissue. Increasing evidence of the role of mechanical property of the ECM is accumulating which shows the influence of the stiffness of the polymer scaffolds on the cell migration, proliferation and differentiation. Soft rubbery polymers are chosen for their application in the mechanically pliant tissues. The freedom of motion of the polymer chain is retained at the local level while a network structure resulting from chemical cross-links and chain entanglements prevents large-scale movement or flow. Thus, rubbery polymers tend to exhibit a lower stiffness and large extensibilities. The fatigue behavior of polymers is also an important consideration in the applications where they are continuously under dynamic strain like in case of heart prosthesis.

The synthetic polymers provide strict control over these properties and thus offer a potentially attractive source for a broad range of biomedical applications. The presence of functional groups on the backbone or side chains of a polymer also means that they can be modified chemically or biochemically, especially at their surfaces. This allows attachment of specific ligands which may play a very important role in cell adhesion and migration. Chemical modification of the polymeric substrates affects the protein adsorption which plays a major role in altering cellular functioning. Patterning of these polymers also gives an additional tool to manipulate and study the various aspects of cell behavior.

1.2.1 Surface immobilized biomolecules

Biomolecules such as cell receptor ligands and affinity proteins have been chemically or physically immobilized within the biomaterial scaffolds for a wide range of cell culture studies. Immobilization of heparin on polymer surface is one of the earliest examples of a biologically functional biomaterial. Living cells are also immobilized on the biomaterial surface for their use in the production of various industrially important enzymes and also as a feeder layer to secrete growth factors for a mixed culture.

Among various classes of functionalized biomaterials, polymers are especially interesting because their surface contains reactive groups *de novo* or they are readily derivatized with reactive groups that are used to covalently link biomolecules. Another advantage of polymers as support for biomolecules is that they are fabricated in variety of forms like films, membranes, tubes, fibers and porous structures.

Cell interaction with a foreign material is usually mediated by biological intermediates such as adsorbed protein molecules. An approach using biologically functional material can be more direct, by adsorption or covalent grafting of ligands for cell-surface adhesion receptors to the material surface [16-17]. The major methods of immobilization of a bioactive compound to a polymeric surface are adsorption via electrostatic interactions, ligand–receptor pairing (as in biotin-avidin) and covalent attachment [18]. Non-covalent adsorption is also used, as in certain

drug delivery applications [19-20]. The biotin-avidin interaction is the strongest reported non-covalent bond with an unbinding force of up to 250 pN[21]. It is attractive in surface bio-conjugations because of the number of biotinylated (and biotinylating) reagents available. However, covalent immobilizations offer several advantages by providing the most stable bond between the compound and the functionalized polymer surface. In the biomedical field, a covalent immobilization can be used to extend the half-life of a biomolecule, prevent its metabolism (as in compounds which provide anti-tumor activity when used locally, but may be toxic if metabolized) or allow for continued bioactivity of in-dwelling devices (as in vascular devices, shunts, or catheters) [22-23].

Specific biomolecules can be immobilized in order to control cellular interactions; one important example being polypeptide growth factors. Such molecules are immobilized and retain their ability to provide biological cues that signal specific cellular behavior such as support of liver-specific function in hepatocytes, induction of neurite outgrowth, induction of angiogenesis and differentiation of MSCs into various lineages[24-27]. These small ligands also provide cell selectivity which is important in drug targeting and tissue engineering [20, 28]. For example, vascular grafts support the adhesion and migration of vascular endothelial cells while at the same time rejects the adhesion of blood platelets [29].

1.3 Biomedical applications of soft polymers

Most organs and biological tissues are soft viscoelastic materials with elastic moduli ranging fromon the order of 100 Pa for the brain to 100,000 Pa for soft cartilage[12]. The combination of good chemical compatibility with physiologically appropriate mechanical properties in these elastomershas increased their potential for use both asimplants and as substrates for tissue engineering[15, 30-31]. These elastomers may be polysilicones, polyurethanes, polyesters, synthetic rubbers or hydrogels. Understanding and controlling mechanicalproperties, especially softness, is important for appropriate physiological functions in numerouscontexts. The properties of various elastomers and their uses in different areas of human body are discussed to understand the role played in different instances.

1.3.1 Silicone elastomers

Silicones make up a vast family of polymers with remarkable properties due to presence of Si-O and Si-C bonds. Many functional groups can be attached to the silicon atoms making them well suited for diverse applications in wide variety of areas. Silicon elastomers are composed of very long polymers containing several thousand silicon atoms per molecule and are amongst most widely used polymers in medical applications because of the strong, highly mobile bonds of their Si-O-Si catenary backbone which provides elevated chemical inertness and exceptional flexibility[15, 32].They are also very stable over time, show little tissue reactivity at the body temperature and are highly resistant to chemical and thermal degradation which allows them to be autoclaved for sterilization. They have exceptional mechanical properties such as high tear strength, and outstanding elasticity which makes them suitable for many medical applications such as contact lenses, special dressings, and air/blood filter membranes[33-34]. The elastic moduli of silicone rubber is in the range of 1-5 MPa which makes it an ideal substrate for the culture of myoblasts and chondrocytes [35].

The hydrophobic behavior of silicone is a major problem for *in vitro* studies since it makes cell adhesion difficult. Increase in the hydrophilic nature of the polymer by various surface treatment methods lead to an elevated cell adhesion and growth levels[36]. SEM analyses of the behavior of cells grown in contact with silicone elastomers showed that the cells grew in aggregates with little spreading and produced numerous adherence structures linking them to one another, but only a few binding them to the substrate[37]. The properties of silicon elastomers described previously affected cell adherence to the substrate and thus cell growth, but had no effect on cell viability. *in vivo* studies on the biocompatibility of elastomer implants showed that a moderate inflammatory response occurs post implantation[38]. Hemocompatibility studies on silicones showed that albumin and fibrinogen strongly adsorbed to these elastomers and platelets also adhere in large quantities[39-40].Polydimethylsiloxane (PDMS) has found increased use in the microelectromechanical systems to study the biomedical problems within the same sizescale of cells and subcellular structures [41-43]. The tunable elasticity and surface properties of PDMS, makes it a desirable candidate for exploring cell-ECM interactions and understanding the mechanical effect on cellular behavior [44-45].

1.3.2 Polyurethanes

Polyurethanes make up the largest family of thermoplastic and thermosetting plastics. They range from very rigid to highly flexible and from compact to cellular and are used for numerous biomedical applications [15, 37, 46-47]. They are the products of polyaddition reactions between polyisocyanates and polyalcohols (polyols).The hard segments cross-link among themselves within the mass of elastomers to form agglomerations that act as fillers which improves the mechanical resistance of the material while the soft segments remain free and randomly arranged(fig.1.2) [48].

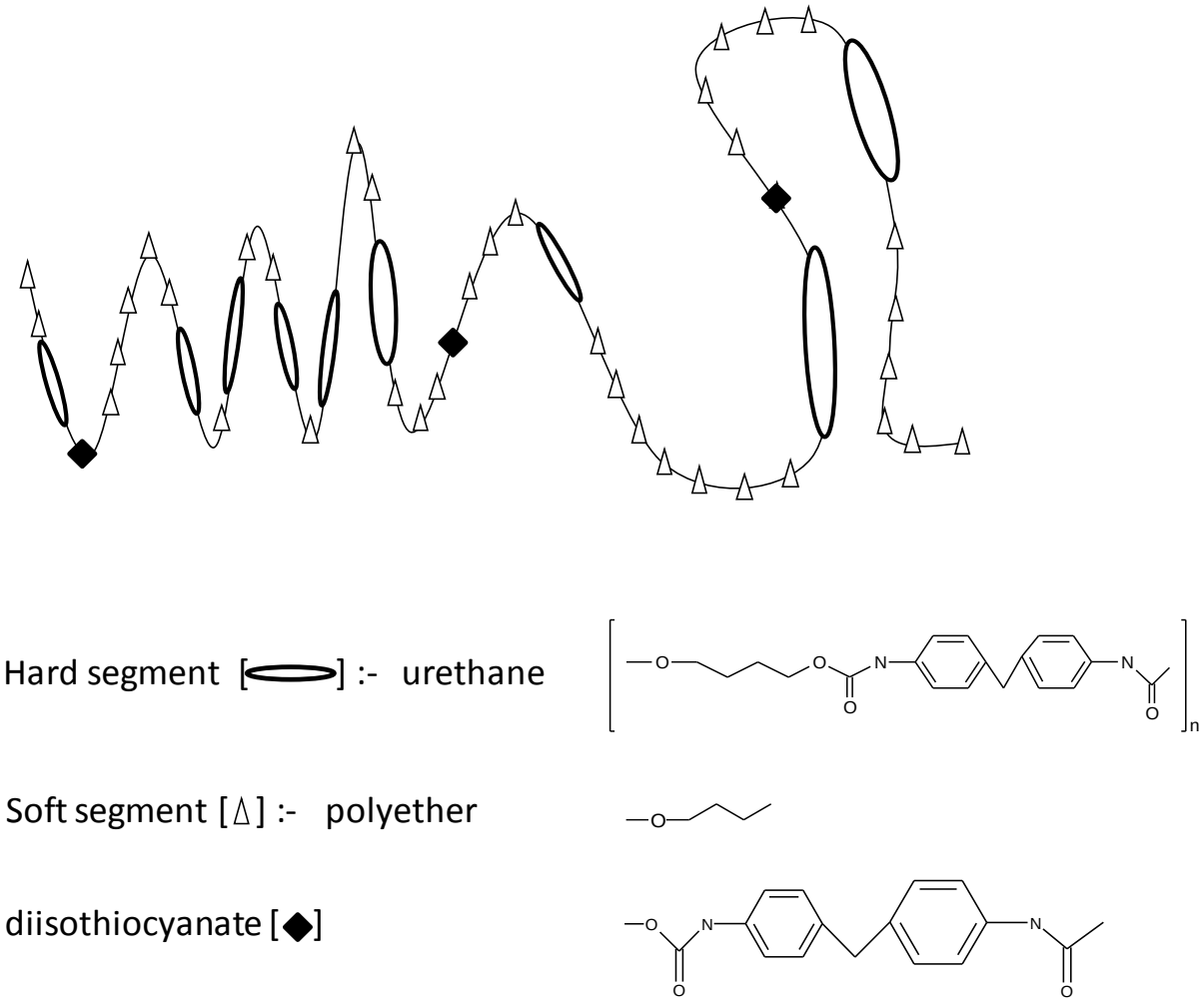

Fig. 1.2-Linear polyurethane chain showing soft and hard segments.

Under a tensile stress of 150%, the polyether soft segments line up along the elongation axis, displacing the urethane hard segments so that they are more or less perpendicular to the vertical axis (fig. 1.3). Soft segments crystallize when brought into close proximity with each other due to application of stress under elongation of around ~ 250%. When the elongation further increases (~500%), the chemical bonds cross-linking the hard segments break down and align these hard segments along the vertical axis. At this point, the soft segments also relax because of the stretching due to the release of the hard segments[49]. Segmented polyurethane elastomers thus have elastic behavior under low stress (deformation) conditions, which becomes plastic when the hard segment network breaks-down. The greater the concentration of hard segments, the more plastic the elastomer becomes while on the other hand, the lower the concentration of hard segments, the more elastic the behavior.

Soft segment polyethersare replaced by polybutadienes,polymethylsiloxanes, polycarbonates and aliphatic hydrocarbons [50-52]. Polysiloxanes are attractive substitutes for polyethers because of their low toxicity, good thermal and oxidative stability, low coefficient of friction, good hemocompatibility and a fact that they do not affect the mechanical properties of the polyurethanes because their modulus of elasticity is similar to that of the soft segment they have replaced [53].

Polyurethanes have found a number of medical uses becauseof their acceptable level of biocompatibility, high mechanical resistance and elastomeric properties. Polyurethanes, together with silicones, are amongst the few elastomers which have been implanted for long periods in the human body [54]. *in vitro* biocompatibility analysis between polyurethane elastomers (polyether and polyester) and copolymers (polyether–polyester) has shown that epithelial cells had same growth patterns and explant morphologies as cells grown on control substrates[55].There wasa strong endothelial cell proliferation within 1 week despite slower spontaneous endothelialization compared to other polymers likePTFE[56]. The biocompatibilities of a polyetherurethane and a porous copolymer (polyether–polyester) has been studied *in vivo* by implantation in rats.

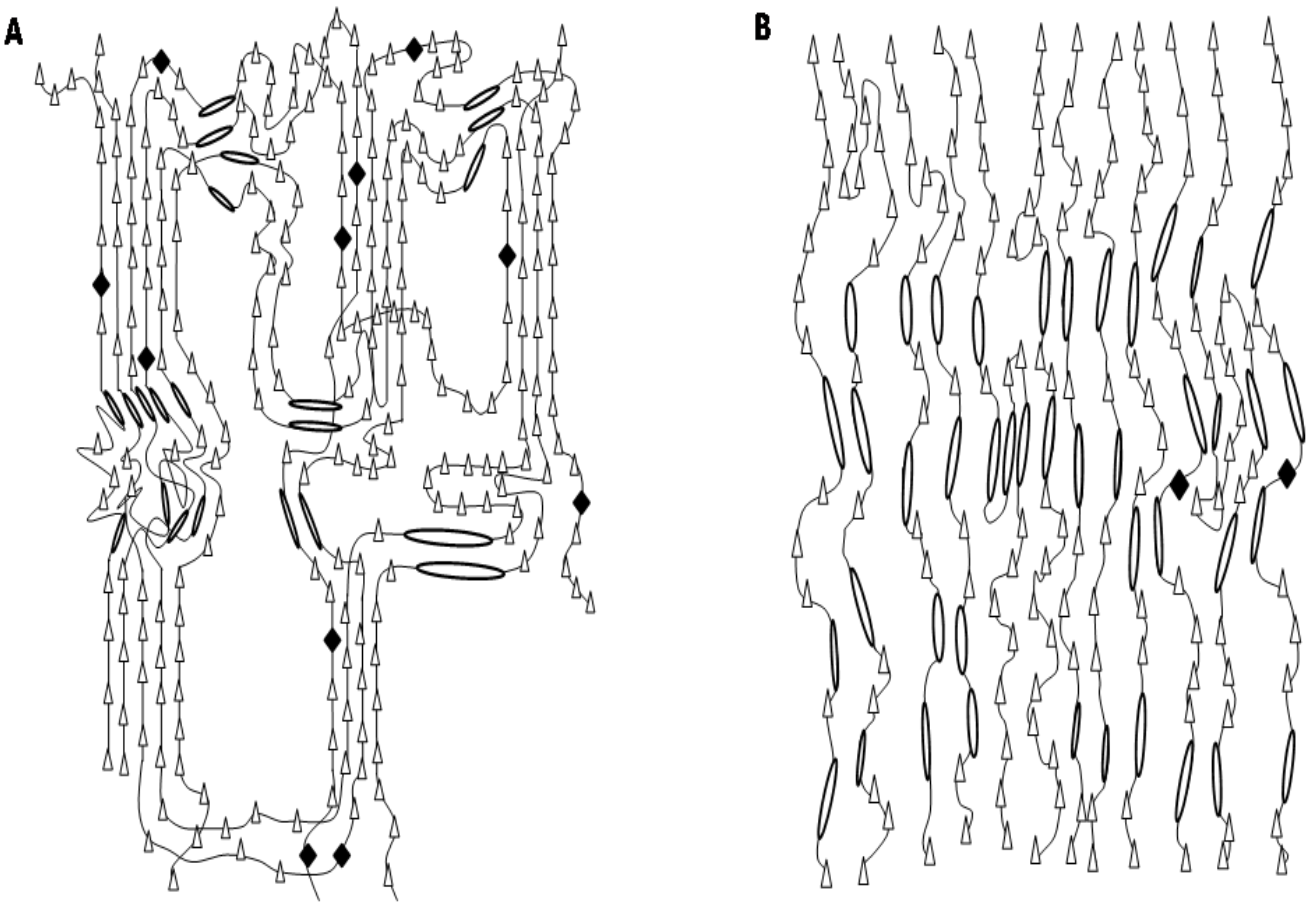

Fig. 1.3- (A) Crystallization of soft segments of polyurethane under a weak vertical stress. (B) Reorientation of hard segments and relaxation of soft segments of the polymer under a strong vertical stress.

The degradation of these polyurethanes is less rapid than other elastomers and does not result in the release of toxic products. The proliferation of fibroblasts and the growth of fibrous and bone tissue are signs of acceptable implant fixation despite the presence of macrophages and foreign body giant cells (FBGC) [57]. The formation of cell monolayers on a hydrophobic substrate is facilitated by the presence of interconnecting pores rather than wettability[58]. A porous structure promotes fibroblast proliferation and the production of new collagen on polyester [59].

The incorporation of glycerophosphocholine as a chain extender in poly(tetramethylene oxide)–based polyurethane significantly decreased bacterial adhesion and protein adsorption. The inclusion of dehydroepiandrosterone (DHEA) in polyetherurethane urea decreased macrophage adhesion and FBGC formation for up to 7 days[60].

The chemical properties of the elastomer have been modified to produce biodegradable products. Studies on the biodegradable polyesterurethanesshowed that these elastomers have good cell compatibility and cell–substrate interactions do not lead to the release of toxic substances or the activation of macrophages[61]. Relatively strong adhesionand acceptable growth of macrophages and osteoblasts occur. The culture of fibroblasts on these polymers showed that the cells were viable for a period of about 12 days [62].

1.3.4 Natural rubbers and their synthetic derivatives

Natural rubbers are the most elastic and resistant of allthe biomedical elastomers, but are also the least hemocompatibledue to the release of dithiocarbamate residues[63]. The synthetic derivatives of these natural rubber compoundswere made to improvetheir blood compatibility. Methylmethacrylate grafts showed great promise because they make natural rubbermore hemocompatible than many silicone elastomers[64]. Another approach was to vulcanize natural rubberby gamma radiation without additives. Natural rubberspolymerized in this way are very pure and demonstratedremarkably good histocompatibility. Untreated naturalrubbers are mainly used to manufacture latex gloves, whiletreated natural rubbers are used to produce catheters and tubing. Latex gloves prevent cross-infections and reduce the cytotoxic and allergic reactions [65]. The well-balanced physical properties ofrubbers (elasticity, tear resistance) make them idealfor various biomedical applications. Co-polymerisedderivates of synthetic rubbers with polystyrenes like Styrene-butadiene-styrene (SBS), Styrene ethylene butylenes styrene (SEBS) are being currently explored for various biomedical applications [66-67].

1.3.4 Hydrogels

Hydrophilic polymers, especially their cross-linked forms, known as hydrogels, are aclass of biomaterials that have demonstrated great potentialfor biological and medical applications.Hybrid materials have been developed to preservethe bulk properties of traditional polymers and their molecular chains resembling proteins. Theelusive goal of molecular recognition in the synthetic polymer systemshas been reached in certain cases. For example, acrylicgels have been designed with recognition capabilities by incorporatingnon-covalently cross-linked antibodies[1, 68]. These proteinscouple the reversible-swelling character of the networkswith molecular recognition by only swelling in the presence ofa specific antigen. The advantage of using synthetic polymericmaterials based solely on proteins or peptides is that it offersa higher degree of control over its properties. Peptides and proteinscan be coded for specific properties using a basic knowledgeof inter- and intrachain interactions.Many of these hydrophilic polymer networks have a highaffinity for water but are prevented from dissolving due totheir chemically or physically cross-linked network. Water canpenetrate in between these polymer chains, subsequently causing swelling and the formation of ahydrogel [1, 69].

The suitability of hydrogels as biomedical materials andtheir performance in a particular application depends to alarge extent on their bulk structure. The most importantparameters used to characterize the network structure of hydrogelsare the polymer volume fraction in the swollen state($v_{2,s}$), the molecular weight of the polymer chain between twoneighboring crosslinking points (M_c), and the correspondingmesh size (ξ).The polymer volume fraction in the swollen state is a measureof the amount of fluid imbibed and retained by the hydrogel.The molecular weight between two consecutive crosslinks,which can be either chemical or physical in nature, is ameasure of the degree of crosslinking of the polymer. The correlation length or distance between twoadjacent crosslinks(ξ), provides a measure of the space availablebetween the macromolecular chains.

Polymer networks can be synthesized using various chemicalmethods (e.g., photo- and thermal-initiated polymerization).Neutral synthetic polymers can be generated from the derivativesof poly(hydroxyethyl methacrylate) (PHEMA), PEG and poly(vinyl alcohol) (PVA). PEG hydrogels are one of the most widely studiedand used materials for biomedical

applications[70].PEG has been applied as a “stealth material”since it is inert to most biological molecules such asproteins. Some of the earliest work on the use of PEG andpoly(ethylene oxide) (PEO) as hydrophilic biomaterials showed that PEO adsorptiononto the glass surfaces prevents protein adsorption[71]. Since then,many forms of PEG surface modification have been used to render asurface, protein resistantand to enhancesurface biocompatibility[72].PEG polymers can be covalently cross-linked using a varietyof methods to form hydrogels. A particularly appealingmethod of cross-linking PEG chains is through photopolymerizationusing acrylate-terminated PEG monomers[73].In thepresence of cells, PEG hydrogels are passive constituents ofthe cell environment since they prevent adsorption of proteins.However, numerous methods of modifying PEG gelshave made them a versatile template for many subsequentconjugations. For example, peptide sequences havebeen incorporated into PEG gels to induce degradationormodify cell adhesion[74]. Fig. 1.4 shows the difference in the attachment of the endothelial cells on RGDS modified PEG hydrogels. Cells show good adhesion and were maintained for longer period of time over these hydrogels.

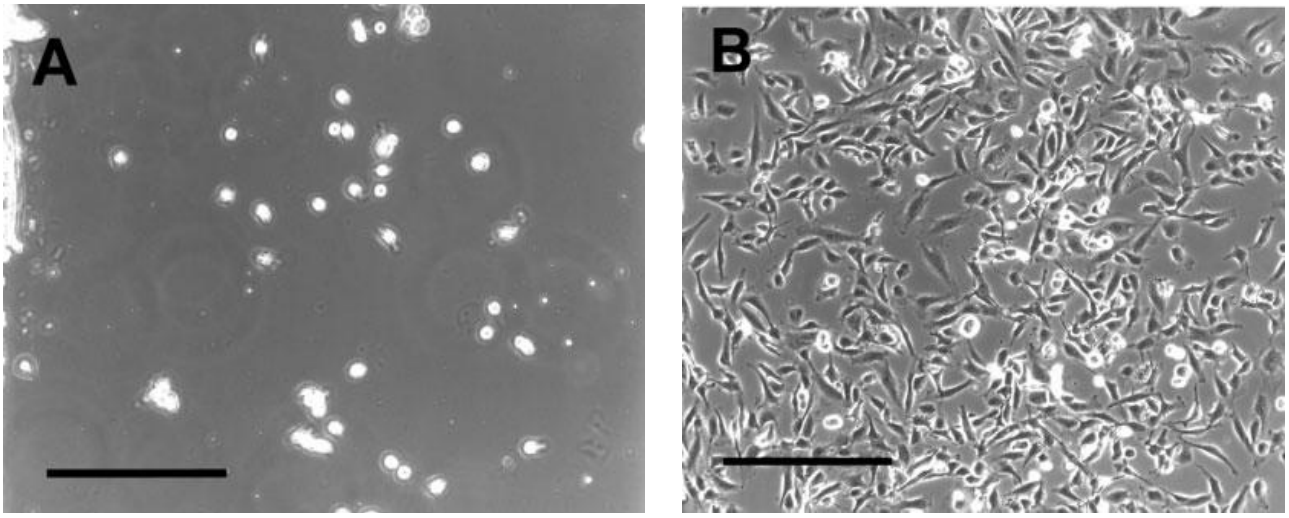

Fig. 1.4- Light microscopy images of endothelial cells attached (3 h after seeding) to the surface of PEG hydrogels fabricated A) without RGDS and B) with 5.0 mMAcr-PEG-RGDS. Scale bar, 200 µm. Reproduced from [2].

PHEMA is another hydrogel that has been extensively studied and used in biomedical applications such as contact lenses and drug delivery [75-76]. The attractive features of PHEMAinclude its mechanical properties, optical transparencyand its stability in water. Surface derivatization of PHEMA gels lead to a modification in its bulk properties. Forexample, dextran-modified PHEMA gels have been synthesizedto modulate the degradation properties of the gel[77].Also, copolymerization of HEMA monomers with othermonomers, such as methyl methacrylate, can be used to modifyproperties such as swelling and mechanical properties[78].

PVA hydrogels are stable, elastic and are formed by repeated freezing and thawing process or chemical cross-linking [79-80].The physically cross-linked PVA hydrogels are biodegradable, and thus can be used forvarious biomedical applications while the chemically cross-linked PVA hydrogels release toxic substances when implanted or used inside the body [81-83].

Environmentallyresponsive hydrogels have been synthesized that are capableof sensing and responding to the changes in external stimuli, suchas changes in pH, p*I*, and temperature[84]. The response mechanism is based on the chemical structureof the polymer network (e.g., the functionality of chain sidegroups, branches, and crosslinks). For example, in networksthat contain weakly acidic or basic pendent groups, water sorptioncan result in ionization of these pendent groups dependingon the solution pH and ionic composition. The gels then act assemi-permeable membranes for the counter-ions, thereby influencingthe osmotic balance between the hydrogel and the externalsolution through ion exchange, depending on the ion-ion interactions. For ionic gels containing weakly acidic pendentgroups, the equilibrium degree of swelling increases as thepH of the external solution increases, while the degree of swellingincreases as the pH decreases for gels containing weaklybasic pendent groups[85].

Temperature-responsive hydrogels are one of the mostwidely studied responsive hydrogel systems. These systems,which are mostly based on poly(*N*-isopropylacrylamide)(PNIPAAm) and its derivatives, undergo a reversible volumephasetransition with a change in the temperature of the environmental conditions. This type of behavior is related to polymerphase separation as the temperature is raised to a criticalvalue known as the lower critical solution temperature(LCST). Networks showing a lower critical miscibility temperatureтend to shrink or collapse as the temperature isincreased above the LCST, and the gels swell upon loweringthe

temperature below the LCST. For example, PNIPAAmexhibits a LCST around 33 °C. PNIPAAm and other thermosensitivehydrogels have been studied for variety of applications,including drug delivery, selective cell detachment and tissue engineering[86].

Hydrogels from natural sources can be derivedfrom polymers such as collagen, hyaluronic acid (HA), fibrin,alginate, agarose, and chitosan[87].Depending on their originand composition, various natural polymers have specific utilitiesand properties. Many natural polymers, such as collagen,hyaluronic acid, and fibrin, are derived from various componentsof the mammalian extracellular matrix. Collagen is themain protein of the mammalian extracellular matrix, whileHAis a polysaccharide that is found in nearly all animal tissues.Alternatively, alginate and agarose are polysaccharides thatare derived from marine algae sources. The advantages ofnatural polymers include low toxicity and biocompatibility.

Collagen and other mammalian-derived protein-based polymersare effective matrices for cellular growth because theycontain many cell-signaling domains present in the *in vivo*extracellular matrix. Collagen gels can be created throughnatural means without chemical modifications[88-90]. HA is a glycosaminoglycan (GAG) that is composed ofrepeating disaccharide units and is particular prevalent duringwound healing and in joints. Covalently cross-linked HAhydrogels can be formed by means of multiple chemical modifications [91-92]. HA is degraded by cells through the release ofenzymes such as hyaluronidase.

Alginate is a linear polysaccharide that is derived frombrown seaweed and bacteria. It gels under benign conditions,which makes it attractive for cell encapsulation. Alginate gelsare formed upon formation of ionic bridges between divalentcations (i.e. Ca^{2+}) and various polymer chains of the alginate[93].The cross-linking density of alginate gels is a function of themonomer units and molecular weight of the polymer. Alginategels degrade slowly in a process in which the mechanicalproperties of the gels are altered with time[94].Chitosan is another naturally occurring linear polysaccharidederived from chitin. Dissolved chitosan can be cross-linkedby increasing pH, by dissolving in a non-solventor byphotocrosslinking[95-96]. Chitosan can be degraded by the lysosomeand is therefore degraded in humans [97].These gelscan be used for many applications, including drug delivery [98].

Biohybrid hydrogels have been synthesized by integrating biological entities with synthetic hydrogels, creating a novel system that synergistically combinewell-evolved biological mechanisms, such as high affinity andspecificity of binding, with tailorable hydrogel properties . Their use has been shown in biosensor applications where glucose oxidase enzyme was incorporated within the hydrogels permitting the glucose sensing and estimation. The stimuli-responsive hydrogelexhibited gating and controlled transport of biomoleculesacross the network, demonstrating its potential for microfluidicsand drug delivery[99].

Hydrogels have also been synthesized containing functionalgroups for enhancing cellular adhesion [74]. The most commonpeptides used to modify hydrogels are amino acid sequencesderived from natural proteins, such as RGD (derived fromproteins such as fibronectin, laminin, or collagen), IKVAV,and YIGSR from laminin. PEG and other hydrogels, such as alginate, have beenmodified with RGD to enhance cellular adhesion [100-101]. PVA gels have also been tailored to enhance cellular adhesionby incorporation of GHK or RGDS sequences foradhesion of hepatocytes and epithelial cells, respectively [102]. Another form of modification of hydrogels is the incorporationof growth factors into the gel. Growth factors can becovalently attached to the hydrogels. For example, transforminggrowth factor beta (TGF-β) has been tethered to PEG toregulate smooth muscle cell function. OtherTGF-βrelated proteins such as bone morphogenic protein 2(BMP-2) have been covalently attached to alginate to regulateosteoblast migration and calcification into the gels[103-104].

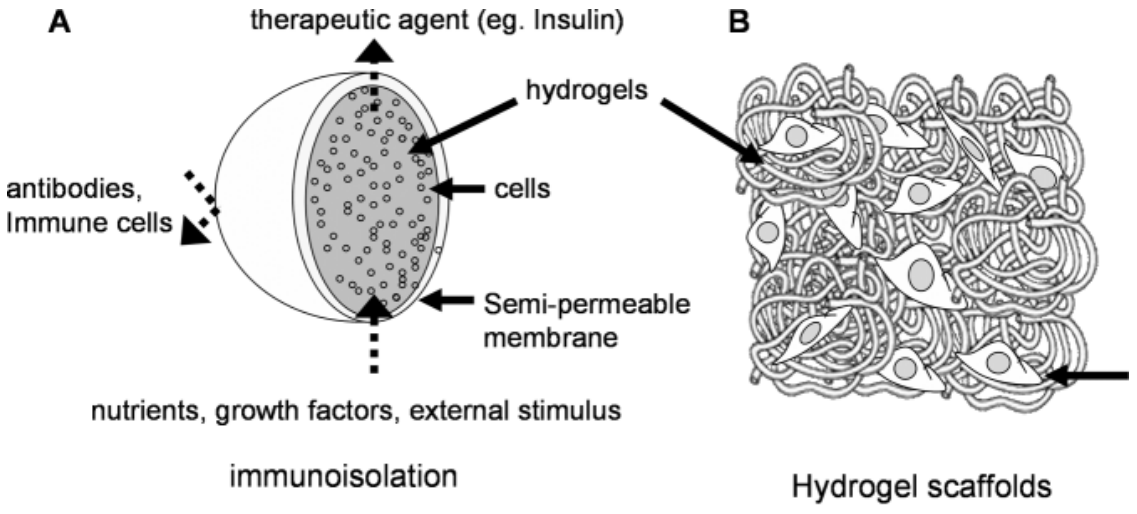

Fig. 1.5-Schematic diagram of the use of hydrogels (A) microencapsulation and (B) tissue-engineering scaffold.Reproduced from[1].

Cell-laden hydrogels are interesting scaffolding materials and their high water content, biocompatibility, and mechanicalproperties which resemble natural tissues make hydrogelsparticularly attractive for tissue-engineering applications. Cells are distributed homogeneously throughout the resultingscaffold, by adding them to the hydrogel before the gelation process begins.Fibroblasts, osteoblasts, vascular smooth muscle cells,and chondrocytes successfully immobilized and attached tothese hydrogel scaffolds[105-106]. Thesescaffolds also facilitated increased growth-factor delivery andshape sculpting with their use in combination with microfluidicchannel technology and photopatterning[78, 107-108].

1.4 Stem cells and their unique properties

Stem cells have remarkable potential to develop into many different cell types in the body during early life and growth. In addition to this, they also serve as an internal repair system in many tissues, dividing essentially without limit to replenish other cells as long as the person or animal is still alive. When a stem cell divides, each new cell has the potential either to remain a stem cell or become another type of cell with a more specialized function, such as a muscle cell, a red blood cell, or a brain cell.

Stem cells differ from other kinds of cells in the body in following three aspects:-

1. These cells are capable of dividing and renewing themselves for long periods.
2. These cells are unspecialized.
3. They can give rise to specialized cell types.

Stem cells are capable of dividing and renewing themselves for long periods[109]. Unlike differentiated cells like muscle cells or nerve cells, which do not normally replicate themselves, stem cells may replicate many times, or proliferate. A starting population of stem cells that proliferates for many months in the laboratory can yield millions of cells. If the resulting cells continue to be unspecialized, like the parent stem cells, the cells are said to be capable of long-term self-renewal.

One of the fundamental properties of a stem cell is that it does not have any tissue-specific structures that allows it to perform specialized functions. For example, a stem cell cannot work with its neighbors to pump blood through the body (like a heart muscle cell), and it cannot carry oxygen molecules through the bloodstream (like a red blood cell). However, unspecialized stem cells can give rise to specialized cells, including heart muscle cells, blood cells, or nerve cells[110-112].

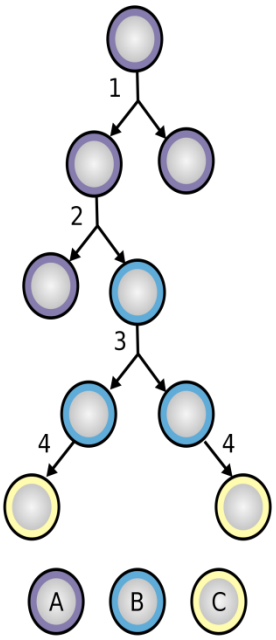

Fig. 1.6-Stem cell division and differentiation. A: stem cell; B: progenitor cell; C: differentiated cell; 1: symmetric stem cell division; 2: asymmetric stem cell division; 3: progenitor division; 4: terminal differentiation.

During differentiation, the cell usually goes through several stages, becoming more specialized at each step (fig. 1.6). The signals,both inside and outside the cells that trigger each step of the differentiation process are currently being investigated in detail. The internal signals are controlled by a set of genes of the cell which are interspersed across long strands of DNA and carry coded instructions for all cellular structures and functions.

The external signals for cell differentiation include chemicals secreted by other cells, physical contact with neighboring cells, and certain molecules in the microenvironment. The interaction

of signals during differentiation causes the cell's DNA to acquire epigenetic marks that restrict DNA expression in the cell and can be passed on through cell division.

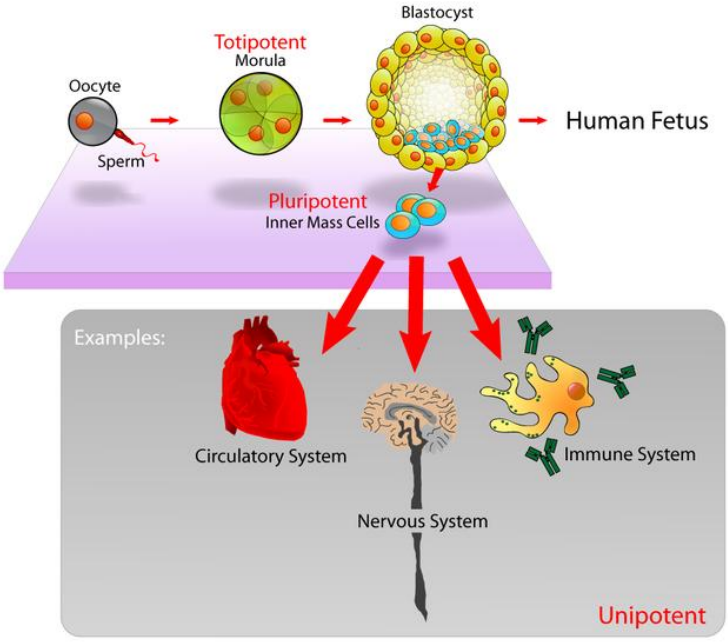

Fig. 1.7-Pluripotent embryonic stem cells derived from the ICM of blastocyst embryo. These cells can differentiate into almost all types of specialized cells in human body except placenta.

1.4.1 Embryonic stem cells

Embryonic stem cells (ES) are derived from the inner cell mass (ICM) of a developing blastocyst (fig. 1.7). This region of the blastocyst gives rise to nearly all the cell types found in the adult organism. ES cells were first derived from rodents and were shown to be pluripotent[113]. Human ES cells were generated later and were shown to have properties similar to those of rodent ES cells, while requiring a different set of culture conditions [114]. The primary focus towards ES cells has been to keep them in an undifferentiated state in long-term cultures, and to standardize the protocols needed to differentiate ES cells into adult cell types in an easy and reliable manner. Mouse ES cells were initially grown on mouse fibroblast feeder layers to keep them in an undifferentiated state.Further studies identified leukemia inhibitory

factor (LIF) as one of the primary molecules secreted by feeder-cell layers that maintained ES cells in their undifferentiated state [115]. With the discovery of LIF as a mediator of differentiation, downstream transcriptional targets of LIF were identified that appear to regulate the pluripotency of ES cells. Transcription factors such as Nanog and Oct3/4 were found to be expressed in ES cells, and their expression decreased as cells differentiated into mature phenotypes.

Human ES cells (hES) behave slightly differently from rodent ES cells. hES cells do not maintain a pluripotent state when treated with LIF,though they can be maintained on feeder layers, or on laminin-coated culture plates when fed with feeder-layer conditioned media[114, 116]. The use of feeder layers was questioned because of the possibility of cross-contamination from animal cellssincea rodent glycopolysaccharide was foundin ahES cultured on mouse feeder layers. These foreign polysaccharides can illicit adverse immune response when transplanted in the human body [117].

1.4.2 Adult stem cells

Unlike ES cells, which are generated from the inner cell mass of a developing blastocyst, adult stem cells have been isolated from numerous adult tissue types, including brain, bone marrow, liver, and skin [118].Like ES cells, adult stem cells are capable of asymmetric division, producing a relatively undifferentiated copy of themselves, and a more-committed daughter cell. Initial isolation and characterization of these adult stem cells showed them to be multipotent, capable of giving rise to only certain cell types of the tissue they were isolated from. Further studies introduced the idea that under certain conditions, these cells could trans-differentiate, or turn into mature cells of other tissue types.

- Hematopoietic stem cells give rise to all the types of blood cells: red blood cells, B lymphocytes, T lymphocytes, natural killer cells, neutrophils, basophils, eosinophils, monocytes, and macrophages.

- Mesenchymal stem cells give rise to a variety of cell types: bone cells (osteocytes), cartilage cells (chondrocytes), fat cells (adipocytes), and other kinds of connective tissue cells such as those in tendons.
- Neural stem cells in the brain give rise to its three major cell types: nerve cells (neurons) and two categories of non-neuronal cells—astrocytes andoligodendrocytes.
- Epithelial stem cells in the lining of the digestive tract occur in deep crypts and give rise to several cell types: absorptive cells, goblet cells, paneth cells, and enteroendocrine cells.
- Skin stem cells occur in the basal layer of the epidermis and at the base of hair follicles. The epidermal stem cells give rise to keratinocytes, which migrate to the surface of the skin and form a protective layer. The follicular stem cells can give rise to both the hair follicle and to the epidermis.

1.4.3 Stem Cell Niche and Extracellular Matrix

One of the most important factors which affect the property of stem cell is the stem cell niche. Stem cells are able to perform their function, because of the environment, and the physical and biochemical cues from this niche influence cell division, differentiation, and migration. The niche first came to prominence in the hematopoietic stem cell (HSC) field, where the composition of bone marrow was found to play an active role in HSC function. Research on niches in regard to neural stem cells has focused on the extracellular matrix comprising the sub-ventricular zone (SVZ) and rostral migratory stream (RMS), and the cytokines and signaling molecules that target this region.The extracellular matrix (ECM) environment of the central nervous system (CNS) is responsible for a large number of regulatory functions both during development and adulthood. The ECM provides signals for cell growth, differentiation and migration [119-121]. These activities are critical for the development of CNS organization, and disruptions of ECM interactions can cause severe developmental defects [119]. During CNS histogenesis, ECM defines functional boundaries for cells and is involved in signaling after injury [120, 122-123]. Permissive substrates for neurosphere differentiation may underlie migratory pathways, whereas non-permissive substrates may mark more sedentary cell zones. In the SVZ

stem cell niche the ECM, composed primarily of tenascin and chondroitin sulfate proteoglycans (CSPG), is believed to act as a barrier, keeping the neural stem cells (NSC) in the SVZ.This ECM composition is set up late in embryonic development and is persistent throughout the life of the animal. During early development the presence of dense ECM may allow the niche to remain undisturbed throughout development and prevent axons from innervating the region, and possibly degrading the ECM matrix.

Laminin and fibronectin are known to be potent permissive substrates for a variety of cell types *in vitro*, including cerebellar and SVZ derived neurospheres[124]. But neither fibronectin nor laminin are present in high levels in an adult animal; however, fibronectin knockout animals demonstrate neural tube abnormalities that are embryonic lethal [125]. Laminin has been shown to be present in the developing cerebellum and acts as a permissive migratory substrate for granule cell precursors to migrate from the external granule cell layer into the internal granule cell layer [126-127]. Laminin has been shown to enhance neurite elongation of cultured neurons and to increase the integration and regeneration of cells within the injury sites[128-129]. Slice co-culture transplants with laminin have been reported to enhance the ability of fetal dopaminergic neurons to reconstruct a damaged nigrostriatal circuit in adult rats[130].

1.4.4 Effect of ECM on stem cell differentiation

Diverse array of environmental factors contribute to overall control of stem cell activity. In particular, increasing role of extra-cellular matrix is being observed on stem cell behavior through physical interaction with cells such as control of cell geometry, ECM geometry/topography at nanoscale, ECM mechanical properties and transmission of mechanical or other biophysical factors to the cell. An improved understanding of the interaction of thesemediators with classical signaling pathways may provide newinsights into the regulation of self-renewal and differentiation ofstem cells. The ability to better engineer artificial ECMs that cancontrol cell behavior, through physical as well as molecular interactionsmay further extend the possibilities in engineering tissuesubstitutes from adult or embryonic stem cells[131-132]. Majority of work in this area has focused on adult stem cells like adult neural cells or

MSCs. Thesecell types generally represent a heterogeneous population withreduced plasticity in comparison to embryonic or hematopoieticstem cells.

1.4.4.1 Cell shape as a potent regulator of stem cell fate

Cell shape is a potent regulator of cell growth and physiology and many events related toembryonic development and stem cell differentiation are influenced by cell shape eg. changes in cell shapehave been implicated as a potential mechanism that regulatesmyocardial development[133-134]. In addition to the physical control of shape, some subsetsof these effects may result from the altered adhesive interactionsbetween the cell and substrate. Growthof chondrocytes in flattened shape in a 2D culture leads to its dedifferentiationand a shift from a chondrocytic phenotype toa more fibroblastic phenotype[135]. But, theretention of these chondrocytes in its native shape using a pellet culture or by encapsulation in a gel such asagarose or alginate helped them retain their normal phenotype[136-137]. Interestingly, the restoration of chondrocyteshape to a rounded morphology by chemical alteration of theactin cytoskeleton also partially restores some of the phenotypicchanges.

Human embryonicstem cell-derived cells maintained in three-dimensional culturein arginine-glycine-aspartate-modified hydrogels show significantlygreater cartilage-specific gene upregulation and ECMproduction than in pellet culture or unmodified poly(ethyleneglycol) gels. The mechanism by which cell shape influences stem cell fatehavebeen explored using micropatternsof proteins which were deposited upon asubstrate, thereby precisely limiting the area of cell attachment.On small ECM micropatterned islands, cells adopteda poorly spread, rounded morphology, whereas cells adhered tolarge ECM islands adopted flattened morphologies typical of 2Dcultures[138]. This shape change fromrounded to flattenedmorphologies profoundly alters the organizationof the actin cytoskeleton and the assembly of focal adhesions[139]. Importantly, this micropatterning approach hasrevealed that cell shape (i.e., rounded versus flattened morphologies)controls the lineage commitment of MSCs into an adipogenicor osteoblastic phenotype[45]. There is a profound change in the

mechanical properties of cell itself which leads to changes in the focal adhesion assembly and F-actin cytoskeleton rearrangement.

1.4.4.2 ECM stiffness as a regulator of stem cell fate

There is a significant evidence that other physicalproperties of the ECM like its mechanical properties may also contribute to the stem cell fate orlineage commitment. Cells that attach to a substrate exert contractile forces, resulting in tensilestresses in the cytoskeleton [140]. Interestingly, therelationship between these forces and the mechanical stiffness,or elasticity, of the ECM can have a major influence on cellbehaviors such as migration, apoptosis and proliferation[141-144].Cells grown onsoft matrigel or on matrigel copolymerized with heat-denaturedcollagen exhibited reduced expression of actin and focal-adhesionplaque in comparison to the cells remaining in a monolayerpattern on a rigid matrigel coat or on matrigel copolymerizedwith type I collagen[145].

Adult neuralstem cells were grown on a synthetic, interfacial hydrogel culture system which varied in moduli between10 and 10,000 Pa[14]. Cell spreading, self-renewal and differentiation was inhibited on soft substrates (10 Pa), whereas the cells which proliferated on substrates withmoduli of 100 Pa or greater and exhibited peak levels ofa neuronal marker, β- III tubulin. Softer substrates (~100-500 Pa) promoted neuronal differentiation, whereasstiffersubstrates (~1,000-10,000 Pa) led to glial differentiation.

MSCs grown on variably compliant polyacrylamide gelwere found to alter their properties in relation to the stiffness ofthe substrate (i.e., stiffer substrates induced stiffer cells).Furthermore, the stiffness of the substrate defined the differentiationlineage of the MSC: soft substrates that mimic the mechanicalproperties of brain tissue were found to be neurogenic,substrates of intermediate stiffness that mimic muscle weremyogenic, and relatively stiff substrates with bone-like propertieswere found to be osteogenic[13].

1.4.4.3 Regulation of stem cells by nanotopography of the ECM

In addition to overt, macroscopicchanges in cell shape, cells also have the ability to sense micro- andeven nanoscale geometrical cues from their environment. Suchcues may represent differences in molecular conformation,surface topography or roughness, fiber diameter, or other parameters.For example, neurite outgrowth from neurogenically differentiatedstem cells was significantly enhanced when grownwithin inert but highly porous 3D polystyrene scaffolds, ascompared to traditional flat surfaces [146].Similar changes have been observed on cell alignment, wherethe directional growth and differentiation of adult rat hippocampalprogenitors cultured on micropatterned polystyrenesubstrates chemically modified with laminin, exhibited over 75%alignment in the direction of the grooves (13 mm wide and 4 mmhigh), as well as significantly increased expression of neuronalmarkers [147]. These findings show that the 3Dtopography of the substrate, in synergy with matrix composition can facilitate neuronal differentiation and neurite alignment.

HumanMSCs grown on nanoscale grooves of 350 nm width showedalignment of their cytoskeleton and nuclei of MSCs along thegrooves [148]. A significant upregulation of neuronalmarkers such as microtubule-associated protein 2 (MAP-2) was observedon these substrates as compared to unpatterned and micropatternedcontrols. While the combination of such nanotopographiccues with biochemical cues such as retinoic acid furtherenhanced neurogenesis, nanotopography showed a strongereffect compared to retinoic acid alone on an unpatterned surface. Neuronal progenitor cells appear to show similar responses toelectrospun fibers with nanoscale properties. Rat hippocampusderivedadult neural stem cells grown on laminin-coated electrospunpolyethersulfone fiber meshes ranging from 283 nm to1452 nm in diameter showed differentiation and proliferationresponses that significantly depended on fiber diameter [149]. Cells stretched multi-directionally tofollow underlying 283 nm fibers but when grown on larger fibers,extended along a single fiber axis. With decreasing fiber diameter,a higher degree of proliferation and cell-spreading andlower degree of cell aggregation were observed.

The mechanisms by which nanotopographic cues influencestem cell proliferation and differentiation is not well studiedbut appear to involve changes in the protein adsorption on

substrates, cellular cytoskeletal organization andstructure, potentially in response to the geometry and size ofthe underlying features of the ECM. That is, changes in thefeature size of the substrate may influence the clustering of integrinsand other cell adhesion molecules, thus altering the numberand distribution of focal adhesions[150]. Alternatively, the influence of nanotopographicfeatures may be mediated through secondary effects, such asalterations in the effective stiffness perceived by the cellor differences in protein adsorption due to the structuralfeatures of the substrate.

Thus, it can be seen that various features of the extra-cellular matrix may affect the properties of stem cells and most importantly its lineage commitment especially into neuronal subtype. The current explosion of studies in this area seeks to explore the variety of facets to provide an ease of control over regulated stem cell differentiation. Neuronal differentiation of ES cells is particularly attractive since it provides an unlimited supply of neurons which is not possibly by traditional cell culture methods. The regenerative potential of neurons in CNS is least in the human body and any injury or disease which may result in the loss of neurons, may be life threatening. The current approaches towards CNS therapies involve development of newer methods to supply stem cells to the adjoining tissues where they may differentiate and replace the injured neurons.

1.6 Scope and overview of the thesis

The field of tissue engineering and biomaterials has greatly benefited from the development of synthetic polymers. These polymers provide tailorable properties which can be engineered for a particular biomedical application. Soft polymers like polyurethanes, elastomers, polystyrene rubbers and hydrogels are finding greater use as implants in our body, drug delivery systems or scaffolds to promote the cell growth. The understanding about the effect of physical environment of ECM on cell growth and proliferation especially stem cells has opened up newer possibilities to tune the cell differentiation towards the desired lineage.

Certain cells like neuronal cells respond to the conducting microenvironment and their properties like neurite length changes with electrical stimulation. A class of polymers which have been utilized in these applications are conducting polymers like Poly(3,4-ethylene

dioxythiophene)-poly(styrene sulfonate) (PEDOT:PSS) and Polypyrrole (PPy). These polymers are interesting class of materials which have excellent optical and electronic properties. The properties of these polymers have been utilized in making biosensors and cochlear impants. They also provide an alternate substrate for neuronal growth which isbeing used for the development of neuroprosthetic devices. Electrically conducting polymers on a soft elastomeric scaffold also provide a rigid scaffold for the differentiation of stem cells. This would play a dual role in promoting development of neurons and acting as a scaffold for the implantation of cells at the injured site.

In this work, the role of conductivity and microstructure of the conducting polymer surface for stem cell differentiation and proliferationare emphasized.The conductivity of the CP coated elastomeric substrate has been shown to be precisely controlled by the application of strain in chapter 2. It is observed that the randomly distributed spherical PEDOT domains transform into ellipsoidal domains within the poly-anionic PSS matrix. This leads to a change in the surface potential distribution of the CP substrates. The application of strain on these substrates also leads to an increase in the stiffness of the substrates due to strain hardening of the underlying elastomer.

In the Chapter 3, detailed studies ofthe differentiation of ES-NPs into neurons on the CP substratesare done and the corresponding results are discussed. The utility of these substrates for stem cell differentiation is analyzed and subsequently neuronal differentiation is induced.The cells are immunostained with specific neuronal marker β-III tubulin to identify the immature neurons. Strained conducting and non-conducting elastomeric substrates arealso used to study the influence of the strain on the neuronal differentiation. The effect of conducting substrates is seen on the neuronal differentiation potential of ES-NPs and this is further investigated in detail.

Chapter 4 discusses the changes in neuronal differentiation and spreading. Actin cytoskeletal arrangement of differentiated neurons is assessed by phalloidinimmunostainingto study its possible role in modulating cellular functioning. The role of the physical guidance provided by the conducting polymers is also investigated to understand the guidance cues provided by the surface during development of neurons on these surfaces. Possible improvements and further

investigation of the role of the conducting component of the substrates in these changes has been highlighted.

CHAPTER 2

MATERIALS AND METHODS

2.1 Introduction

Polymer scaffolds are being increasingly explored for their role in tissue engineering and biomedical applications. Soft polymers provide a diverse array of scaffolds for cell culture which enable us to engineer and control the cell behavior for variety of purposes like promoting cell differentiation to a particular lineage, manipulating or studying the cell movement, migration and controlling the cell adhesion. The modulation of stem cell lineage specificity by the change in material properties of the soft substrates provides specific control over cell behavior [151].

Conducting polymers are being explored extensively in the area of neuroprosthetics and functional analysis of neurons. The role of these polymers in controlling stem cell fate can open up numerous possibilities especially in the area of neural tissue engineering. Conducting polymers have also shown to support the neuronal culture for a much longer period of time than traditional cell culture materials. This is especially important since the adult neurons do not have the potential to regenerate which is a major concern during a brain or spinal cord injury or related diseases. Neuronal differentiation on conducting polymer interface also provides an intricate connection between cell machinery and conducting polymer surface. This can be an important step in the development of biomedical applications for neural interfacing.

Current chapter dealswith the properties of these polymers which makes them attractive scaffolds for stem cell differentiation. The change in their conducting properties upon the

application of strain attracted particular interestsince it may play a significant role in providing guidance cues during the developmental stages ofES cells. The last section of the chapter deals with the protocols followed for the differentiation of ES cells into neurons and glial. The analytical and quantitative methods used in the experiments have also been discussed in detail.

2.2 Styrenic copolymers

The styrene family contains a wide variety of polymers.Liquid styrene can be polymerized in two ways:

1. Bulk polymerization- delicate method
2. Suspension polymerization- fine droplets (0.1 to 10μm) of styrene monomer dispersed in an aqueousphase.

During the polymerization of styrene, one carbon-carbon double bond (in the vinyl group) is replaced by a much stronger carbon-carbon single bond; hence it is very stable and difficult to depolymerize. About a few thousand monomers typically comprise a chain of polystyrene, giving a molecular weight of 100,000–400,000.

A 3-D model shows that each of the chiral backbone carbons lie at the center of a tetrahedron, with its 4 bonds pointing toward the vertices. In fig. 2.1, consider that these -C-C- bonds are rotated so that the backbone chain lies entirely in the plane of the diagram. From this flat schematic, it is not clearly evident which of the phenyl (benzene) groups are angled outward from the plane of the diagram, and which ones are inward. The isomer where all of the phenyl groups are on the same side is called isotactic polystyrene, which is not produced commercially.

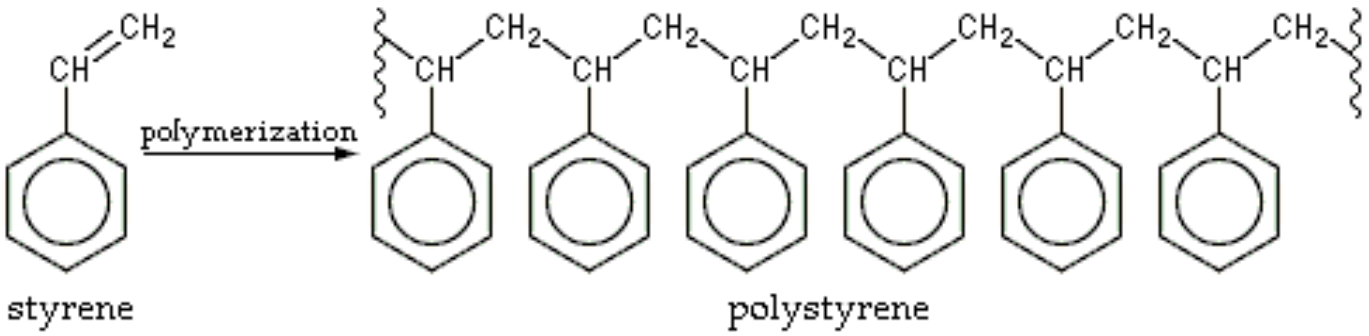

Fig. 2.1- Polymerization of styrene to give a polystyrene polymer.

Polystyrene can either be a thermoplastic or a thermoset polymer. A thermoplastic polystyrene is in solid (glassy) state at room temperature, but flows in liquid state if heated above its glass transition temperature of about 100 °C (for molding or extrusion), and becomes solid again when cooled. Pure solid polystyrene is a colorless, hard plastic with limited flexibility and can be casted into molds with fine details.

The property of the polymer isdetermined by short-range Van der Waal forces between the polymer chains. The total attractive force between the molecules is large since they are long hydrocarbon chains that consist of thousands of atoms. When heated (or deformed at a rapid rate, due to a combination of viscoelastic and thermal insulation properties), the chains are able to take on a higher degree of conformation and slide past each other. This intermolecular weakness (versus the high intramolecular strength due to the hydrocarbon backbone) confers flexibility and elasticity. The ability of the system to be easily deformed above its glass transition temperature allows polystyrene (and its derivatives) to be readily softened and molded upon heating.

Styrene is also copolymerized with polybutadiene or ethylene/ butylene to produce graft styrene-butadiene-styrene (SBS) and styrene-ethylene/butylene–styrene (SEBS), which are widely used in medical applications[15, 37, 67].

Fig. 2.2 shows the chemical structure of SEBS, which is sold under the brand name KratonG ,isa linear triblock copolymer which exhibits high stability under UV exposure and processing conditions.This elastomer has improved shock resistance, does not require additives, very flexible, pure and does not release any residues *in situ*[152]. However, it is not very histocompatible and numerous attempts have been made to improve its biocompatibility. Polyhydroxyethylmethacrylate (PHEMA) grafts improve blood compatibility and polysiloxane grafts impart the properties of silicone elastomers. while N^+, F^+, and Ar^+ions improve cell adhesion [153]. The SBS and SEBS elastomers can be sterilized by heat, vapor, gamma radiation, or ethylene oxide without losing their physical properties. They are used to manufacture catheters, stoppers, non-rigid containers, surgical fields, gloves etc.

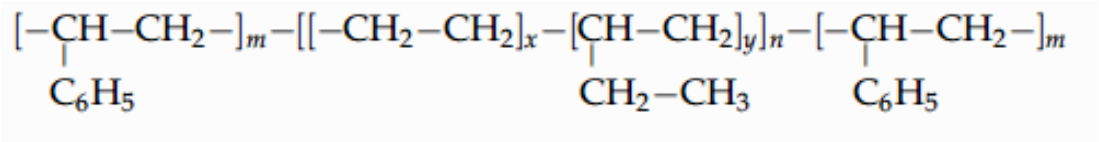

Fig. 2.2- Chemical structure of SEBS.

SEBS offers some attractive properties which may find its usage in cell culture experiments as a scaffold over which cells are cultured. The polymer can be easily patterned at micro or nanometer length scales providing directional guidance to the proliferating cells. The flexibility of SEBS provides an implantable material which can withstand higher degree of strain over a long period of time.

The properties of SEBS are also comparable with PDMS which is commonly used for cell culture experiments. SEBS provides a unique surface for studying the behavior of cells modulated by the tunable viscoelastic properties of the polymer. Mechanical effect of the polymer and the effect of strain on cell growth can be better understood on the highly flexible SEBS polymer than PDMS. The ease of processing conditions and cost of SEBS makes it a

cheaper alternative amongst all the soft polymers used for biological studies. Table 2.1 provides a comparison between the properties of SEBS and PDMS:-

Table 2.1- Comparison between the properties of SEBS and PDMS.

	SEBS	PDMS
Content	Polystyrene-30% Rubber-70%	Silicones
Physical form	Solid(dusted pellet)	Solid(viscous gel like)
Specific gravity(gm/cc)	0.91	0.76
Glass transition temperature(K)	213	150
Hardness(Shore A)	70	25-40
Elongation(%)	450	250
Ultimate tensile strength(MPa)	2.413	2.24
Viscosity(cP)	140-220	0.65-10
Water contact angle(Θ)	82-88	95-113

2.3 Conducting polymers

Conductingpolymers (CP) were reported as a novel generation of organic materials.They exhibit both electrical and optical properties similar to those of metals and inorganic semiconductors coupled with the attractive properties associated with conventional polymers, such as ease of synthesis and flexibility in processing[154-156]. The fact that several tissues are responsive to electrical fields and stimuli has made CPs attractive for a number of biological and medicalapplications[2, 157-159].

2.3.1 PEDOT:PSS

Poly(3,4-ethylene dioxythiophene (PEDOT) is one of the well-studied π-conjugated polymers, mainly because of its excellentelectrical conductivity, electro-optical properties, andits processability. Preparedwith standard oxidative chemical or electrochemicalpolymerization methods, PEDOT was initiallyfound to be an insoluble polymer, yet it exhibitedsome very interesting properties. In addition to ahigh electrical conductivity (ca. 550 S/cm)andmetallic behavior,PEDOT was found to be almosttransparent and highly stable in thin oxidizedfilms[156, 160-162]. The solubility problem was circumventedwith a water-dispersible polyelectrolyte,poly(styrene sulfonate) (PSS), used as a chargebalancingcounter-ion during polymerization which yielded poly(3,4-ethylene dioxythiophene)-poly(styrene sulfonate) (PEDOT:PSS).

This combination yielded a water-soluble polyelectrolyte with good film forming properties, high conductivity (ca. 10 S/cm), high visible light transmissivity, andexcellent stability. A minimal change in the conductivity of PEDOT:PSSwas observed upon heating the CP films at 100^{o}C forover 1000 hours.

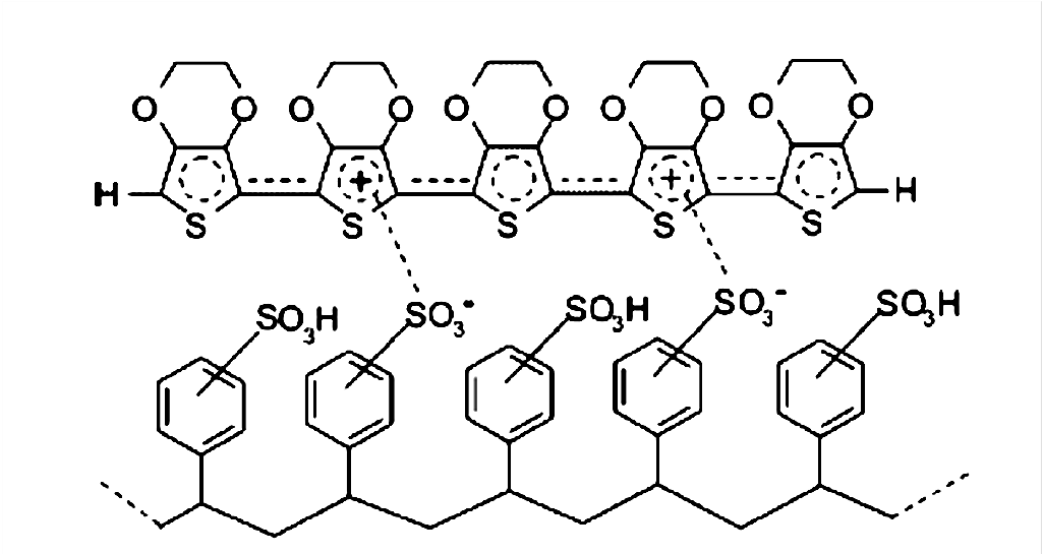

Fig. 2.3- Molecular structure of PEDOT:PSS.

Both PEDOT and PSS contain one sulfur atom per repeat unit. The sulfur atom inPEDOT is within the thiophene ring, whereas in PSS, it is included in the sulfonatemoiety (fig. 2.4) [163].Theelectronic and ionic (cation) conductivities makePEDOT:PSS attractive for capacitorsandhigh-power Li batteries[164-167]. New applications for PEDOT:PSShave emerged in the field of organic polymer-based optoelectronics.PEDOT:PSS has been used as a buffer layer, sandwichedbetween indium tin oxide (ITO) and anactive organic layer, in organic-based light-emittingdevices (OLEDs)and photovoltaiccells[168-169]. PEDOT is also a good candidatefor use asprocessable electrode in electrochromicdisplaysand has also found application inphotoelectrochemical cells as an absorbing material[170]. BothPEDOT and PEDOT:PSS have found their way intocommercial applications, under the commercial name of BAYTRON P by Bayer industries and ORGACON by AGFAfor antistaticcoatings in photographic films[171]. The difference in the properties of PEDOT:PSS manufactured by both companies makes them suitable for different applications. Table 2.2 summarizes the differences in the properties of both variants of PEDOT:PSS :-

Table 2.2- Comparison between the PEDOT:PSS variants, ORGACON and BAYTRON P.

	ORGACON	BAYTRON P
Molar ratio of PEDOT to PSS	5:8	1:6
Conductivity(S/cm)	300-460	120-240
Additives	Ethylene glycol	None
Adhesion property on elastomers	Good	Poor
Viscosity(cP)	8-10.5	5-5.6

2.3.1.1 Conductivity enhancement of PEDOT:PSS

The conductivity of PEDOT: PSS film is enhanced by more than two orders of magnitude by addition of compounds with two or more polar groups, like ethylene glycol or sorbitol,into an aqueous solution of PEDOT: PSS.The additive induces a conformational changein the PEDOT chains in the PEDOT: PSS film (fig. 2.5).

Both coil and linear or expanded–coil conformations exist in untreated PEDOT: PSS films, whereas the linear or expanded–coil conformation becomes dominant in high conductivity PEDOT: PSS films. This conformational change results in an increase in the intrachain and interchain charge-carrier mobility, which increases the conductivity [172]. PEDOT:PSS from AGFA contains these additives as well as an increased molar ratio of PEDOT to PSS which results in its higher conductivity.

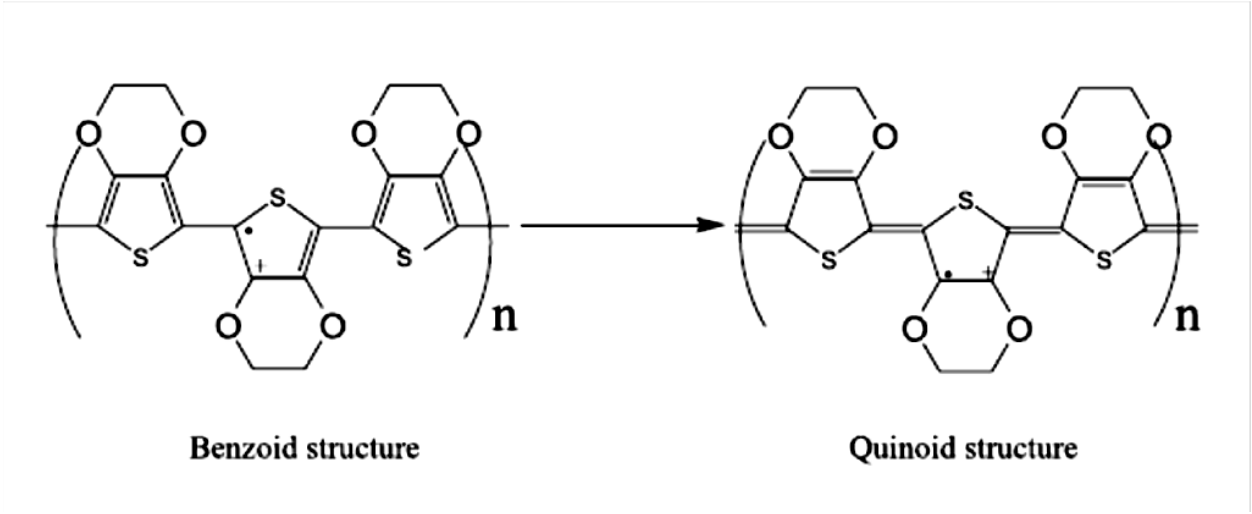

Fig. 2.4- Conformational change in PEDOT after treatment with an additive.

2.3.2 Biological applications of conducting polymers

CPs offer a number of advantages over conventional polymers used for biomedical applications. The electrical activity, conductivity, high stability and ease of fabrication of these polymers is particularly helpful in using them as cell culture scaffolds and implants [155]. CPs have shown, via electrical stimulation, to modulate cellular activities, including cell adhesion, migration, DNA synthesis, and protein secretion[173-176]. But, certain modification are neededfor specific CP applications like in case of biosensors, it is important to tune the hydrophobicity, conductivity, and reactive functionalities for modification of CPs to successfully incorporate biomolecules and to improve detection of binding events. For tissue engineering, CP properties like biomolecule functionalization, surface roughness, hydrophobicity, three-dimensional geometry, redox stability, and degradability are critical. Neural probeapplications require materials with high surface area, hydrophobicity, and cell specificity to improve and maintain good signal-to-noise ratio for detection of neuron signals.

A popular strategy for optimizing the biological properties of a CP is the incorporation of bioactive molecules. This can be achieved through a number of techniques, including physical adsorption, entrapment, doping, and covalent attachment of desired biomolecules. The process of doping CPs, necessary to induce conductivity, can also be exploited to modify CPs non-covalently and to introduce new properties for a desired application. The range of possible dopants is vast as long as the selected dopant is charged. Alternatively, covalent methods can be used to more permanently functionalize CPs in which the monomers can be synthesized with desired functional groups and then polymerized[177].

CP systems are also used in monitoring and diagnosing metabolites (e.g., glucose, hormones, neurotransmitters, antibodies, antigens) for clinical purposes[178]. They are extensively used as transducers that integrate the signals produced by the biological sensing elements such as enzymes.The most common types of transducers are amperometric and potentiometric. An amperometric biosensor measures the current produced when a specific product is oxidized or reduced (e.g., redox reaction of a substrate in an enzyme) at a constant applied potential[178]. The CP mediates the electron transfer (e.g., via hydrogen peroxide) between an enzyme, such as an oxidase or dehydrogenase, and the final electrode. Potentiometric biosensors use ion-

selective electrodes as physical transducers. For example, detection of urea by ureases was done via the production of NH_3, which interacts with polypyrrole (PPy) to produce an electrical signal[179].

CPs are explored as biomaterials for different cell types and functions because previous studies have shown that cells such as fibroblasts, neurons, and osteoblasts respond to electrical fields created by electretsor between electrodes *invitro* and *in vivo*[175-176, 180]. Both, PEDOT:PSS and PPy havebeen readily used to support cell adhesion and growth of a number of different cell types, including endothelial cells , rat pheochromocytoma (PC12) cells , neurons and support cells (i.e., glia, fibroblasts) associated with dorsal root ganglia (DRG), primary neurons, keratinocytes and mesenchymal stem cells[158, 181-182]. Different counter-ions like heparin, tosylate etc. have been used during polymerization of PEDOT which improved its biocompatibility. Electro-adsorbed polylysine enabled long-term neuronal survival and growth on the conducting polymer (fig. 2.5). The neurite extension was strongly inhibited by an additional layer of PSS orheparin, which in turn could be coated with spermine to activatecell growth. Binding of basic fibroblast growth factor (bFGF) to the heparin layer inhibited neurons butpromoted proliferation and migration of precursor cells[2]. Electrical stimulation of neurons grown on conducting polymer layers resulted in the elongation of neurites[159].

The ability of CPs to maintain neuronal culture for long periods without showing any adverse reaction translated their use towards neural interface development. The basic need of such a device is to intimately interface electrodes with neural tissue and to relay signals efficiently between the cells and the electrode, thus integrating the device seamlessly with the native neuronal signaling network. CPs are attractive candidates for interfacing electrodes with neurons because they can achieve high surface area, helping to promote effective ion exchange between recording sites and the surrounding tissue[183].

PEDOT has been explored as an alternative to PPyin this direction because it is much more stable to oxidation and more conductive than PPy and unlike PPy, PEDOT was found to retain 89% of its conductivity under similar conditions[184]. Electrode arrays coated with PEDOT:PSS were successfully used to obtain neural recording from mouse for over six weeks without illiciting any adverse immune reaction [185-186].

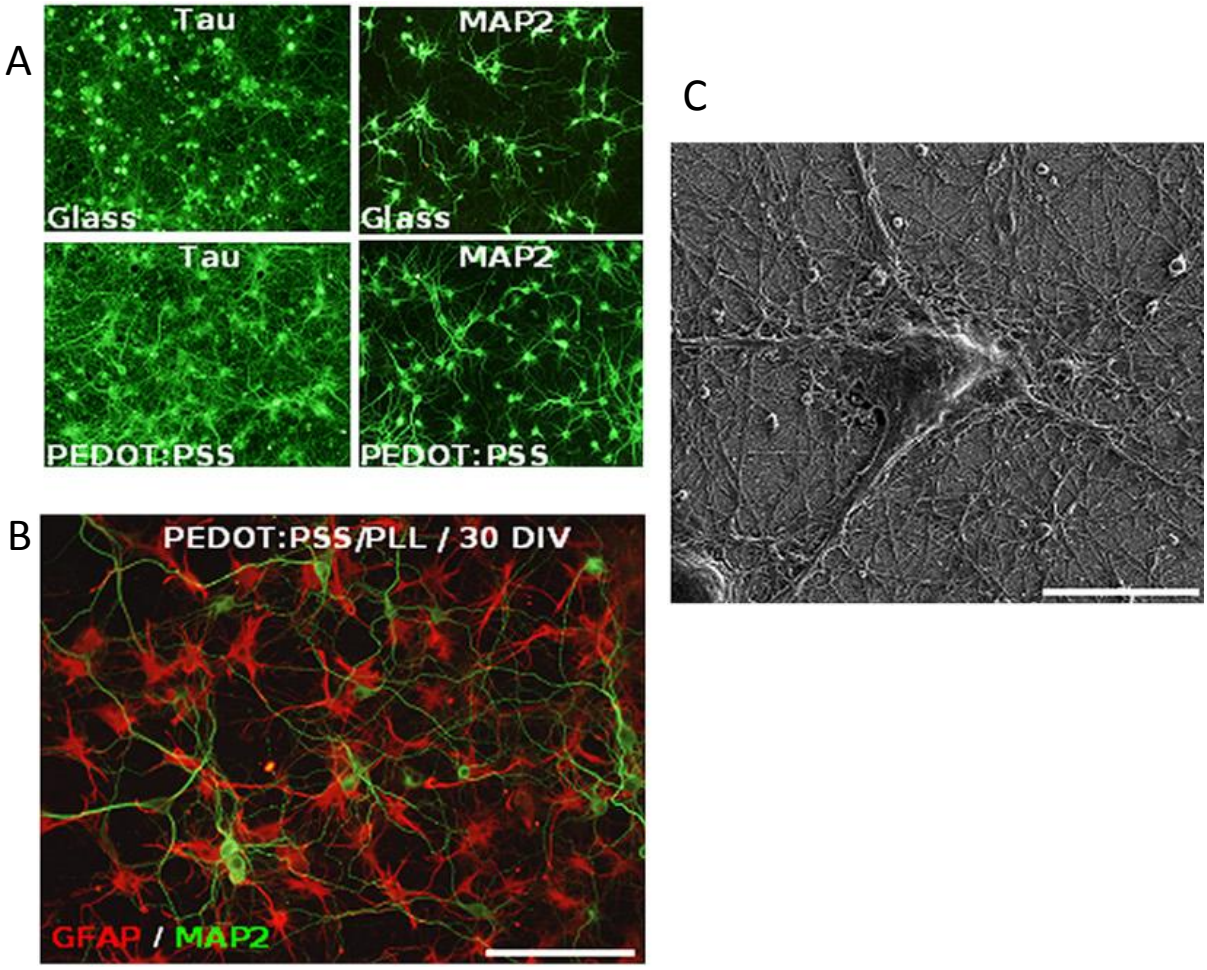

Fig. 2.5- Electro-adsorption of poly-L-lysine (PLL) on PEDOT:PSS enables long-term neuronal growth. A) Neurons survived and showed profuse development of axons (Tau immunostained) and dendrites (MAP2 immunostained) B) Neuronal culture after 30 days *in vitro* C) SEM images showing 10 DIV neurons on electroadsorbed PLL on PEDOT:PSS surface. Scale bar 20µm. Reprinted from [2]with permission from Elseiver.

2.4 Substrate architecture and fabrication

SEBS(KRATON 1726-G)was solvent processed with chloroform as solvent to form thin stretchable films of SEBS. Briefly, SEBS was dissolved in chloroform by sonication and stirring for around 4-5 hours till a translucent solution was obtained. This solution was carefully poured in a flat bottom glass petri-dish to allow the solvent to evaporate which left behind a thin film of SEBS. Subsequently, the film was peeled off and 1 ×1.2 cm rectangular substrates were cut and plasma treated for 2 minutes, at 0.5 bar pressure and 0.08 A current. This reduced the hydrophobicity of the substrates which prevented the delamination of PEDOT:PSS films when incubated in the cell culture media.

The aqueous dispersion of PEDOT:PSS (Agfa, Orgacon Printing Ink EL-P3040) was spin coated on SEBS films at 2500 RPM, 60 s to obtain the films of thickness ~ 90 nm and they were post annealed at 65 ^{0}C for 12 hrs.. These substrates were further heat treated in vacuum at around 60^{o} c for 2 hours to prepare PEDOT:PSS coated substrates (CP substrates) [187].

The setup for straining the PEDOT:PSS coated SEBS substrates was a homebuilt setup with a calibrated screw gauge of least count (L.C.) ~ 32μm (fig. 2.6). Substrates were strained by clamping at the two ends and were uniaxially strained to different strain regimes of 10%, 20%, 30% and 5 cycles of 30% strain. The strained conducting substrates were maintained in stretched condition by wedging them cleanly to a glass slide of the same dimension using araldite. The glass slide was previously cleaned to remove any impurity by sonicating in 1:1:1 (volume ratio) solution of isopropyl alcohol (IPA), acetone, and chloroform for 10 min. Glass slides were then boiled for 3 min in trichloroethylene (TCE) and IPA separately, followed by rinsing in deionized water and blow drying.

The pristine SEBS substrates were prepared in the similar manner following the similar procedure barring the coating with conducting polymer PEDOT:PSS. The stretched cycles substrate was left with a residual strain without wedging it to a glass slide.

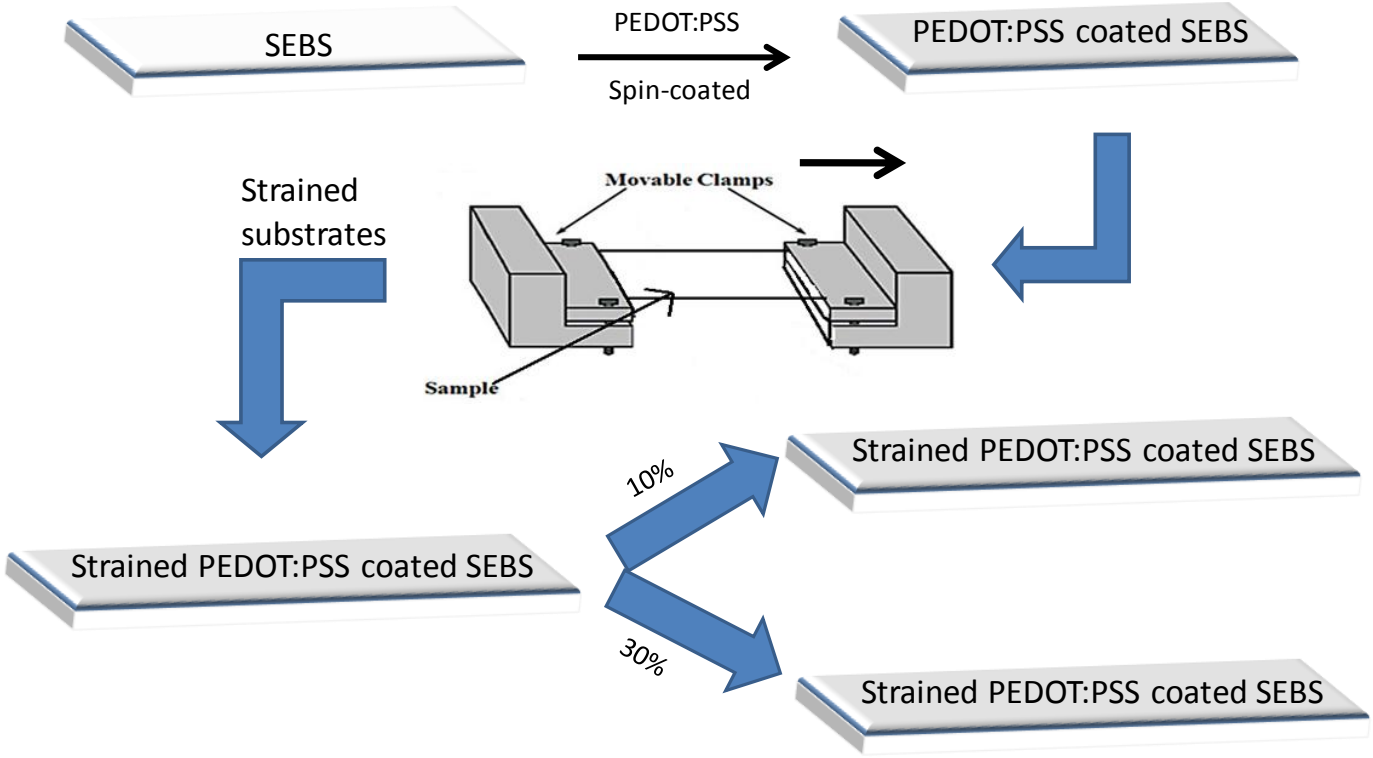

Fig. 2.6- Schematic of substrate architecture and preparation. Pristine SEBS and PEDOT:PSS coated SEBS substrate were stretched using the straining set-up to obtain different substrates.

2.4.1 Surface characterization of substrates

Prior to the investigation of the effect of the CP substrates on stem cell differentiation, surface characterization was carried out to study the changes in the substrates upon application of strain.

Application of strain results in an increase in the conductivity of the CP coated substrates [187]. Detailed characterization of the surface potential of the conducting substrates was done by Kelvin probe microscope (KPM) imaging of 2µm × 2µm area of the conducting substrates by *JPK instruments,* Singapore. Fig. 2.7 shows the KPM images of CP substrates and it is observed that the thin conducting film of PEDOT:PSS is organized in horizontal layers of flattened PEDOT rich particles which are separated by quasi-continuous PSS lamella. PEDOT rich clusters are arranged in form of circular domains of around 100-150 nm in PSS matrix. These domains become elliptical (~ 200-250 nm) on application of strain on these substrates (indicated by the arrowheads) and their distribution also changes. Prior to straining, the circular PEDOT domains were arranged uniformly in PSS matrix which subsequently redistribute along the strain direction when elongated, leading to a change in the distribution of surface potential on these conducting substrates. Charge transport in PEDOT:PSS occurs by variable range hoping in the direction of strain while it occurs by nearest neighbor hopping in the perpendicular direction [188]. In variable range hoping, conduction is about 10 orders higher since the separation between PEDOT lamella is not completely closed by the constrictions of PSS lamella while in perpendicular direction thick PSS lamella impedes the conduction.

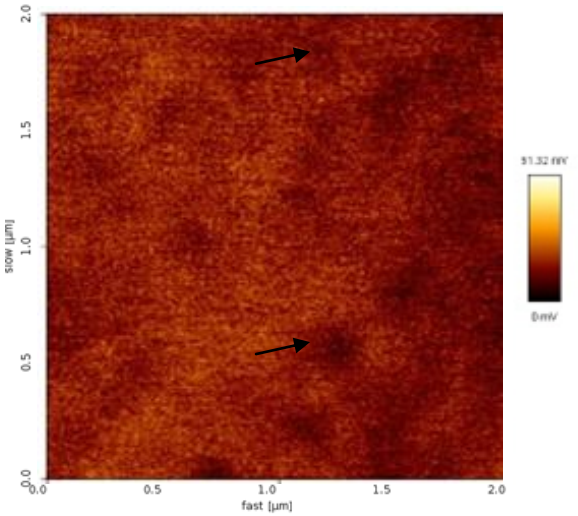

SEBS PEDOT: PSS
0% Stretched

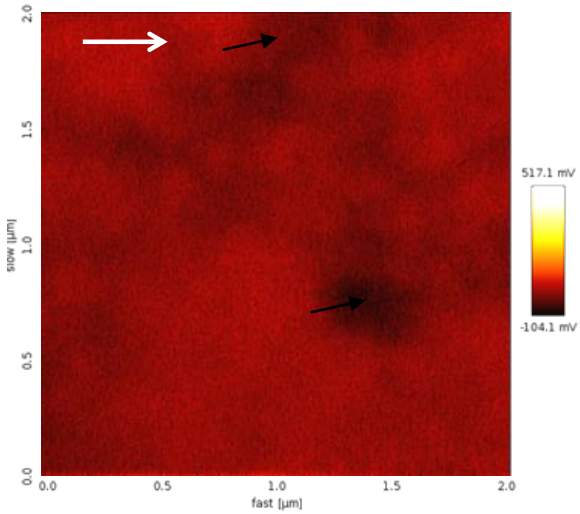

SEBS PEDOT: PSS
30% Stretched

Fig. 2.7- KPM image of PEDOT:PSS coated SEBS substrates showing changes in the PEDOT domains upon straining. The bold arrowhead indicates the direction of strain while the smaller arrowheads indicate the PEDOT domains which are uniformly distributed and circular in SEBS PEDOT:PSS 0% strained substrate while they become elliptical in SEBS PEDOT:PSS 30% strained substrates.

Surface roughness plays a major role in determining the behavior of cultured cells and it has been observed that neurons are able to sense the variations in surface roughness at nanometer length scale and respond to it. Fig. 2.8 shows the atomic force microscope (AFM) images of these substrates which was done to study the changes in the surface roughness of the substrates. Surface roughness was measured over an area of 1 μm × 1 μm of the substratum and surface roughness values were obtained. It was observed that the surface roughness of the substrates decreased upon straining while the conducting polymer coating on SEBS substrates increased their surface roughness values. This was probably due to the underlying surface inhomogenity of the SEBS substrates that the coated film was rougher.

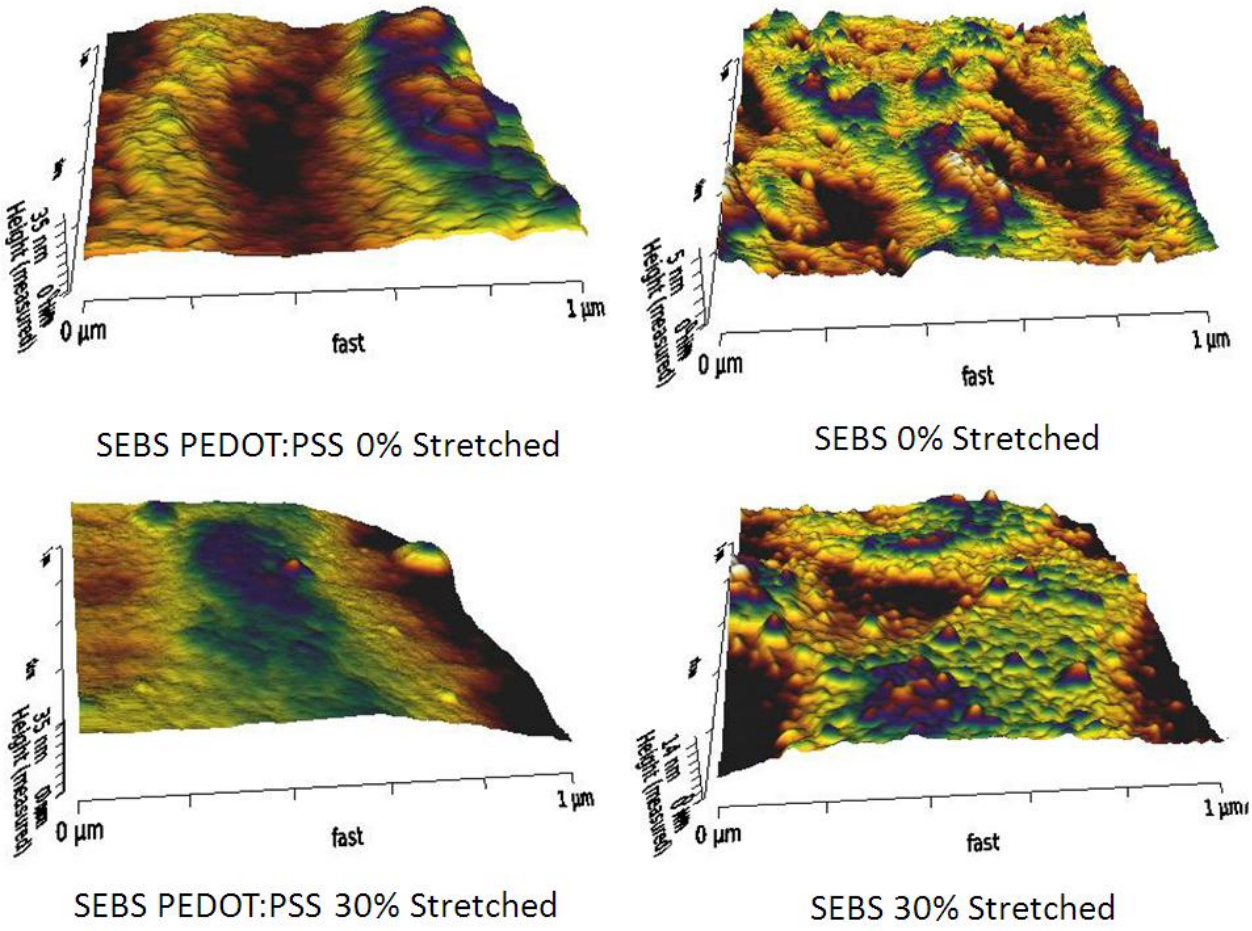

Fig. 2.8- AFM image of the pristine SEBS and PEDOT:PSS coated SEBS substrates.

Hydrophobicity of the substrate affects the adsorption of proteins which in turn affects the cell adhesion. Hence, the hydrophobicity was measured by sessile water drop method in which a small water droplet is placed on the substrate and the contact angle with the surface is measured. Contact angle is the angle formed between the liquid/solid interface and the liquid/vapor interface. The value of contact angle varies with the hydrophobicity of the material and an increase in the contact angle is observed with the increase in hydrophobicity. Highly hydrophobic surface like a lotus leaf has a contact angle around 130^{o} while the contact angle in hydrophilic materials is much smaller than 90^{o}.

Fig. 2.9- Contact angle measurement of PEDOT:PSS coated substrates.

Contact angle on the conducting substrates was measured to observe the effect of straining on the hydrophobicity of the substrates (fig. 2.9). The measurements were averaged over 50 sets to rule out any variation in the results and no change in the value of contact angle was observed, which negated any role of straining on the hydrophobicity of the substrates.

2.5 *in vitro* neuronal differentiation of ES cells

The differentiation of neural cell lineages from ES cells is attractive since it provides a continuous supply of specific neural cells for potential cell therapy and also because it allows the study of early neural development. The spontaneous differentiation of ES cells can be achieved by expanding the ES cell culture at high density, which leads to overgrowth of surviving ES cells and subsequent spontaneous differentiation [189-191]. Hence, the differentiation process is generally less controlled and the cultures obtained are heterogeneous, with modest efficiency of neural differentiation. This neural progenitor population can be further enriched under a neural cell culture condition containing appropriate signals.

Highly enriched ES cell derived neural progenitors (ES-NP) can be attained through various protocols [112, 189, 192]. One such widely used protocol employs stromal cell derived inducing activity (SDIA) by co-culturing ES cells on bone marrow derived stromal cells [193-195]. The direct contact of ES cells with stromal cells has been interpreted in favor an inductive mechanism for neural differentiation although the exact molecular nature of the inducing signal remains elusive. The co-culture of ES cells with these cells for 4 weeks result in greater than 90% of ES cells differentiating towards a neural precursor phenotype which expresses markers of neuroectoderm such as Pax6, nestin and Musashi[194-195].

Alternative strategy for neural differentiation from ES cells involves a step in which ES cells form free-floating aggregates, referred to as embryoid bodies (EB) [192]. This step removes self-renewing signals and initiates cellular differentiation through cell-cell interactions. EB formation takes place after ES cell colonies are detached via enzymatic treatment or by mechanical scraping from the feeder cell and subsequent culture in suspension [196]. ES cells within these aggregates differentiate spontaneously into heterogeneous cell types of all the

three embryonic germ layers. Hence, addition of signaling molecules is necessary at certain stages to bias the differentiation process towards the neural lineage. Retinoic acid(RA), a morphogen, for multilineage differentiation, is one of the most commonly used chemicals for promoting neural differentiation. Treatment of differentiating cultures with RA yields reasonable neural differentiation from ES cells [197]. Within the differentiated neural cells, there is a wide range of developmental stages, from nestin and polysialylated neural cell adhesion molecule (PSA-NCAM)-expressing precursors to β-III tubulin positive neurons within a week of differentiation [192, 197-198].

2.5.1 Embryonic stem cell culture

Mouse D3 ES cells (ES-D3; ATCC#CRL-11632) were grown on Mitomycin-C treated primary mouse embryonic fibroblast (MEF) feeder layer on 0.1% gelatin substrate in embryonic stem cell growth medium [ESGM - consisting of DMEM, 10% defined FBS, 10% NCS, 2mM L-Glutamine, 1X Nucleoside, 0.1mM β-mercaptoethanol and 1000U/ml LIF]. Briefly, culture flasks were incubated with 0.1% gelatin solution for 30 minutes at room temperature and washed with 1X PBS. Frozen vials containing ES cells were thawed rapidly in 37^0C water bath and washed twice with 1X PBS. Finally, cells were re-suspended in ESGM and incubated at 37^0C in 5% CO_2 incubator for 1-2 days. ES cells grown on MEF feeder layer were used for making stocks while for regular experiments, feeder free ES culture protocol was used [192]. Proliferating ES cells appeared as spherical colonies with intact boundary and individual cells were seen separately. ES cells generally do not grow well in low numbers hence appropriate number of cells should be cultured in culture dishes and should not be splitted more than 1:10 ratio.

2.5.1.1 Preparation of MEF feeder layer

ES cells are usually grown on a layer of mitotically inactivated primary mouse embryonic fibroblasts (MEF) to promote growth and prevent differentiation. Since these cells stop dividing after a couple of passages, embryonic fibroblasts need to be isolated freshly, each time from E13 embryos. For MEF isolation, pregnant mouse was sacrificed by cervical dislocation and E13.5 embryos were transferred into 1X PBS in a Petri-dish. Embryos were washed in 1X PBS and their head, heart, viscera and liver were removed. Decapitated embryos were transferred to 0.25% Trypsin/EDTA solution and minced finely with curved scissors. The minced tissue was incubated at 37^0C for 10-15 minutes and the trypsin was inactivated by adding 100-200 µl FBS. Subsequently, it was transferred to a conical tube and allowed to settle down and the supernatant was removed and washed with DMEM. The tube was centrifuged for 10 minutes at 1000 rpm and the pellet was re-suspended in the MEF medium. Cells were allowed to grow for 24-48 hours and were subsequently frozen. For Mitomycin-C treatment, confluent primary MEF cells were plated on gelatin coated culture flask and incubated at 37^0C overnight in MEF medium.10 µg/ml Mitomycin(dissolved in MEF medium) was added to recover the cells and incubated for 3 hours, the cells were then washed with MEF medium thrice after removing the Mitomycin containing medium completely. Finally, MEF medium was replaced with ESGM and the plate was incubated until ES cells were seeded.

2.5.1.2 ES cell passaging

~70-80% confluent ES cells were washed with 1X PBS and trypsinized using 1ml of 0.05% Trypsin-EDTA for 3-5 minutes at 37^0C. Trypsin was inactivated by adding 100µl of serum and the cells were washed twice with 2ml 1X PBS and pelleted down by centrifugation at 1800 rpm for 5 minutes. Pelleted cells were re-suspended in 4ml fresh ESGM and ~$1x10^6$ cells were plated on inactivated MEF/gelatin coated T-25 flask.

2.5.1.3 ES cell freezing

One confluent T-25 flask was trypsinized and washed in 1X PBS. After washing, ~2x10^6cells /vial were re-suspended in freezing medium (ESGM with 10% DMSO). The tubes were then transferred to cryo-baby and placed at -70^0C for overnight (for cooling the cells at the rate of 1^0C/min) and the cells were transferred to liquid nitrogen next day.

2.5.2Embryoid body (EB) generation and RA induction

Proliferating ES cells were trypsinized and plated on uncoated plates in EB medium (ESGM without LIF and β-mercaptoethanol) for four days followed by 0.5µM RAfor an additional 4 days to promote the neuronal induction in the EB.RA acts as a morphogen and induces neuronal lineage since activation of RA receptors in EB leads to the development of neuronal subtypes.

2.5.3 ES cell derived neural progenitors (ES-NP) generation

ES-NPs were generated from ES cells by modifying previously described protocol [199]. RA-induced EBs was partially differentiated on poly-D-Lysine (150µg/ml) and laminin (1µg/ml) substrates for two days in neuron differentiation medium (DMEM/F12 supplemented with 1% N2 supplement, 0.5% FBS, heparin (2µg/ml) and FGF2 (10ng/ml). Partially differentiated EBs were further trypsinized and plated on uncoated 6-well plates (~1.5x10^6 cells/well) in ES-NP proliferation medium consisting of DMEM/F12 supplemented with 1% N2 supplement, Heparin (2µg/ml) and combinations of FGF2 (20ng/ml) or EGF (10ng/ml).

2.5.4 Substrate preparation for cell culture

Polymeric substrates (conducting and non-conducting) were prepared as described earlier. In addition to these substrates, controls were used in the experiments which consisted of glass coverslips and PEDOT:PSS coated glass coverslips. All the substrates were first washed with ethanol and then irradiated with UV for 2 hours. These substrates were dried and incubated overnight with penstrep solution to prevent any contamination. Substrates were re-washed with 1x PBS next day and subsequently coated with poly-D-lysine (150µg/ml) for 4-6 hrs. The substrates were again washed with 1x PBS and coated with laminin (1µg/ml) which was diluted in DMEM/F12 medium for 1 hr at 37^{o}c. Substrates were washed twice with 1x PBS before seeding ES-NPs on them.

2.5.5 ES-NP differentiation on polymeric substrates

ES-NPs were differentiated onpoly-D-lysine (150µg/ml) and laminin (1µg/ml) coated polymeric substrates.The differentiation medium consisted of DMEM/F12 supplemented with 1% N2 supplement, FGF2 (10ng/ml) or EGF (10ng/ml), Heparin (2µg/ml) and 1.0% FBS. Heparin was added in medium in combination with FGF2 only. Differentiation procedure was carried out for 6-8 days post which cells were fixed for immunofluorescence analysis and processed with DAPI, β-III tubulin, GFAP or phalloidin.

2.5.6 Immunofluorescence analysis

Immunoflourescence analysis was carried out for detection of cell specific markers. Briefly, 4% paraformaldehyde-fixed cells were blocked in 5% NGS (Sigma-Aldrich) and permeabilized with 0.2–0.4% Triton-X 100 followed by an overnight incubation with primary antibodies at 4°C (β- III tubulin, 1:200, GFAP 1:400).For visualizing actin cytoskeleton, cells were incubated with FITC conjugated phalloidin(1:750).Cells were examined for fluorescence

following incubation with appropriate secondary antibody conjugated to FITC (1:400), cy3 (1:400) and DAPI (1:50000) in an upright fluorescent microscope (Olympus BX-61) and images were captured using a cooled CCD camera with a 20x objective. Confocal imaging was done using Nikon A1 and Zeiss LSM 510 Meta confocal microscope.

2.5.7 Quantitative analysis

Cell counting was done from the acquired immunostained images of neuronal and glial cells. Briefly, 7–8 fields of each polymeric substrate were imaged, and the number of β-III tubulin positiveand GFAP positive cells were obtained by manual counting of the merged images. Cells stained with nuclear stain DAPI were used for counting total number of cells. One-way ANOVA analysis was performed in all the statistical analysis and significance is depicted at $p < 0.5$.

Neurite length was measured by Simple Neurite Tracer plug-in of the Image J software [200-201]. The neurite length was measured from the point of attachment of the neurite to the cell body along its entire length till its end. The branched terminals of the neurites were considered individually and their length was measured as described. The area of the aggregates was measured by binarizing the DAPI images of the differentiated cells on the substrates by Image J software [201-202]. The aggregate was chosen with the help of Wand tool and the area was measured and saved with ROI manager.

All the experiments were performed in duplicates (n=2) and repeated three times (N=3) for performing the quantitative analysis thus negating the chances of sudden variations in the data. The immunostained images shown in subsequent chapters are the average representative of all the experiments performed on the particular substrate.

Chapter 3

Differentiation of Embryonic stem cells on polymeric substrates

3.1 Introduction

The field of tissue engineering and regenerative medicine encompasses the repair of damaged organs and tissues *in vivo* as well as generating tissue constructs for subsequent *in vitro* transplantation. The lack of available donor cell sources severely hampers the clinical applicability of this concept. Moreover, tissue rejections and use of immunosuppressive can have possible lethal effects on the patients. Stem cells provide an attractive alternative for cell therapy due to their pluripotent nature and self-renewal capacity.

ES cells in particular have garnered a lot of interest owing to their unique ability to differentiate into any of the three germ layers: ectoderm, mesoderm and endoderm[203]. Although ES cells are attractive because of their pluripotency, they are also difficult to work with because of the same characteristic. Maintaining large number of ES cells in an undifferentiated state and subsequently directing them to differentiate, in a reliable and reproducible manner, into specific cell lineages are the foremost challenges in ES cell-based cell therapy[204]. If ES cells remain undifferentiated after implantation in the body, they will spontaneously differentiate into multiple cell types and form a type of tumor called teratoma[205-206]. So, it is utmost important to drive them towards a particular cell lineage prior to implantation but a critical balance needs to be maintained between undifferentiated and differentiated populations, so that we have a large pool of undifferentiated cells available whenever required and they are differentiated into specific cell type prior to implantation. Hence, the most fruitful strategy for cellular

therapeutics is to create reserves of undifferentiated stem cells and subsequently driving their differentiation to a lineage of choice in an efficient and scalable manner [207].

Directing the differentiation of ES cells into specific lineages would require precise control over the developmental pathways followed by the undifferentiated cells during their transit to differentiated cells [208]. The extracellular microenvironment surrounding the ES cells *in vivo* presents a number of spatially and temporally instructive biochemical and physical cues within a complex and interactive milieu that guide and govern the sequential development and cell fate decisions. Scaffold based tissue engineering provides a viable alternative to mimic the intricate stem cell niche. Biomaterials serve as biointeractive stages for promoting cell attachment, proliferation and organization in addition to acting as delivery vehicles for bioactive molecules during various developmental stages. The fate specific decision and directed differentiation into specific lineage is controlled primarily by growth factors and other soluble signals and the extracellular niche provided by the scaffold also plays an influential role [209-211].

The versatility of such a concept was demonstrated by the induction of human ESCs differentiation into distinct embryonic tissue types within a biodegradable 3D polymer scaffold made from a 50:50 blend of PLGA and PLLA. The type of tissue produced depended on the differentiation growth factor that was supplemented. RA and transforming growth factorβ(TGF-β) induced ES cell differentiation into 3D structures with characteristics of developing neural tissues and cartilage, respectively, whereas activin-A or insulin-like growth factor induced liver-like tissues.

The effect of conducting polymer environment on stem cell differentiation is a relatively untapped area and they offer unique surfaces to modulate the cellular differentiation to a desired lineage. The strict control on the properties of these conducting polymers by simple physical methods provides a very attractive and feasible approach for tuning the cell properties. Neurite length of the regenerating neurons was found to increase when their culture was electrically stimulated on the conducting polymers.

In this chapter, we discuss the differentiation of embryonic stem cell derived neural progenitors (ES-NPs) into neurons and glial cells on conducting polymer as well as non-conducting

elastomeric substrates and investigate the potential guidance cues provided by them which may be assimilated in the developmental program of these stem cells.

3.2 Proliferation and differentiation of green fluorescent protein (GFP) tagged ES cells

Mouse ES cells are commonly cultured on glass coverslips coated with poly-D-lysine and laminin.ES cells differentiate uniformly into neuronal cells on these glass coverslips in presence of a differentiation medium. In this study, the primary requirement was to differentiate the neuronal progenitors derived from ES cells into neurons on the conducting polymer scaffolds consisting of PEDOT:PSS coated on SEBS substrates. Biological compatibility of conducting polymer PEDOT:PSS has been demonstrated in various studies and it is widely used as a viable substrate for primary culture of mouse brain and hippocampus. In many studies, PSS was replaced with biological materials like poly-D-lysine or nerve growth factor which promoted the neuronal differentiation on the tailored substrates [2, 212]. Conducting property of these polymers has been exploited to suit the differentiation and proliferation of neurons which bear longer neurites extending along the desired direction. The combination of electrical property of the conducting polymers with the mechanical property of elastomers can provide ideal scaffolds for tissue engineering and neuroprosthetics. In this study, SEBS, a linear triblock co-polymer of Styrene, ethylene and butylene is used as a flexible and stretchable elastomer over which conducting polymer PEDOT:PSS is coated. One of the monomeric units of this triblock polymer is styrene and its homopolymer polystyrene is regularly used for tissue culture. The attachment of cells to the polystyrene dishes takes place even in the absence of the serum which shows its biocompatibility and ability to mediate cell adhesion.

The viability of these substrates for stem cell differentiation was confirmed by seeding with GFP transfected ES-NPs. GFP is widely used in molecular biology as a biosensor or as a reporter for expression of a certain gene. The protein was first isolated from jellyfish *Aequorea victoria* **[213]**.ES cells were transfected with the pce-3 plasmid and GFP was expressed constitutively under CAG promoter [214]. The cells which were transfected with the plasmid and

expressed GFP were selected by pluromycin resistance and cloned subsequently to form a stable GFP tagged ES cell line. This cell line allowed us to follow the proliferation and differentiation of ES cells on both conducting and insulating substrates for a period of eight days. Post differentiation, cells were fixed as described in chapter 2 and immunostained with DAPI which specifically marked the nuclei of cell.

Florescence microscopy analysis of the cells in fig. 3.1 revealed the adhesion of ES-NPs on the tested substrates followed by their differentiation into a heterogeneous population of cells. Neuronal cells, differentiated from ES-NPs, were pointed out by their morphology since immunocytochemical staining with specific neuronal marker was not performed. It was clearly observed that they extendedneuritesand formed inter-connections with other permeated neurons. This demonstrated the viability of all the substrates for cell attachment, spreading and neuronal differentiation.

The physical guidance provided by the conducting microenvironment of the CP-substrates was studied by observing the variations in the ES-NP differentiation and neuronal spreading. The guidance cues provided by the application of strain on both conducting as well as non-conducting substrates during neuronal differentiation were also examined.

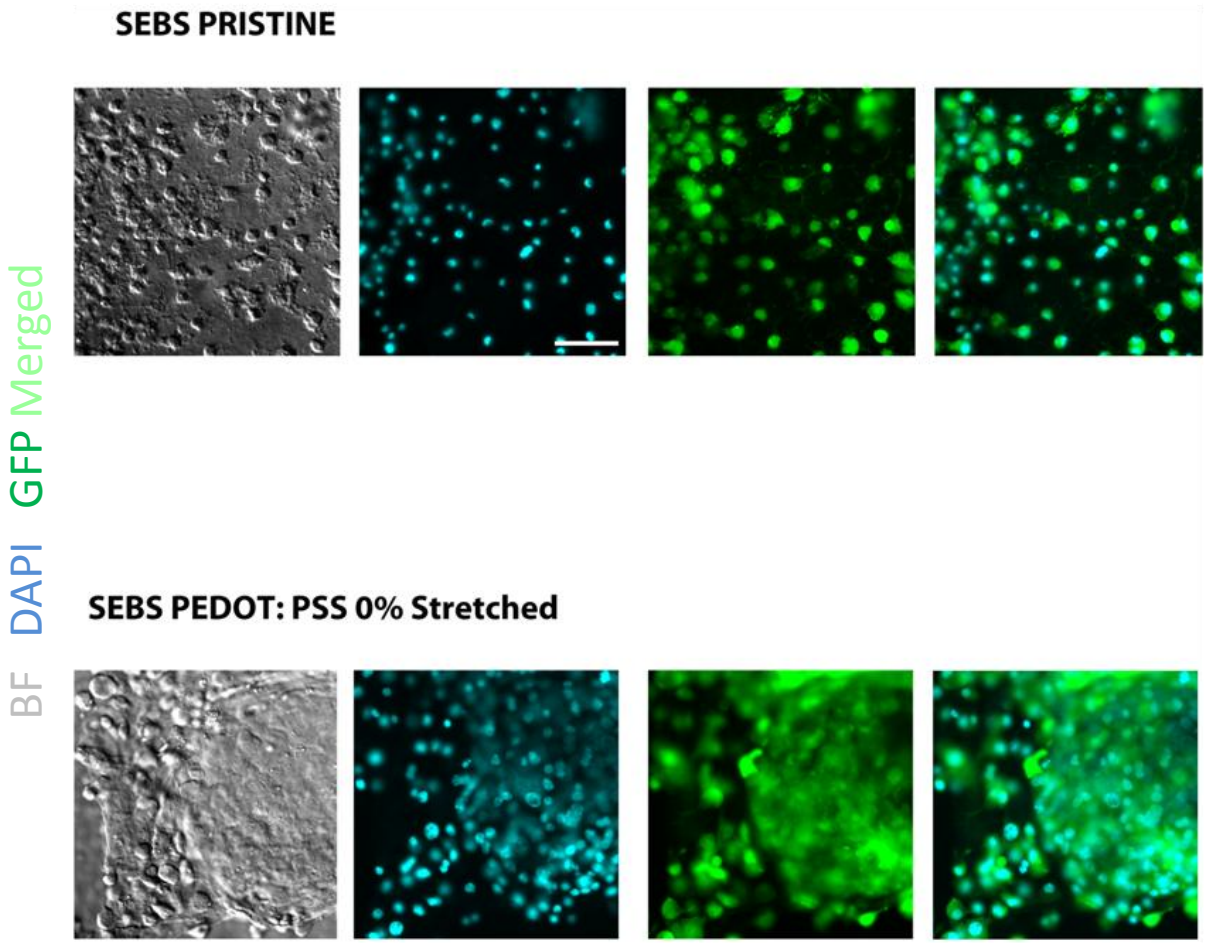

Fig. 3.1-Differentiation and Proliferation of GFP tagged ES-NP cells. ES cells were transfected with pce-3 plasmid and GFP was constitutively expressed under CAG promoter. Heterogeneous population of cells differentiated from ES-NPs express GFP. Scale 50 µm.

3.3 Cell spreading on polymer substrates post differentiation

Prior to the analysis of immunostained images of neurons, cell spreading was assessed to study the change in the distribution of cells on the polymeric substrates. DAPI staining was done after 8 days of cell culture on the substrates as described previously in chapter 2 and the images were used for the surface area analysis. DAPI images clearly illustrated the distribution of all possible cell types present on the substrates and hence they were used for the cell spreading analysis. Images were taken through a 4x objective to give a wider field of view (2 mm × 2 mm) of the cell attachment and spreading on the substrates. The surface area of the aggregates formed by cell clustering was measured as described previously in literature [201-202]. The DAPI images were first binarized using Image J software available from NIH [202]. The aggregates were then selected using the wand tool and their surface area was measured and stored in the ROI manager.

Figs. 3.2 and 3.3 depict the DAPI images of cells on CP-coated SEBS substrates and non-conducting pristine SEBS substrates. The following inferences about the cell spreading were drawn from the images:-

1. The cells were uniformly distributed on the surface of glass coverslips and pristine SEBS substrates while they tend to aggregate on CP-coated substrates.
2. The aggregates formed on the unstrained CP substrates were comparatively larger in size than those on glass coverslips or pristine SEBS substrates.
3. The tendency of cells to aggregate increased with the increase in the applied strain regime on the conducting substrates. Therefore, larger cell aggregates were observed on 30% strained CP substrates in comparison to 10% strained conducting substrates. Majority of cells were present within these aggregates and an uneven distribution of cells was observed on 30% strained CP substrates.
4. The observations on the strained non-conducting SEBS substrates were starkly opposite to the strained CP substrates. The cells permeated uniformly on the surface and the aggregate area also decreased with an increase in the applied strain regime on these substrates.

Interestingly, the application of increasing strain regime had opposing influence on the cell spreading on polymeric substrates. The number of aggregates on the surface of pristine SEBS substrates increased, accompanied by a decrease in their average surface area,which resulted in a fewer number of cells within these aggregates. Meanwhile, the number of aggregates on strained CP substrates decreased with a similar increase in the applied strain regime but they exhibited an increase in surface area and consisted of more number of cells within them.

Fig. 3.4 shows the quantification of the surface area of the cellular aggregates present on the conducting as well as non-conducting substrates. On unstrained CP substrates, the cellular aggregates of approximately 10^4 μm^2 surfacearea were present while on highly strained (30%) CP substrates, aggregate size increased to approximately $10^5 \mu m^2$. The elevated strain levels remarkably produced uniform spreading of cells on the surface of non-conducting SEBS substrates which was accompanied by the presence of smaller aggregate sizes. The surface of the unstrained pristine SEBS substrates bore cellular aggregates which had an average surface area of approximately 10^4 μm^2. In comparison, the average surface area of the cellular aggregates on 30% strained pristine SEBS substrates was approximately 10^3 μm^2.

These observations show an elevated tendency of cell spreading on unstrained CP substrates while application of strain resulted in their aggregation. In contrast, straining the non-conducting SEBS substrates assisted in cell spreadingand resulted in a decrease in the number of cells within these aggregates.

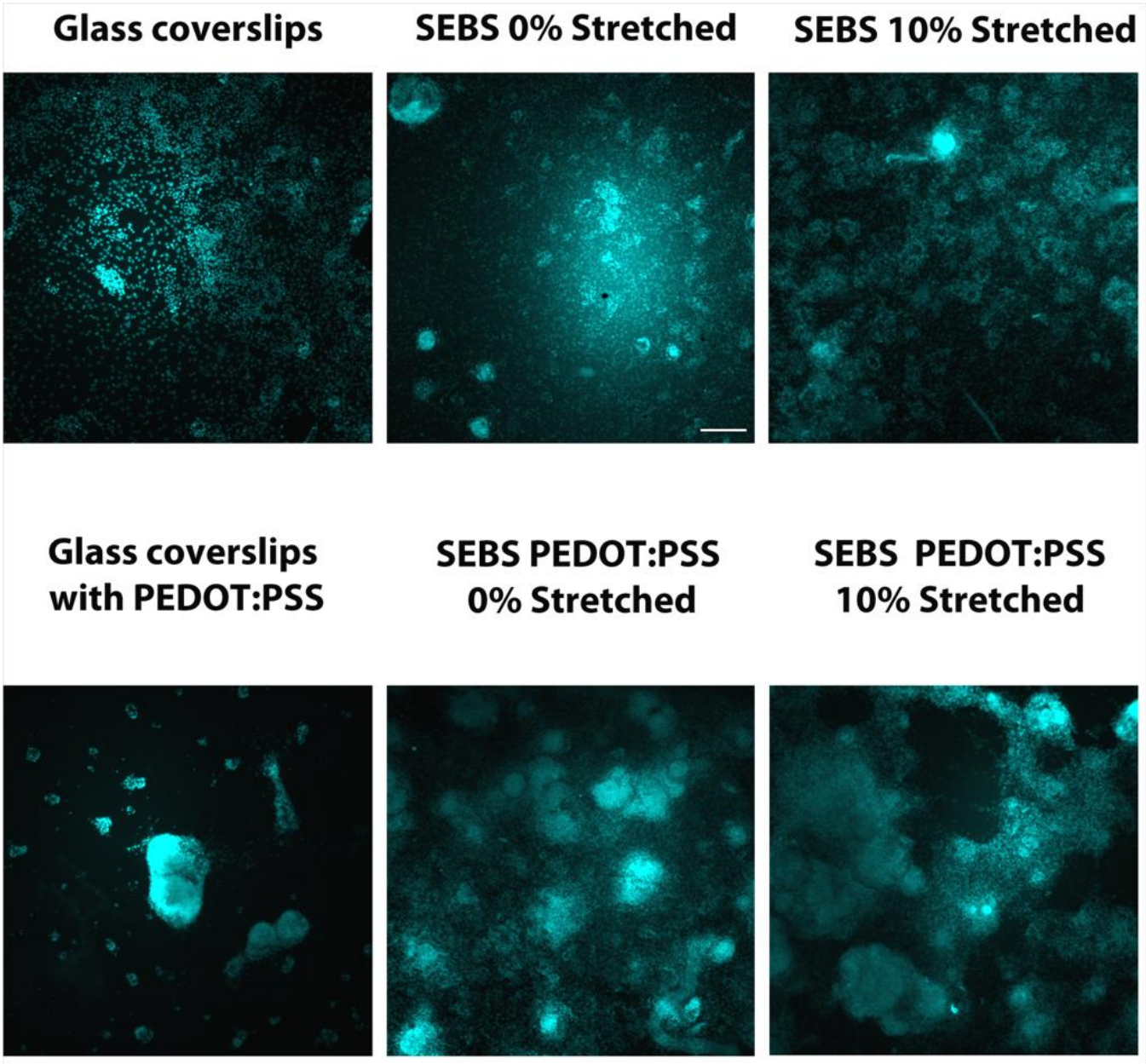

Fig. 3.2- DAPI images of cells on polymeric substrates showing the distribution of cells on the surface. Uniform distribution of cells is seen on most of the substrates with more aggregates present on CP substrates. Scale bar 100µm.

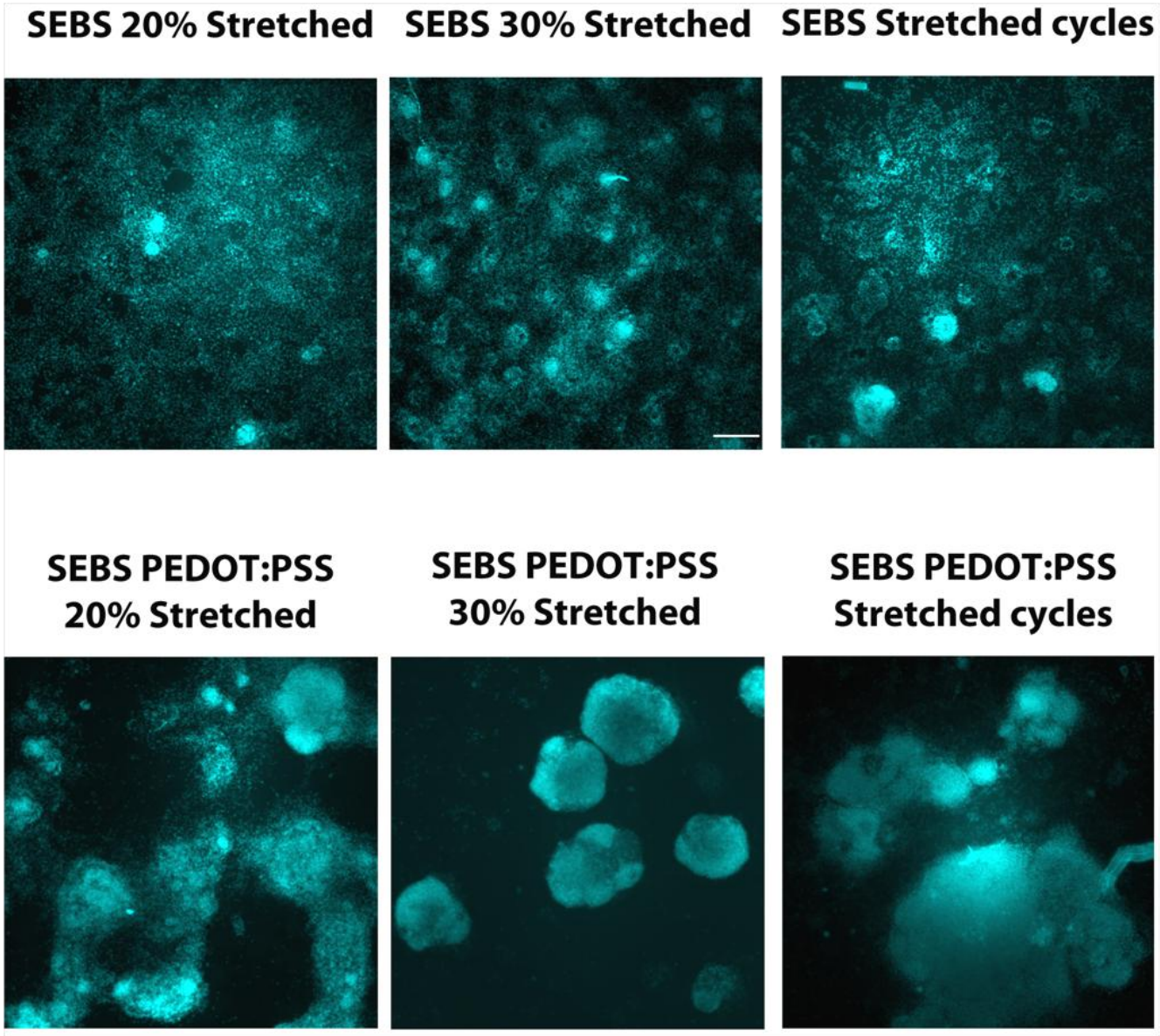

Fig. 3.3- DAPI images of cells on polymeric substrates showing the distribution of cells on the surface. Increase in tendency of aggregation of cells is seen on strained CP-substrates increase which results in the formation of larger cellular aggregates. Scale bar 100µm.

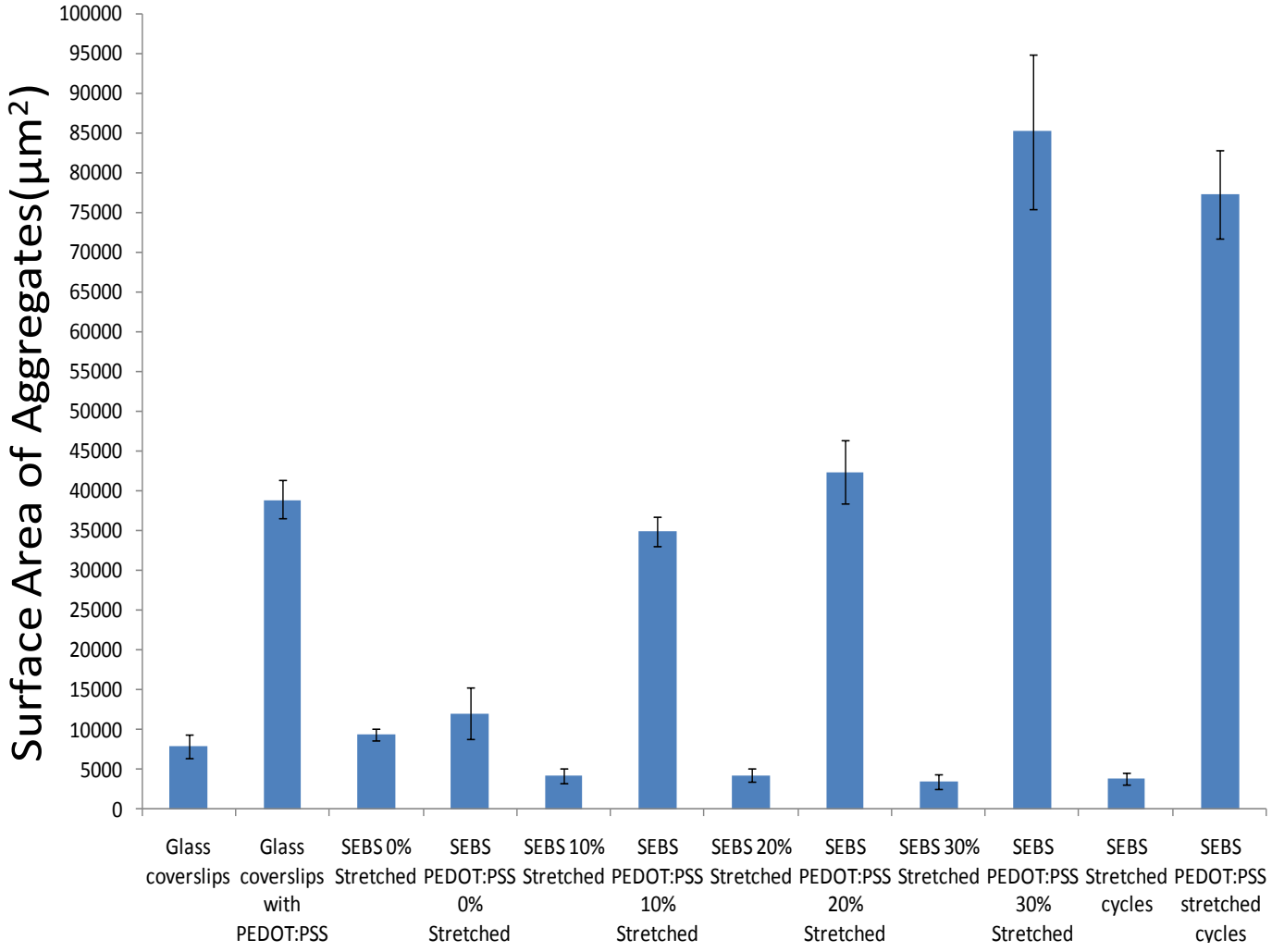

Fig. 3.4- Surface area of the aggregates formed on the polymeric substrates. An increased tendency of cells to remain within aggregates is seen on strained CP substrates with a significant increase in surface area. Data is represented as mean± SD, (n=3).

3.4 ES-NP differentiation on glass coverslips and PEDOT: PSS coated glass coverslips

Glass coverslips and their conducting counterparts, PEDOT: PSS coated glass coverslips, were used as controls over which ES-NPs were differentiated. It should be noted that the biochemical medium for the differentiation of ES-NP on all the substrates was kept uniform. The substrates were pretreated with poly-D-lysine and laminin as described in the preparation of substrates in chapter 2. Poly-D-lysine provides a positively charged surface for the attachment of cells while laminin is one of the key ECM proteins which favors neuronal differentiation on these substrates.

Cells were fixed for immunocytochemical staining analysis, post ESNP differentiation period of 8 days. Immunostaining was performed by-

1. β-III tubulin which specifically binds the immature neurons differentiated from ES-NPs. The secondary antibody used in this case is FITC (green).
2. DAPI to stain the nuclei of cells.

Cells were observed under upright fluorescent microscope (Olympus BX-61) and images were captured using a cooled CCD camera.The co-localized image of DAPI and β-III tubulin pointed out the neurons differentiated from ES-NPs.

Fig. 3.5 depicts the neuronal differentiation on glass coverslips and CP-coated glass coverslips. The following inferences about neuronal differentiation were drawn from these images:-

1. The neuronal differentiation and spreadingwas promoted on glass coverslips. Neurons exhibited longerneuriteswhich formed inter-connections with other neurons.
2. The number of differentiated neuronal cells was markedly low on PEDOT:PSS coated glass coverslips. Neuronal spreading was significantly diminished and neurite length was also less on these substrates in comparison to the uncoated glass coverslips. Increased tendency of cell aggregation was also observed on these substrates.

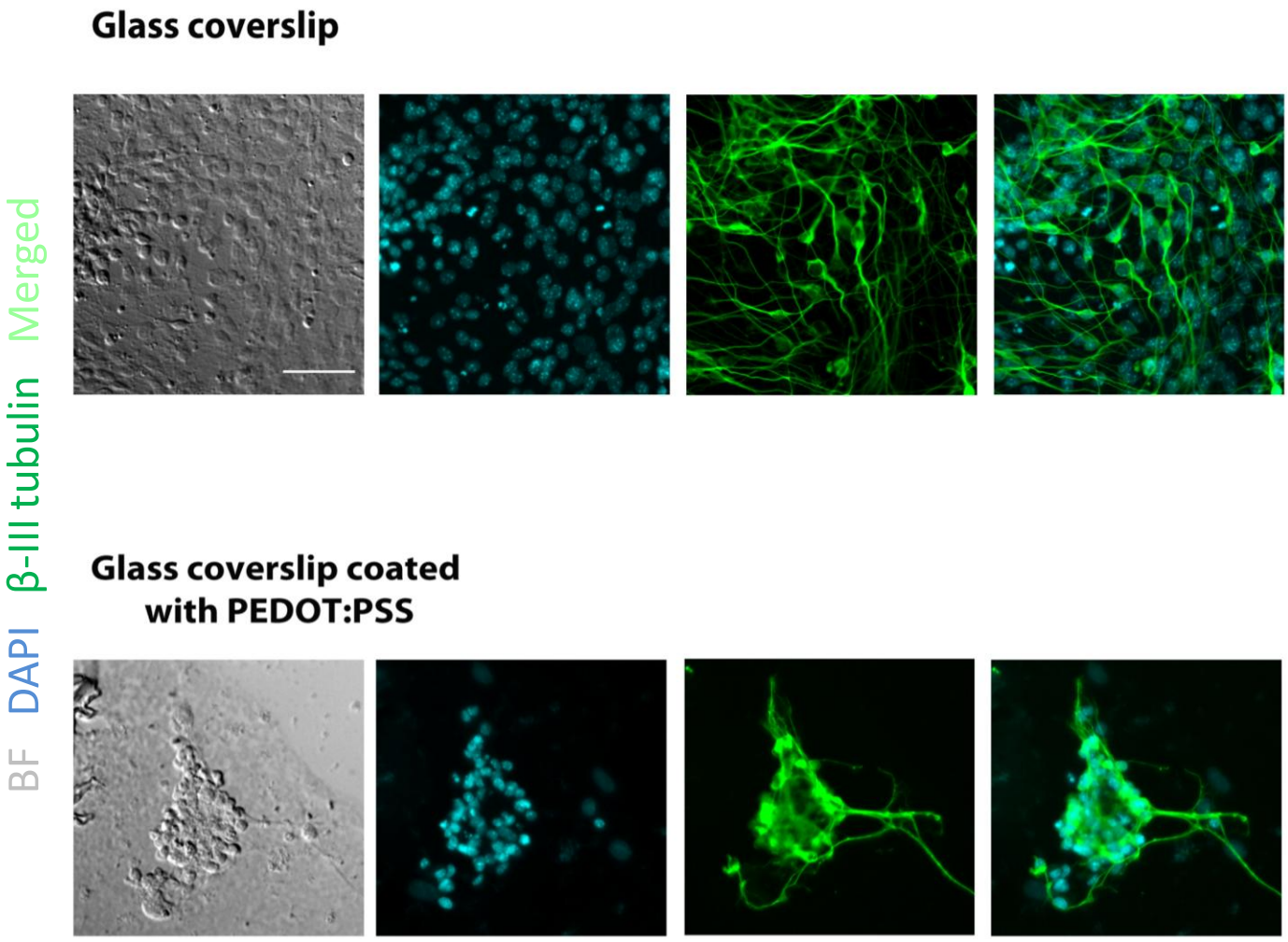

Fig. 3.5- Differentiation of ES-NPs on glass coverslips and PEDOT:PSS coated glass coverslips. The difference in the pattern of cell spreading is quite evident with longer neurites and better cell spreading on non-conducting glass coverslips in comparison to the PEDOT:PSS coated ones. Scale bar 50µm.

These observations clearly indicated the contribution of the physical cues provided by the conducting polymer component on neuronal differentiation and spreading. This role was further investigated by differentiating the ES-NPs on the PEDOT:PSS coated SEBS substrates and non-conducting pristine SEBS substrates.

3.4.1 ES-NP differentiation on CP-coated and pristine SEBS substrates

ES-NPs were differentiated on CP-coated SEBS substrates and pristine elastomeric substrates as described previously. DAPI and β-III tubulin images were merged and used for counting the β-III tubulin^{+} cells (neurons) and DAPI^{+} (total number of cells) for quantitative analysis of neuronal differentiation. Fig. 3.6 shows the immunostained images of differentiated neurons from ES-NPs. Differentiation of ES-NPs on unstrained pristine SEBS are shown in the top panel while the lower panel indicates the neuronal differentiation on CP-coated SEBS (unstrained).

The observation of neuronal differentiation and neurite length on these substrates revealed following inferences:-

1. Significant number of neurons differentiated from ES-NPs on pristine SEBS substrates and majority ofthese neurons permeated uniformly on the substrates and exhibited longer neurites. These neurites formed inter-connected networks with the neurites of other neurons.
2. Majority of neurons segregated out from the aggregates post differentiation on pristine SEBS substrates.
3. The number of differentiated neuronal cells was comparatively reduced on these conducting substrates. Post differentiation, diminished neuronal spreading wasobserved on CP-coated SEBS substrates.
4. The tendency of differentiated neuronal cells to aggregateincreased on CP substrates in comparison to pristine SEBS substrates. The neurite length, which is closely associated with the spreading of neurons on the surface, also reduced on the CP substrates.

These images clearly indicated that CP substrates provided guidance cues during the differentiation of ES-NPs which prevented their spreading, post differentiation, and assisted in their aggregation, a trait which was also evident on CP-coated glass coverslips. Neuronal aggregation also resulted in the decrease in neurite length of the developing neurons. ES-NP differentiation on these substrates was significantly different from that observed on the pristine SEBS substrates or glass coverslips. Neuronal differentiation on pristine SEBS substrates occurred in a similar manner as on glass coverslips where neurons spread out well on the surface and significant neuronal population was present. Hence, a potential role of conducting polymer PEDOT:PSS on embryonic stem cell differentiation was seen which promoted the aggregation of differentiated neurons on the surface.

Application of strain had a significant role in manipulating the cell spreading on the substrates as was observed in the previous section. Similar role of strained CP substrates on neuronal differentiation was studied by differentiating the ES-NP on pre-strained substrates under varying strain regimes. These studies have suggested a role of conducting microenvironment provided by the CP substrates on ES-NP differentiation. The changes in the surface of the CP-substrates due to strain hardening and alignment of PEDOT domains upon the application of strain were described in the previous chapter. These investigations will reveal any possible role of these physical changes in the substrates on the differentiation of stem cells.

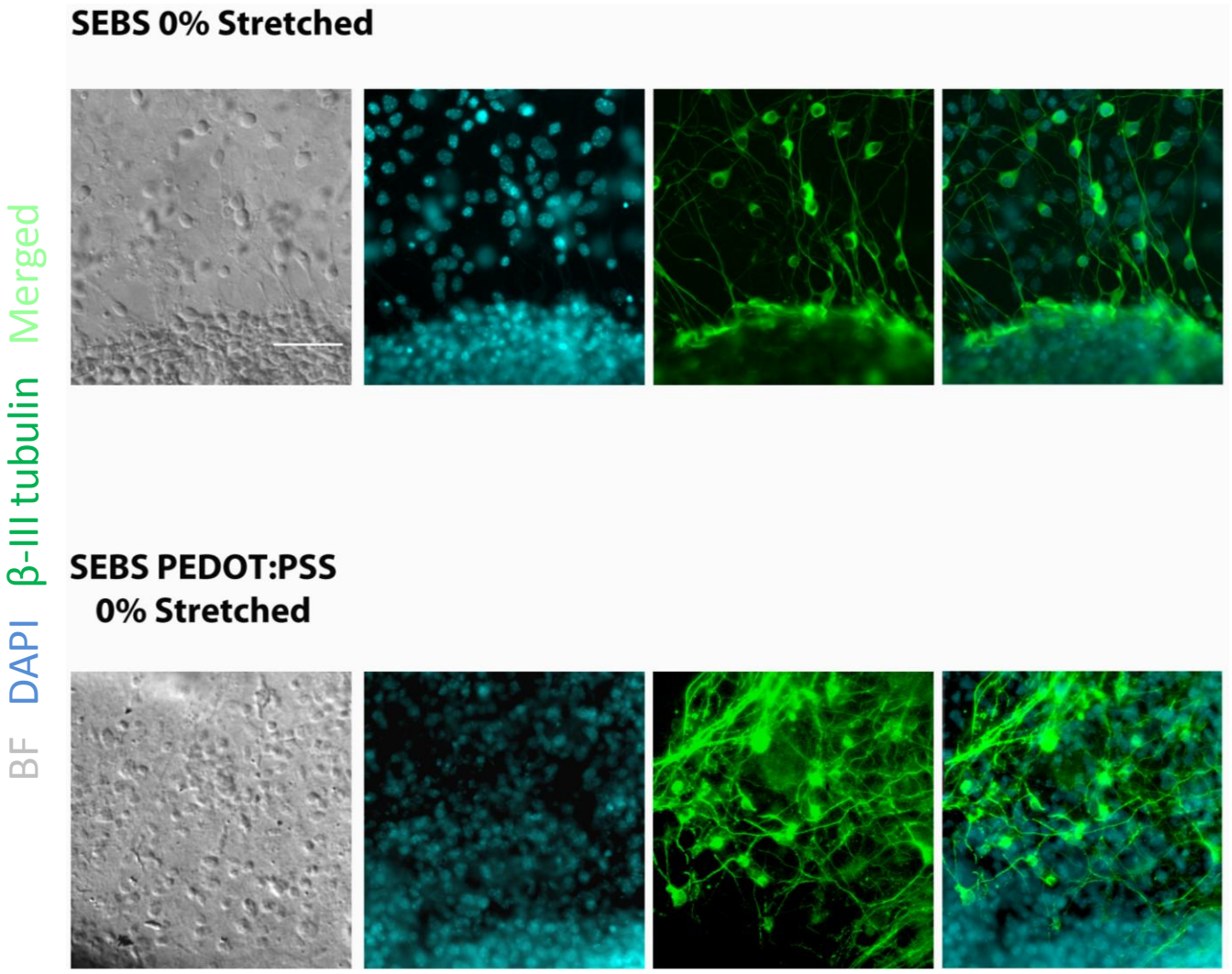

Fig. 3.6- Differentiation of ES-NPs on conducting CP-coated SEBS and non-conducting pristine SEBS substrates. The difference in neuronal differentiation is clearly evident on both the substrates with neurons present within the aggregates on conducting substrates while an even distribution is observed on pristine SEBS substrates. Scale bar 50µm.

3.4.2 ES-NP differentiation on strained substrates (CP-coated and pristine SEBS substrates)

ES-NPs were differentiated on strained polymeric substrates as described previously. β-III tubulin^{+} and DAPI^{+} cells were counted from their respective images to analyze the neuronal differentiation and perform quantitative analysis. Neurite lengths were analyzed to see the effect of straining on these cell parameters.

Fig. 3.7 shows the immunostained image of neurons on 10% strained CP-coated SEBS and pristine SEBS substrates. The aggregation tendency of cells further accentuated and neuronal spreading reduced considerably on CP coated strained polymeric substrates. Increased cell aggregation resulted in a decrease in the neurite length of the neurons accompanied by a decrease in neuronal differentiation potential of ES-NPs. Fig. 3.8 depicts further corroboration of this trend in the images of neuronal differentiation on 20% strained CP-coated substrates. Neuronal population decreased further on these substrates which were accompanied by a decrease in the neurite length. These substrates promoted neuronal aggregation which resulted in an increase in the aggregate surface area and hence more number of cells was present in these aggregates. The neurons, within an aggregate, formed inter-linking networks with the other neurons confined in the neighboring aggregates.

Fig. 3.9 depicts the neuronal differentiation on 30% strained CP-coated substrates. The number of differentiated neuronal cells markedly reduced on these substrates. Cell spreading was also reduced significantly with a majority of differentiated neurons present within the aggregates. This resulted in an abrupt decrease in the neurite length while the surface area of the aggregates increased considerably. Fig. 3.10 depicts the change in the neuronal differentiation on CP-coated stretched cycles substrates in which the substrates were subjected to 5 cycles of 30% strain, as described in chapter 2, and left with a residual strain. Cell spreading increased on these substrates while neuronal differentiation and neurite length also increased in comparison to the 30% strained CP-coated substrates. This could be attributed to the relaxation of strain applied on the polymeric substrates.

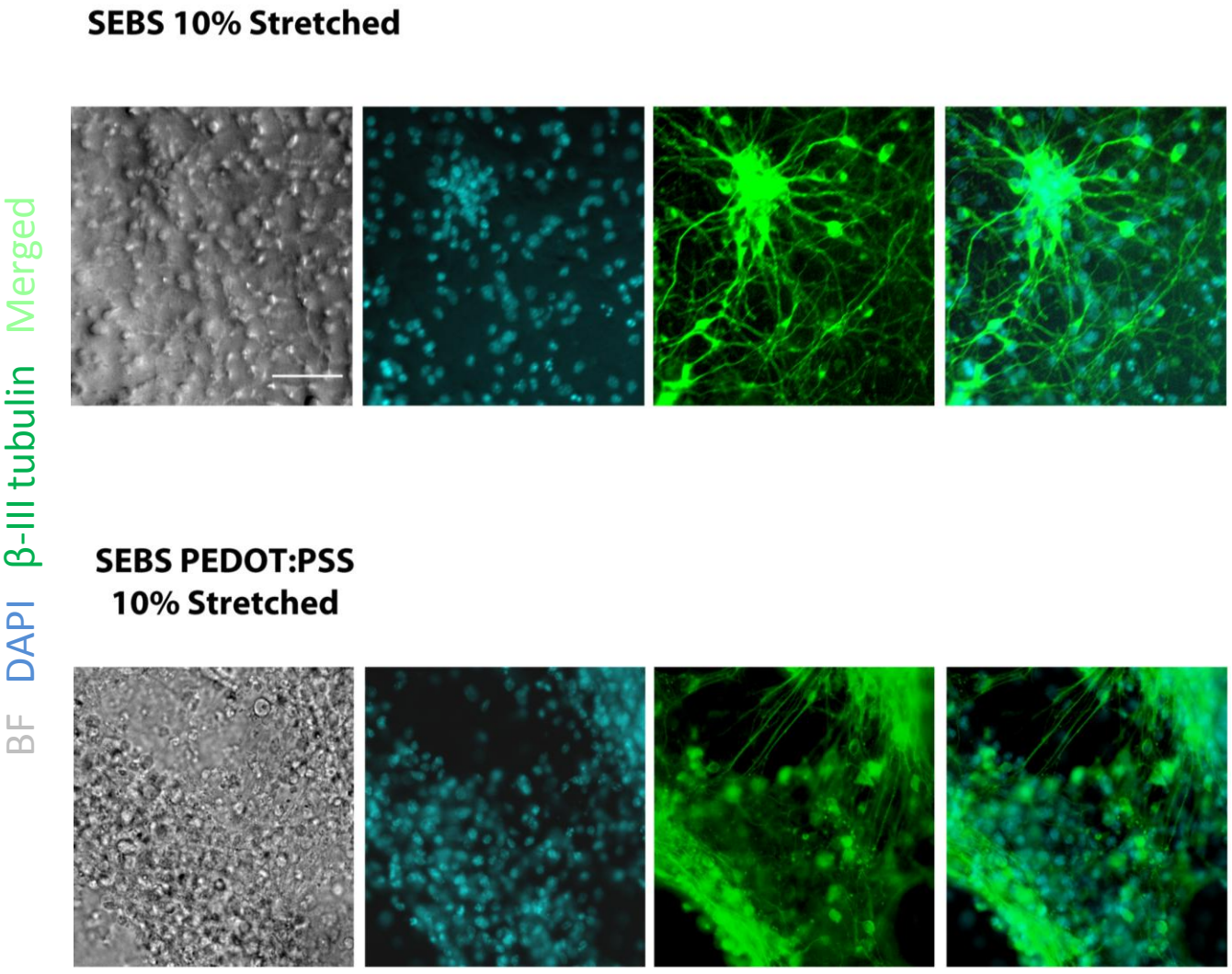

Fig. 3.7- Differentiation of ES-NPs on strained (10%) CP coated SEBS and non-conducting pristine SEBS substrates. Neuronal differentiation decreases on straining CP coated substrates and tendency to remain within the aggregates increases. Differentiated cells on strained SEBS substrates show similar behavior as unstrained substrates. Scale bar 50µm.

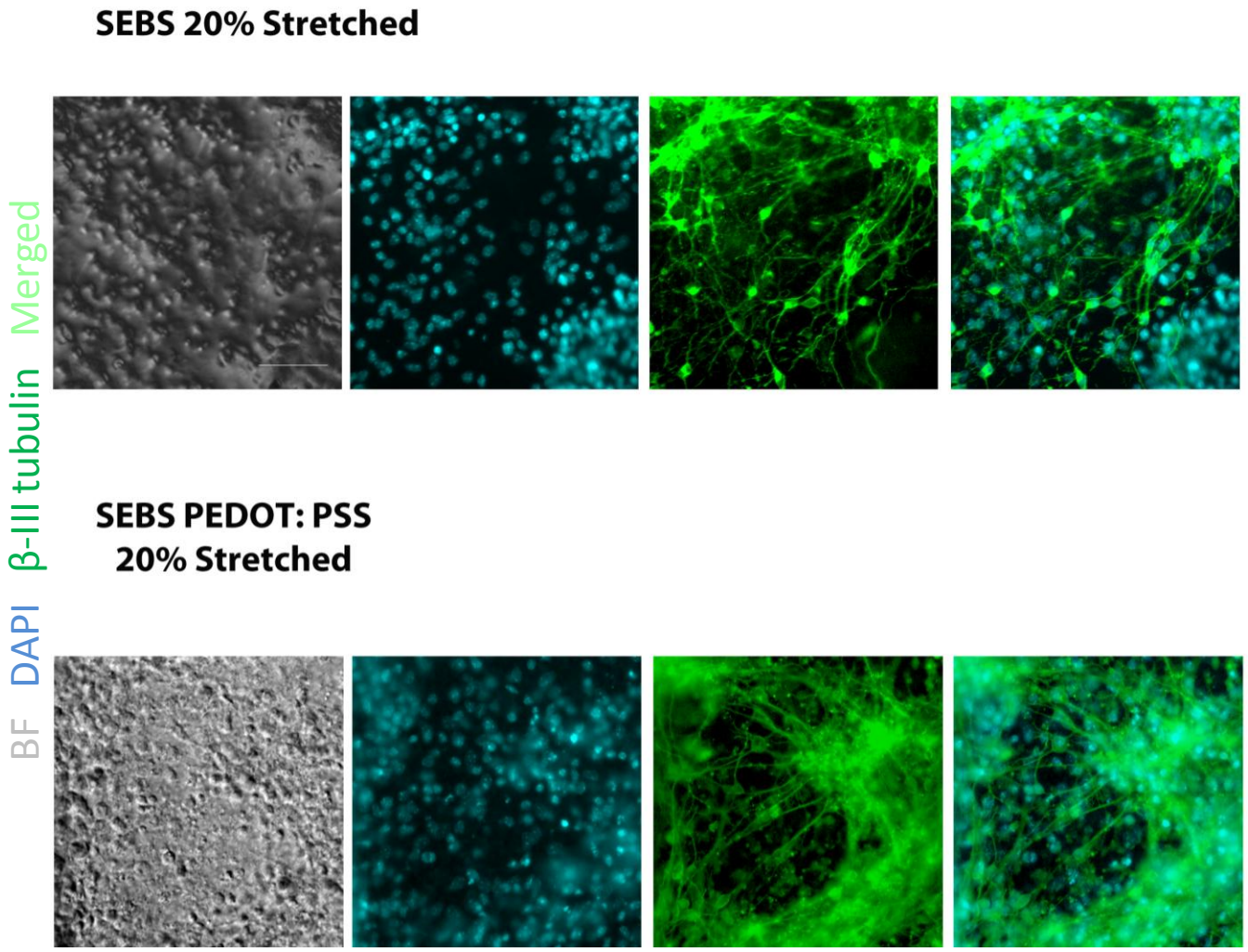

Fig. 3.8- Differentiation of ES-NPs on strained (20%) CP coated SEBS and non-conducting pristine SEBS substrates. Neuronal differentiation decreases further on straining CP coated substrates and tendency to remain within the aggregates markedly increases. Differentiated cells on strained SEBS substrates show more spreading and less tendency to remain within aggregates. Scale bar 50µm.

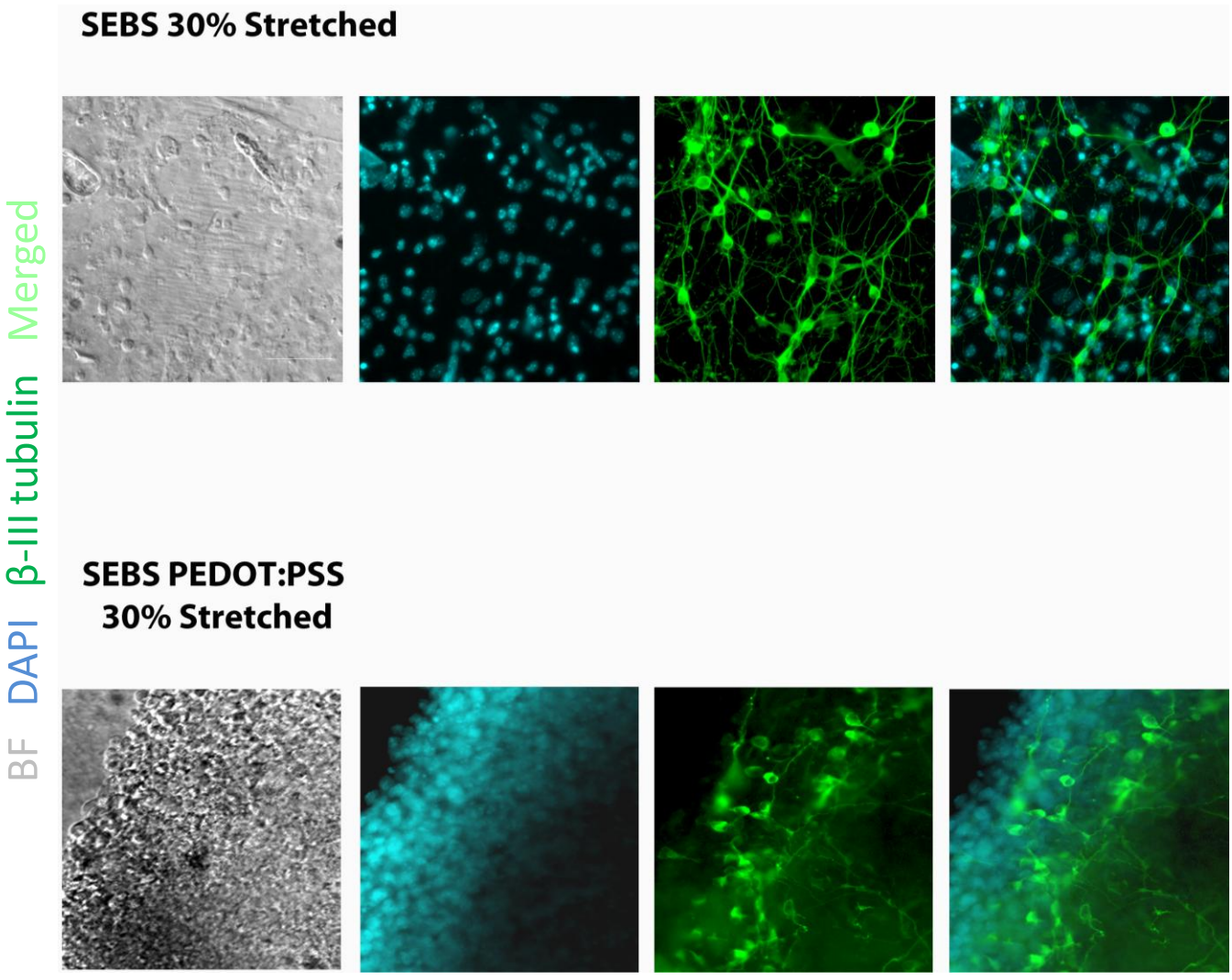

Fig. 3.9- Differentiation of ES-NPs on strained (30%) CP coated SEBS and non-conducting pristine SEBS substrates. Neuronal differentiation decreases further on straining CP coated substrates and tendency to remain within the aggregates increases significantly on these substrates. Differentiated cells on strained SEBS substrates show more spreading and tendency to remain within aggregates is further minimized. Scale bar 50µm.

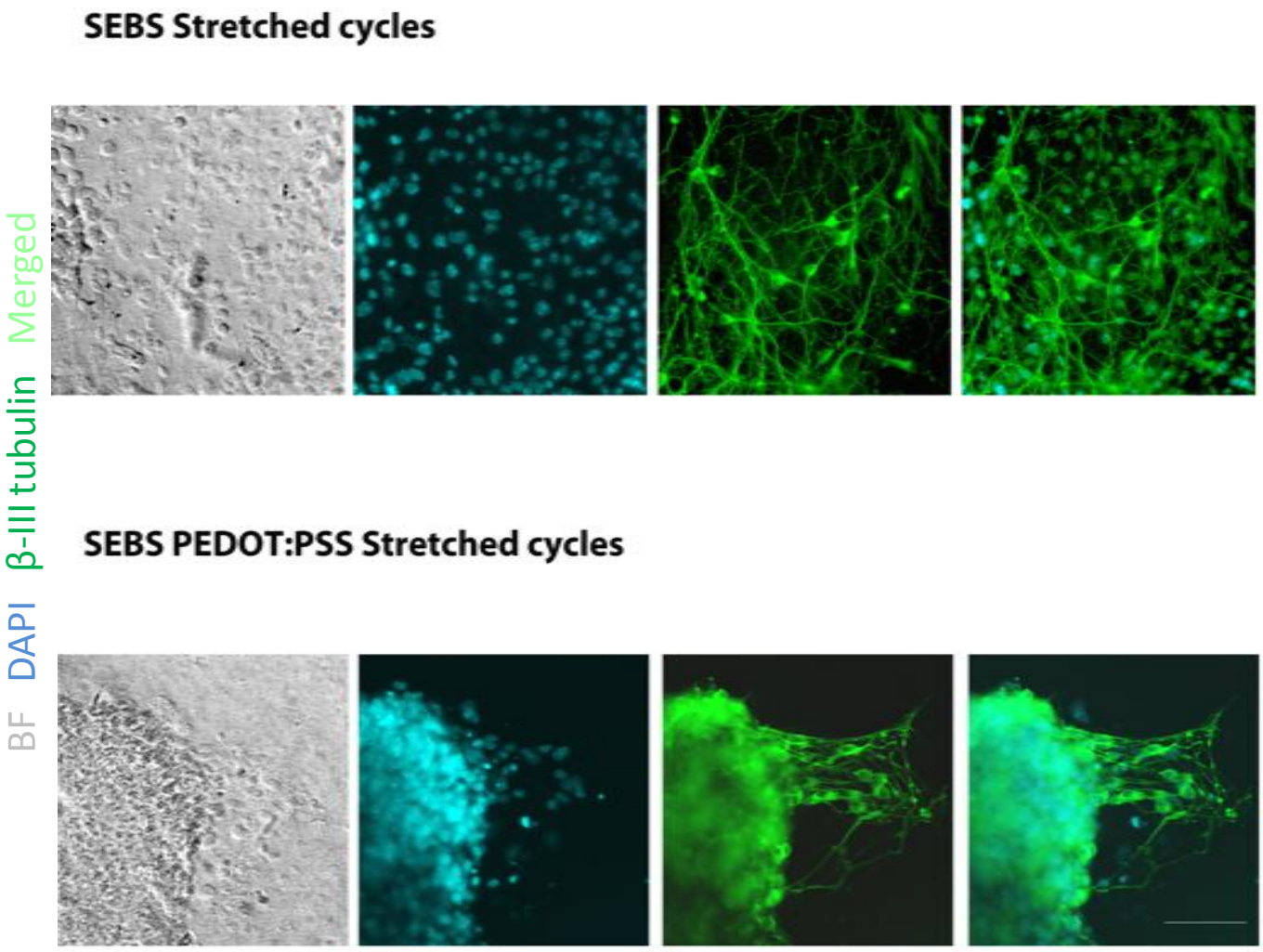

Fig. 3.10- Differentiation of ES-NPs on strained (cycles) CP coated SEBS and non-conducting pristine SEBS substrates. Neuronal differentiation and spreading improves compared to 30% strained CP substrates. Differentiated cells on strained SEBS substrates show similar spreading and possess good dendritic arbor. Scale bar 50µm.

A contrasting trend was observed in the neuronal differentiation of ES-NPs on strained non-conducting pristine SEBS substrates. Fig. 3.7 shows the immunostained image of the differentiation of ES-NPs on strained (10%) pristine SEBS substrates and a similar trend was observed as was seen on pristine SEBS substrates.Neuronal differentiation increased marginally on these substrates in comparison to CP substrates strained to similar regime. But, neurite length increased significantly on these substrates. The cell spreading increased considerably with a very few differentiated cells present within the aggregates. A decrease in the surface area of the aggregates was also seen which corroborated with the uniform distribution of cells on the polymer surface.

Figs. 3.8, 3.9 and 3.10 depict the neuronal differentiation of ES-NPs on highly strained (20%, 30% and cycles) pristine SEBS substrates. There was a significant increase in the number of differentiated neurons on these substrates. Neuronal spreading increased considerably with only a small proportion of neurons present within the aggregates. In comparison to the strained conducting counterparts of these substrates, neurons bore much longer neurites and a dense dendritic arbor was seen. The surface area of the aggregates decreased significantly with the increase in the application of strain and smaller cell aggregates were seen segregated throughout the surface of the 30% strained SEBS substrates.

Fig. 3.11 shows the quantitative analysis of the neuronal differentiation on the above polymeric substrates which corroborated the observations seen from the immunocytochemical stained images.Differentiation on unstrained (0%) PEDOT:PSS coated substrates resulted in $26.7 \pm 2.5\%$ neurons while on highly strained (30%) PEDOT:PSS coated substrates $11.8 \pm 1.7\%$ neurons were present ($p<0.5$). In comparison to the CP coated substrates, straining the pristine SEBS substrates (30%) lead to an increase in the differentiation with $36.2 \pm 1.2\%$ neurons in comparison to $30.3 \pm 2.0\%$ neurons on unstrained pristine SEBS substrates.

Fig. 3.12 shows the neurite length analysis which was done on all the substrates as described in chapter 2. Neurons bore longer neurites on pristine SEBS substrates in comparison to the CP-coated substrates. The average neurite length of neurons on unstrained (0%) PEDOT:PSS coated substrates was 115.5 ± 4.7 µm in comparison to 145.7 ± 3.1 µm long neurites on unstrained pristine SEBS-substrates. Application of strain on conducting substrates lead to a decrease in the average neurite length while the opposite trend was seen on strained pristine

SEBS substrates. On 30% strained CP substrates, neurons bore neurites of average length 41.7 $\pm$ 2.6 µm while average neurite length on 30% strained SEBS substratewas found to be 215.5 $\pm$5.6 µm ($p<0.5$).

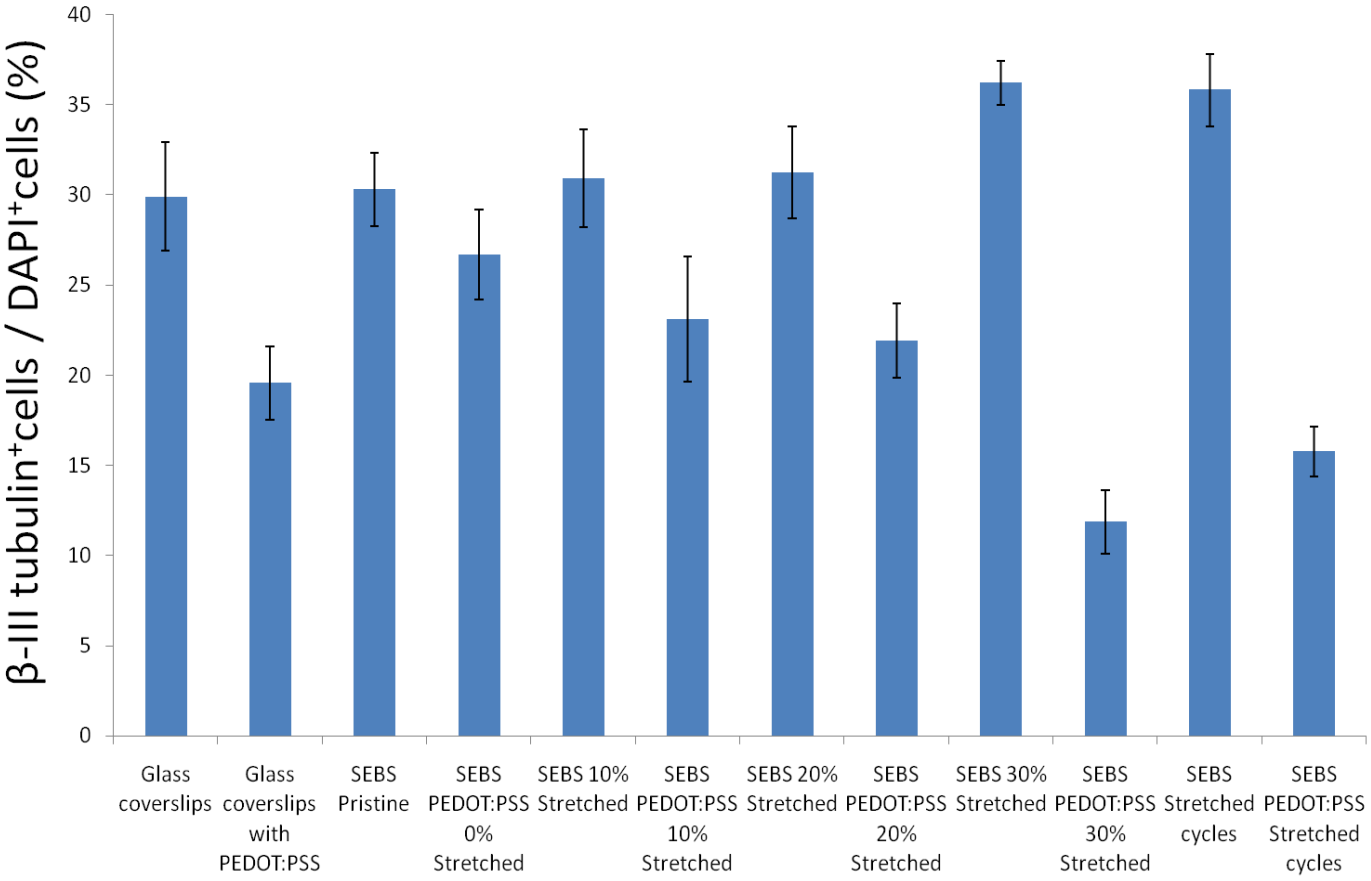

Fig. 3.11- Quantification of percentage of β-III tubulin positive cells on polymeric substrates. Data is represented as mean± SD, (n=3), p<0.5.

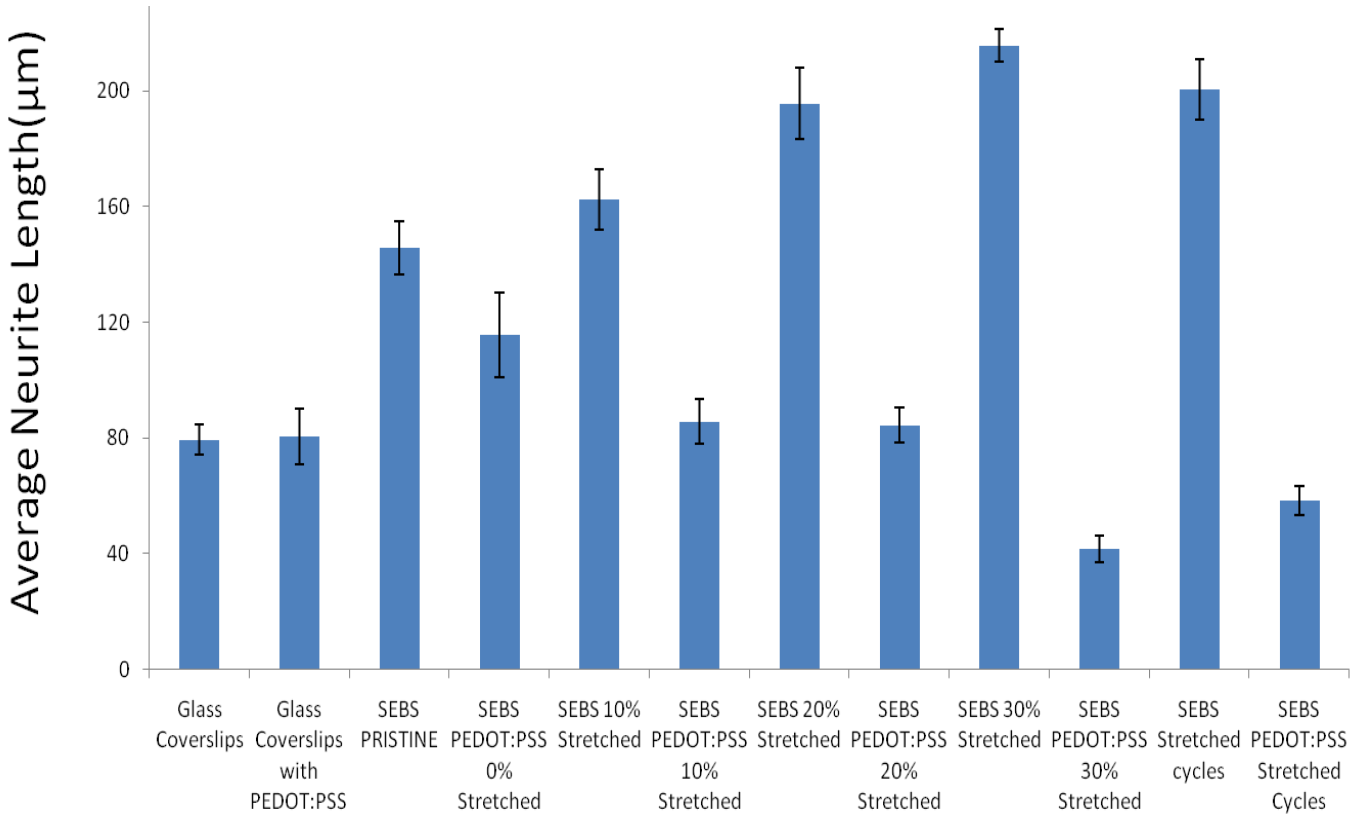

Fig. 3.12- Average neurite length of β-III tubulin positive cells in fig.3. Neurite length was measured from the soma to the tip of neurite along its length. Data is represented as mean± SD, (n=3), p<0.5.

3.5 Confocal imaging of cell aggregates on polymer surface

ES-NPs consist of a mixture of population of aggregated neurospheres and individual neuronal progenitor cells. Subsequent differentiation of neurospeheres or progenitor population resulted in the development of immature neurons. Segregation of the differentiated neurons away from these aggregates was seen on the glass coverslips and pristine SEBS substrates while on CP substrates their permeation was hindered leading to the presence of differentiated cells within the aggregates. In either case, the investigation of cell aggregates was done by vertical z-stack imaging through a confocal microscope.

The presence of the differentiated neurons at all the strata of the aggregates indicated a multilayered growth pattern of the neurons. The obstruction in the spreading of the differentiating neurons resulted in their proliferation over each other. The height of the aggregates, which indicated the number of layers of cells, increased on the highly strained CP substrates (30%) while on the strained pristine SEBS substrates, relatively smaller aggregates were present. This corroborated the tendency of cells to be present within the aggregates on strained CP substrates.

Figs. 3.13 and 3.14, are the confocal images of the aggregates and represent the topmost layer of cells in the aggregates and the layer of cells at the aggregate-polymer interface respectively. These images showed that the number of differentiated cells decreased as one moved away from the solid substratum. This was supported by the presence of increased number of differentiated neuronal cells near the aggregate-polymer interface than at the top of the aggregates.

This tendency was evident on strained conducting as well as non-conducting substrates because the neurons preferred to adhere on the surface rather than proliferate on top of each other. The necessary traction forces for firm attachment and subsequent spreading of cells was not provided by the soft neuronal layer and hence neurons prefer a solid substratum underneath them. Neurons formed well defined network of interconnected neurites in all the aggregates with a decrease in neurite length as the function of distance from the substratum.

Top of aggregates

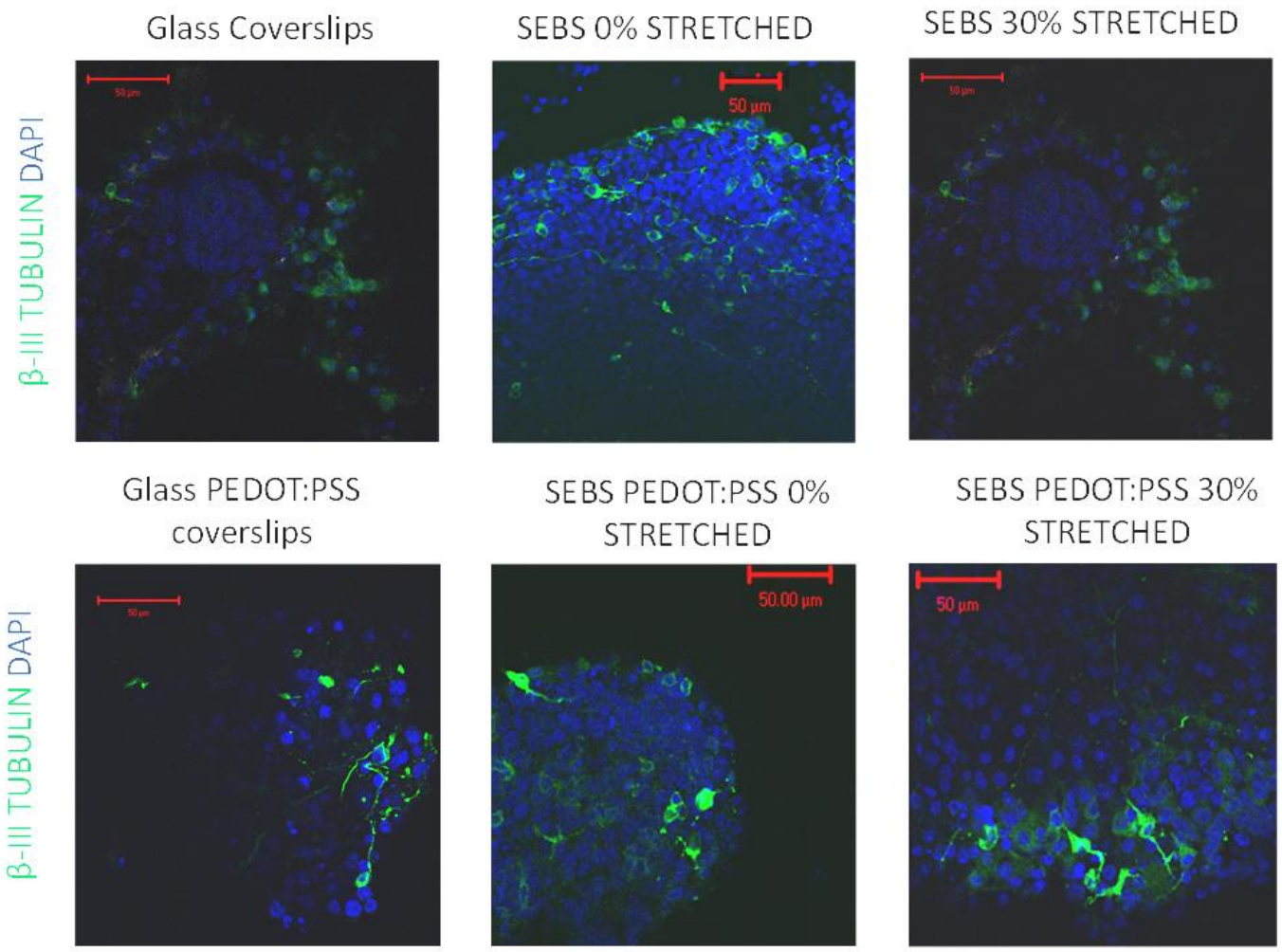

Fig. 3.13- z stack confocal imaging of the cell aggregates formed on polymeric substrates.The image shows the region at the top of the aggregates. Scale bar 50µm.

Aggregate-Polymer interface

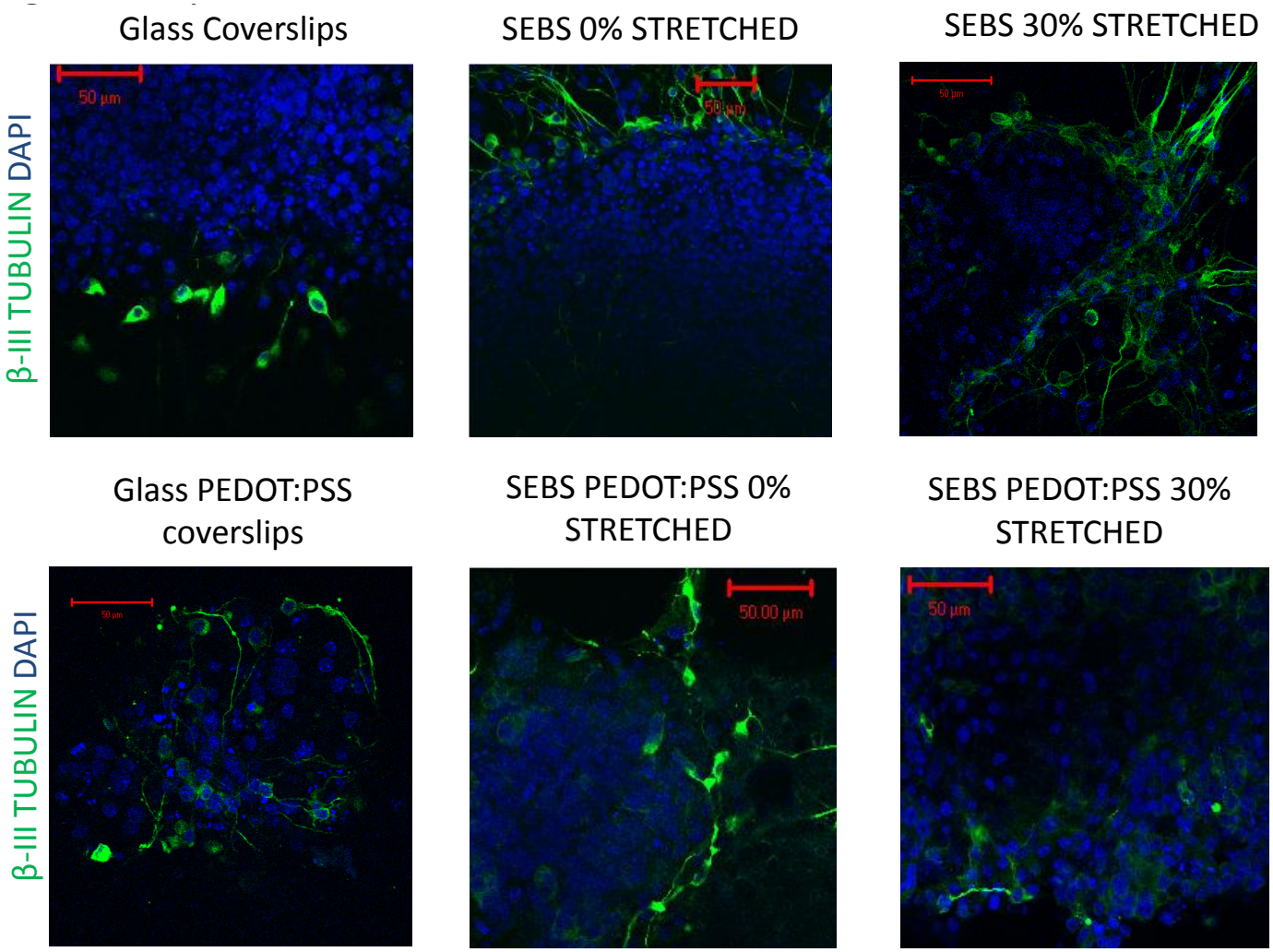

Fig. 3.14- z stack confocal imaging of the cell aggregates formed on polymeric substrates. The image shows the region at the aggregate-polymer interface. Scale bar 50µm.

3.6 'Defect patterning' of cell aggregates on polymeric substrates

The strained bilayered-substrates were expected to have crack-type defects which emerged orthogonal to the strain direction. The delamination of PEDOT:PSS film resulted in the appearance of these slip defects on the top conducting layer of the strained substrates. This resulted in the generation of local defect patterns due to which underlying SEBS surface was exposed. These local defect patterns or crack edges could possibly dock and immobilize the cells. These jagged crack features offered the aggregate a preferred direction, which was indicated by the ellipsoidal geometry of the aggregates where the long axis was largely distributed within 20^{o} angle, perpendicular to the strain direction as shown in the cartoon below.

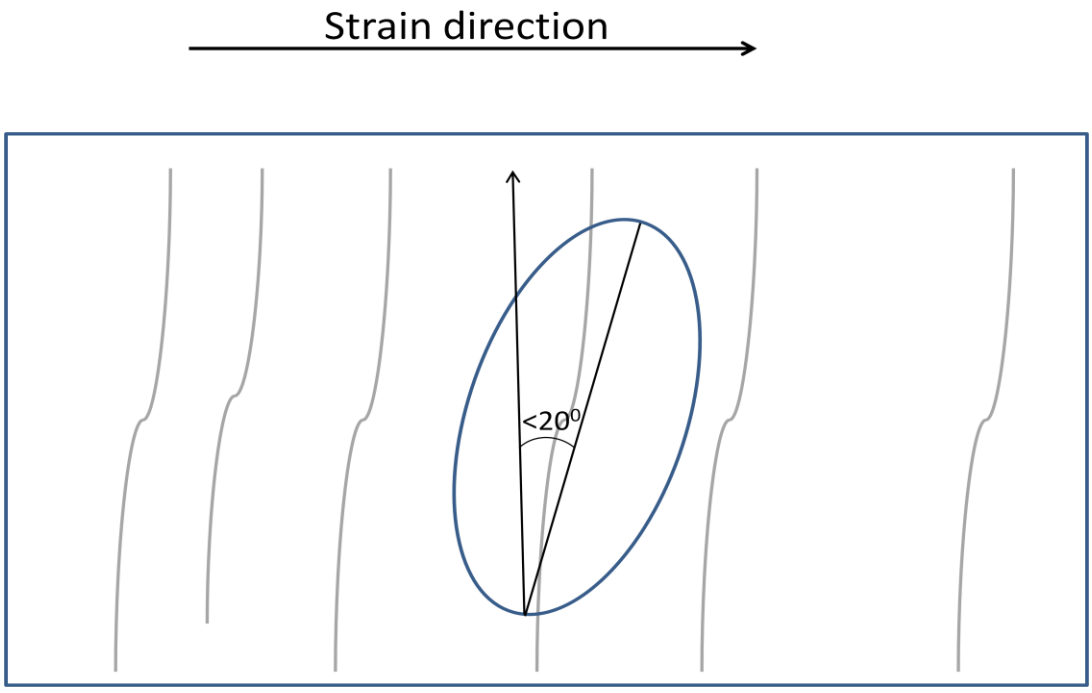

Fig. 3.15- Pictorial representation of the aggregate aligned along the crack patterns on the strained CP substrates

The aggregates were positively scored for the alignment if they fulfilled the conditions as depicted in fig. 3.15. The presence of heterogeneous population of cells within these cellular aggregates necessitated the use of DAPI images for the directional alignment analysis. DAPI images of the aggregates were taken with a 10x objective in various fields on all the substrates to investigate the role of defect patterns. Fig. 3.16 and 3.17 showed that on unstrained substrates (both conducting and non-conducting), the aggregates were randomly oriented throughout the surface. The alignment of the aggregates increased with the increase in strain regime on CP substrates. Some aggregates were found to align along the direction of defects and the percentage of such aggregates increased significantly on 30% strained CP substrates. Meanwhile, aggregates were found to align only on 30% strained pristine substrates and not on lower strained substrates.

The above observations were consistent with the quantitative analysis of the directional alignment of aggregates. It was seen that on 30% strained CP substrates, 70.2 $\pm$ 5.3% of aggregates were aligned along these local defects in contrast to only 21.9 $\pm$ 4% of aggregates being aligned on pristine SEBS substrates strained to similar regime ($p<0.5$;fig.3.18). The alignment of aggregates along the defects decreased sharply with the diminishing value of the strain applied on the substrates. 39.8 $\pm$ 6.4% of aggregates were aligned along the defect patterns on 20% strained CP substrates while no significant alignment was observed on the corresponding non-conducting strained SEBS counterparts. The 'crack patterning' of the aggregates is solely due to the defects formed in the PEDOT:PSS layer on SEBS which yields easily to allow the generation of these defects. SEBS surface in comparison maintains its texture and the defects arise only on the application of larger strain levels.

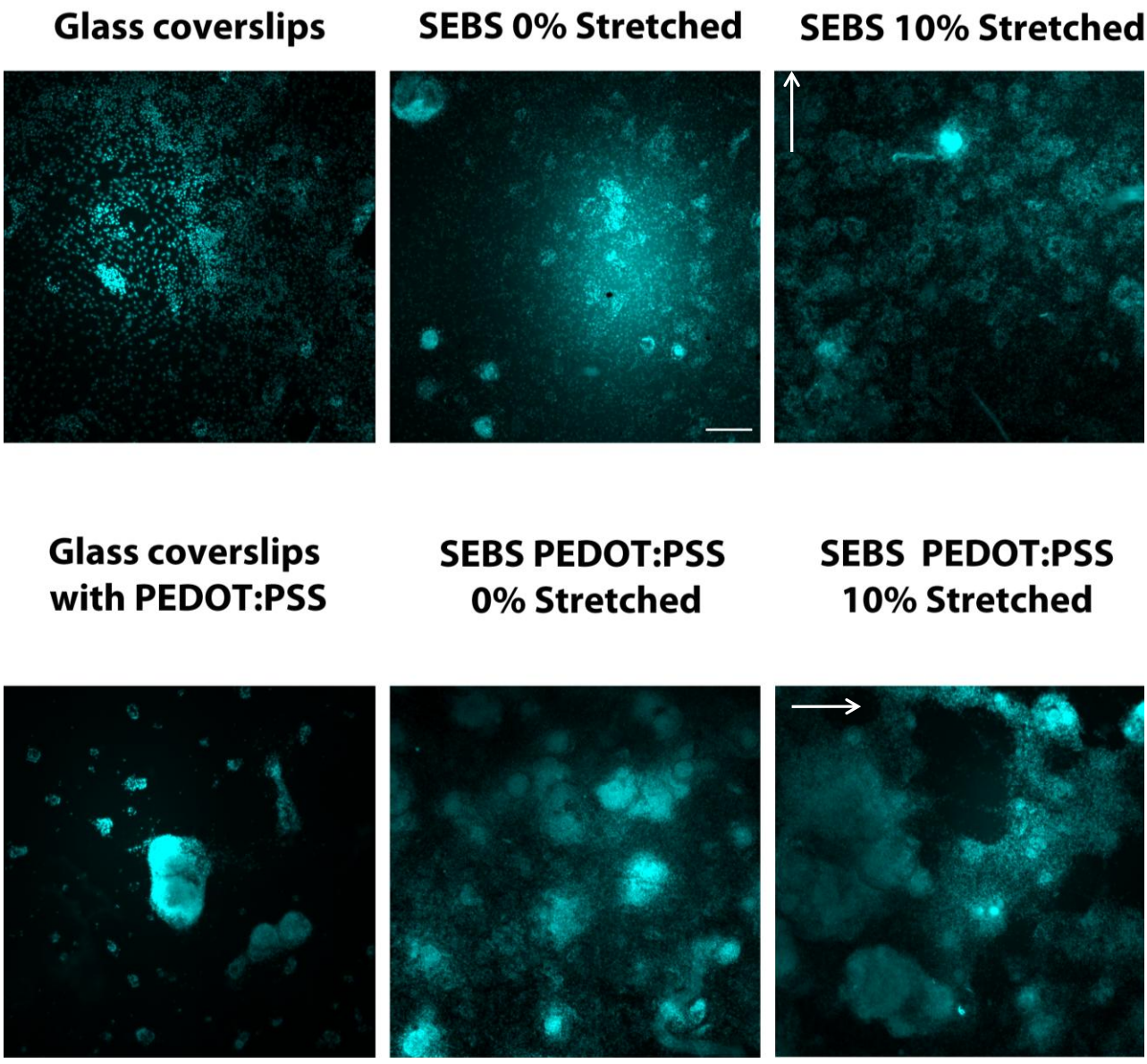

Fig. 3.16- DAPI images of cells on polymeric substrates for analyzing the role of directionality provided by the defect patterns. The arrows indicate the strained direction. Scale bar 50µm.

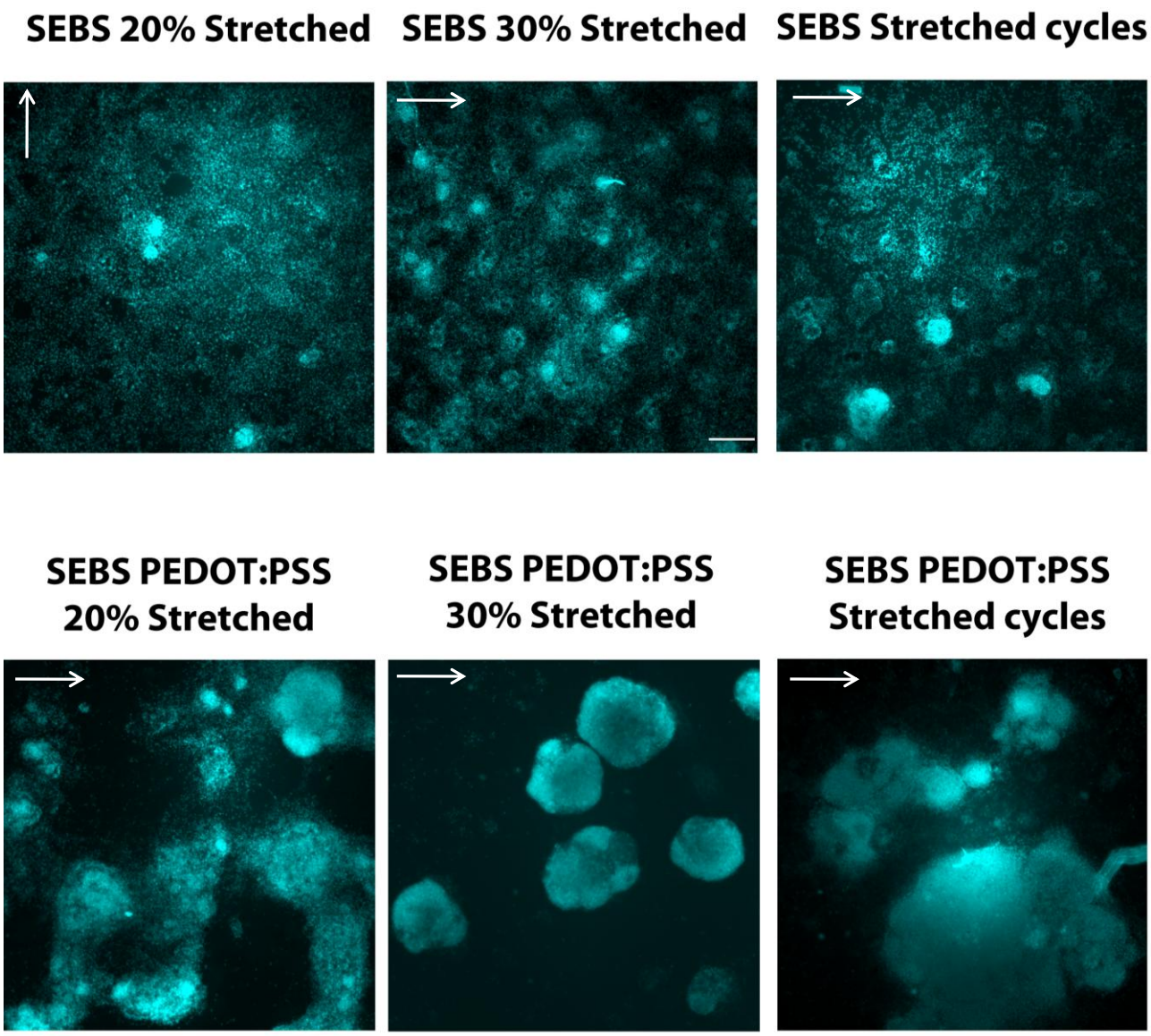

Fig. 3.17- DAPI images of cells on polymeric substrates for analyzing the role of directionality provided by the defect patterns. The arrows indicate the strained direction. More number of aggregates was aligned along the direction orthogonal to strained direction on CP substrates. Scale bar 50µm.

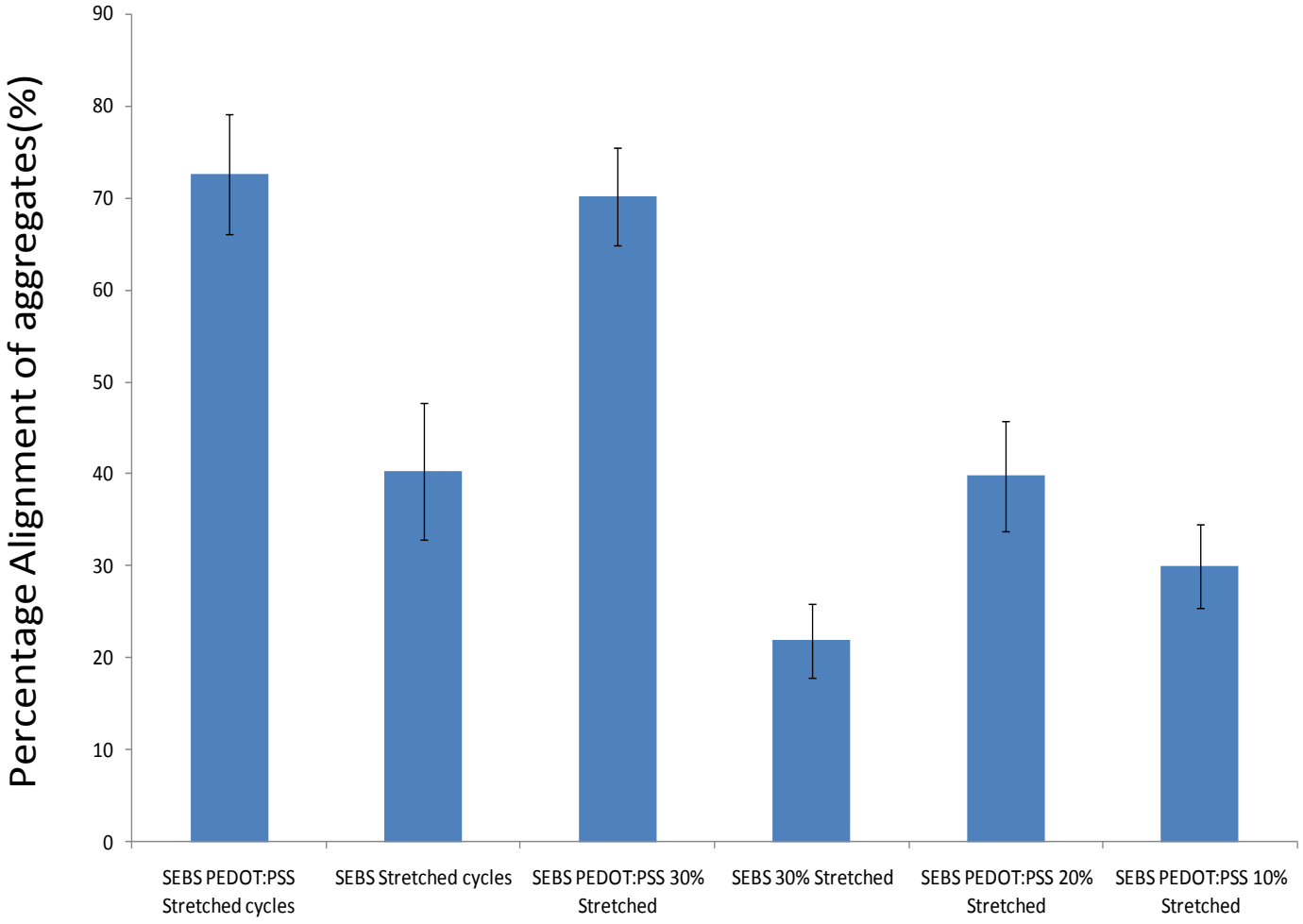

Fig. 3.18- Quantification of the directional alignment of cellular aggregates along the 'defect patterns' generated on polymeric substrates. The alignment of aggregates increases with the application of strain on CP coated substrates. Data is represented as mean± SD, (n=3), p<0.5.

3.7 Glial differentiation on polymeric substrates

The potential of these substrates to support glial differentiation of ES-NPs was also assessed. Addition of FGF2 in N2 differentiation medium promotes mixed neuronal/glial population. During ES-NP differentiation, neurons are formed at earlier stages of development while glial population appear late followed by the development of glial population which further gives rise to astrocytes and oligodendrocytes at the later stages. The number of glial cells exceeds neurons if the ES-NP differentiation is maintained for a longer period of time. It has also been reported by many groups that astrocytes secrete some neurotrophic factors which are essential for the differentiation and proliferation of neuronal population.

ES-NP differentiation on polymeric substrates was carried out as described earlier. Briefly, the substrates were coated with poly-D-lysine and laminin and subsequently ES-NPs were seeded on it. The differentiation of ESNPs was carried out for around 8 days in N2 differentiation on these substrates. After differentiation period was over, the cells were fixed and immunocytochemical staining was performed using following antibodies to ascertain the glial population:-

1. GFAP (glial fibrillary acidic protein) antibody is a specific glial marker. This primary antibody was used with cy3 as secondary antibody and cells appeared red in color.
2. DAPI staining to stain the nuclei of the cells (blue).

Cells were observed under upright fluorescent microscope (Olympus BX-61) and images were captured using a cooled CCD camera.The co-localized images of DAPI and GFAP pointed out the glial cells differentiated from the ES-NPs. These images were also used for the quantification of the glial population to assess the potential of polymeric substrates for glial differentiation.

Figs. 3.19 and 3.20 show a typical image of glial differentiation on the glass coverslips and polymeric substrates. The following inferences were drawn from the

immunocytochemicalanalysis on the control substrates (glass coverslips and CP-coated glass coverslips), CP-coated SEBS substrates and pristine SEBS substrates.

1. Glial cells were well distributed throughout the surface of glass coverslips and a large population of glial cells was present.
2. The number and spreading of glial cells did not differ significantlyon CP-coated glass coverslips and a significant glial population was differentiated from ES-NPs.
3. A similar trend in glial differentiation was observed on unstrained pristine SEBS substrates. The substrate promoted glial population and most of the glial cells spread throughout the surface.
4. The potential for glial differentiation did not vary much on CP-coated substrates. Glial cell did not tend to aggregate and were uniformly distributed throughout the surface.

Thus, the effect of guidance cues from the CP substrate which were so prominent during neuronal differentiation was not observed on glial differentiation. The consequence of the application of strain on polymeric substrates and change in their substrate properties were then investigated on glial differentiation.

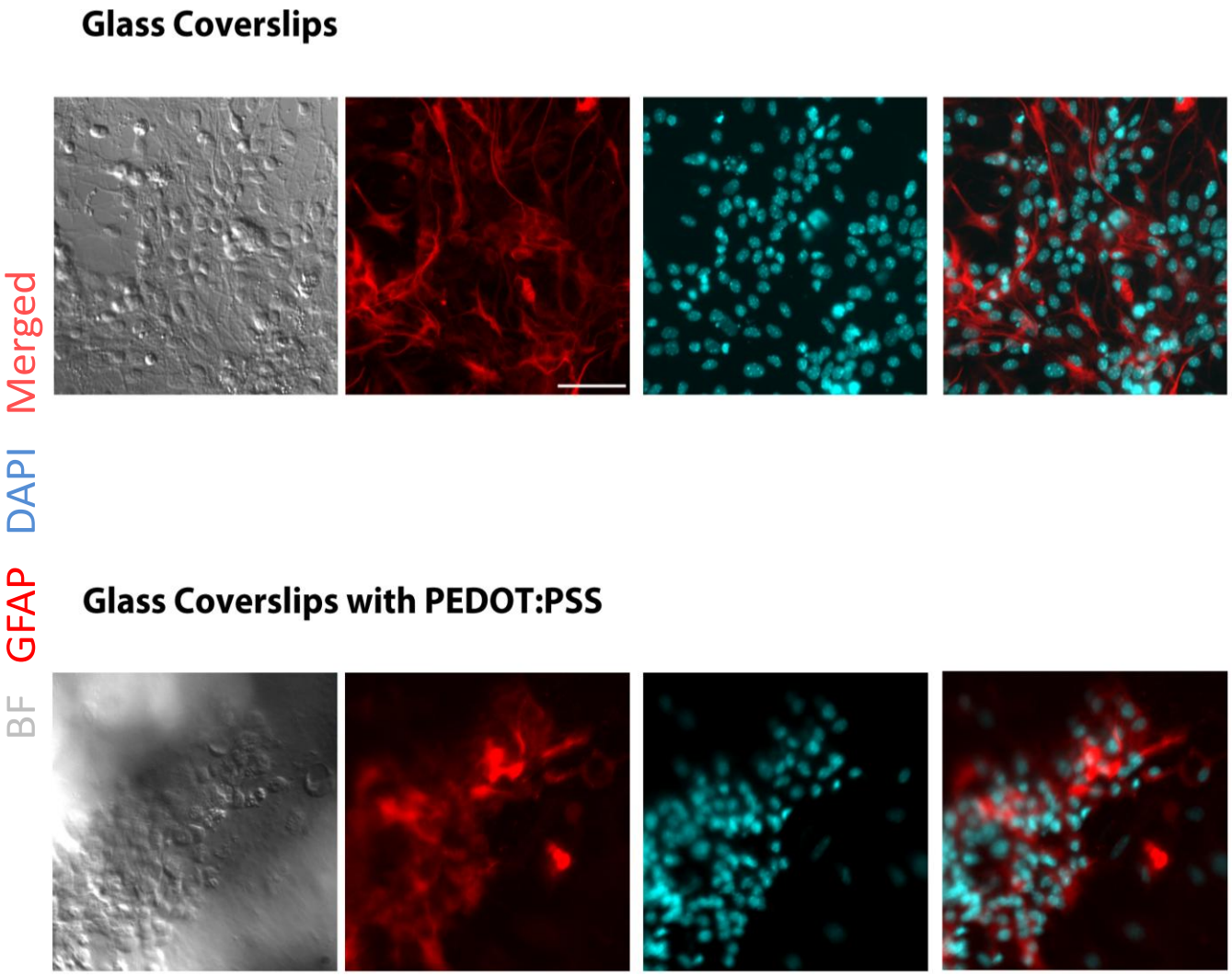

Fig. 3.19- Differentiation of ESNPs into glial cells on glass coverslips and PEDOT: PSS coated glass coverslips. Glial cells do not show aggregation tendency as was present in neurons. Scale bar 50µm.

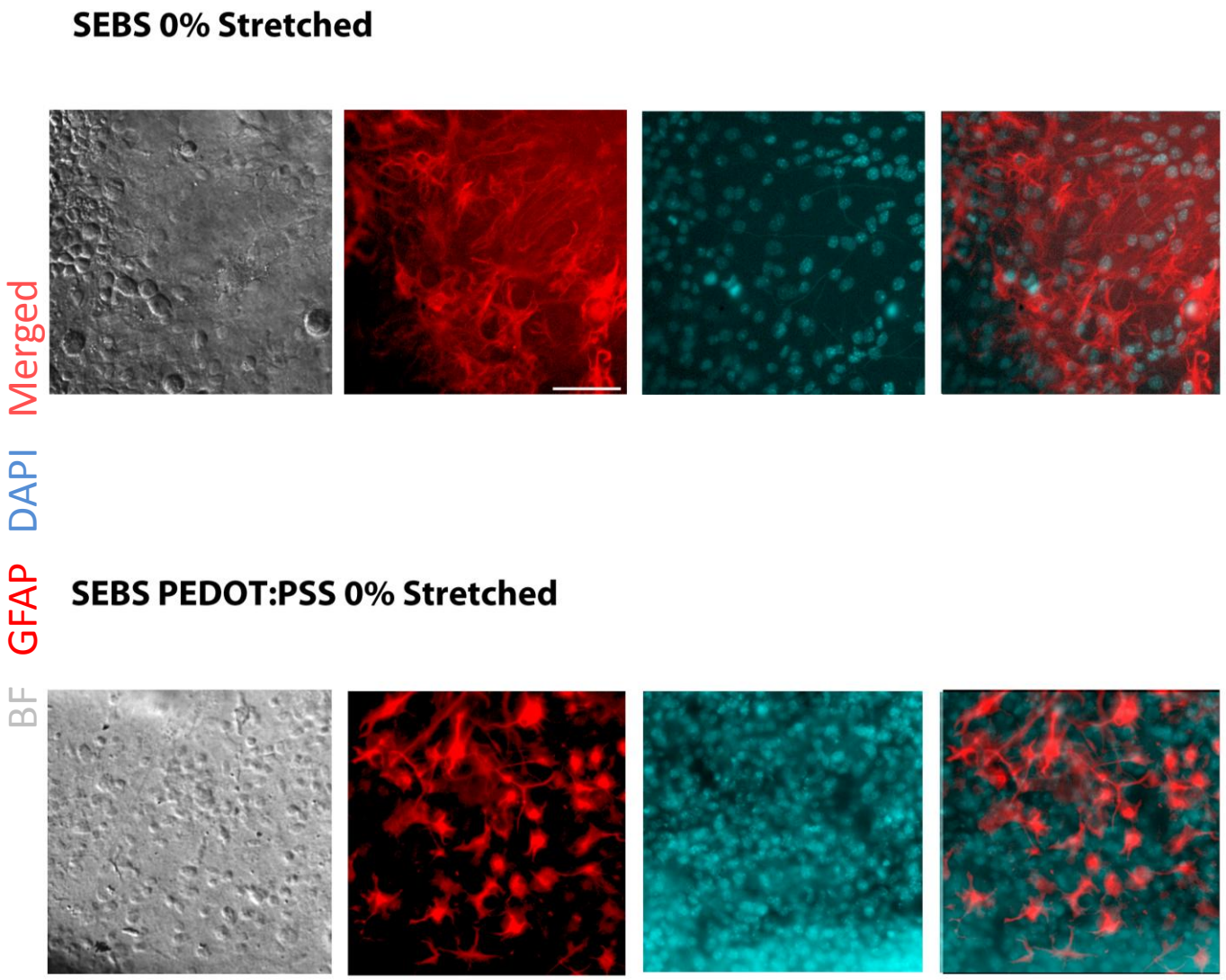

Fig. 3.20- Differentiation of ESNPs into glial cells on pristine SEBS and CP-coated SEBS substrates. There is no significant variation in number or spreading of glial cells on both the substrates. Scale bar 50µm.

3.7.1 Glial differentiation on strained substrates

Glial cells were differentiated from ES-NPs as described previously. Merged images of GFAP and DAPI staining were used for counting the glial cells ($GFAP^+$) and total number of cells ($DAPI^+$) respectively to quantitate the glial differentiation on strained polymeric substrates(conducting CP-coated and non-conducting pristine SEBS substrates).

Fig. 3.21 depicts the glial differentiation on 10% strained substrates (both CP and pristine SEBS) which does not show any significant deviation from the trends observed on unstrained substrates. In both these substrates, considerable population of glial cells was spread out on the surface with very few cells present in the aggregates on the CP substrates. This observation remained consistent with the glial differentiation on 20% strained CP-coated as well as their counterparts (fig. 3.22). The majority of glial cells were spread out on the surface but a marginal increase in the aggregation of glial population was also found.

Figs. 3.23 and 3.24 show the glial differentiation on 30% strained and cycles substrates. The differentiation of glial cells markedly reduced on strained (30% and cycles) CP coated substrates and most of the cells were present within the aggregates (figs. 3.23 and 3.24). The spreading of glial cells on these substrates reduced drastically which was similar to the neuronal cells on these substrates. Contrastingly, on 30% strained SEBS substrates, the glial cells were well-spread and the tendency to aggregate was minimal. The number of differentiated glial cells also increased marginally on these substrates.

Fig. 3.25 shows the quantitative analysis of the glial differentiation on the above polymeric substrates. The results from this analysis corroborated with the observations seen from the immunocytochemical stained images.Differentiation on unstrained (0%) PEDOT:PSS coated substrates resulted in $26.2 \pm 1.5\%$ glial cells while on highly strained (30%) PEDOT:PSScoated substrates, $16.7 \pm 2.6\%$ neurons were present ($p<0.5$). In comparison to the CP-coated substrates, straining the pristine SEBS substrates (30%) lead to a marginal increase in the glial differentiation with $28.5 \pm 1.2\%$ glial cells in comparison to $26.5 \pm 2.3\%$ glial cells present on unstrained pristine SEBS substrates.

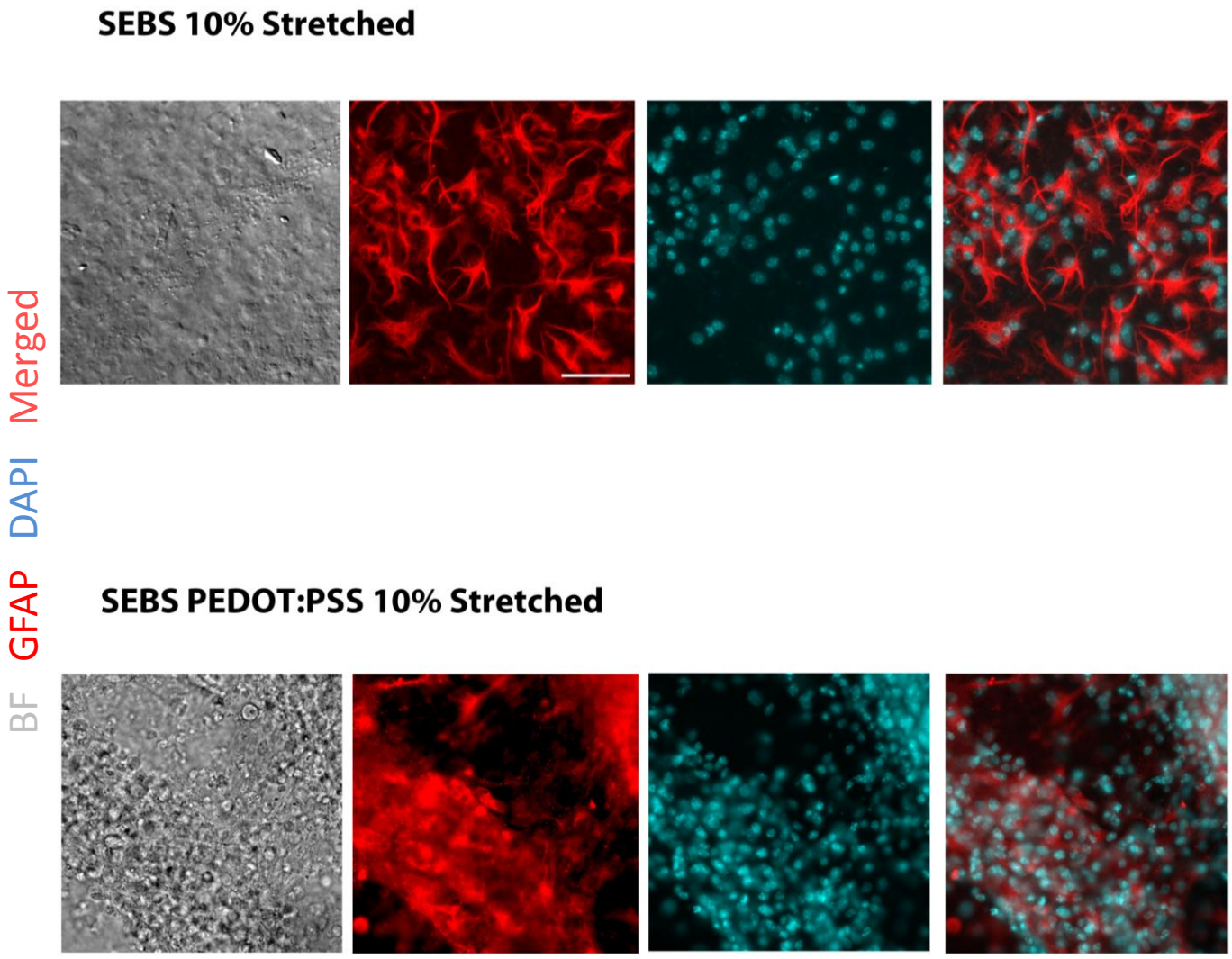

Fig. 3.21- Differentiation of ESNPs into glial cells on strained (10%) SEBS and CP-coated SEBS substrates. The number of glial cells on both the substrates is nearly equal and few glial cells tend to be present within the aggregates on CP-coated substrates. Scale bar 50µm.

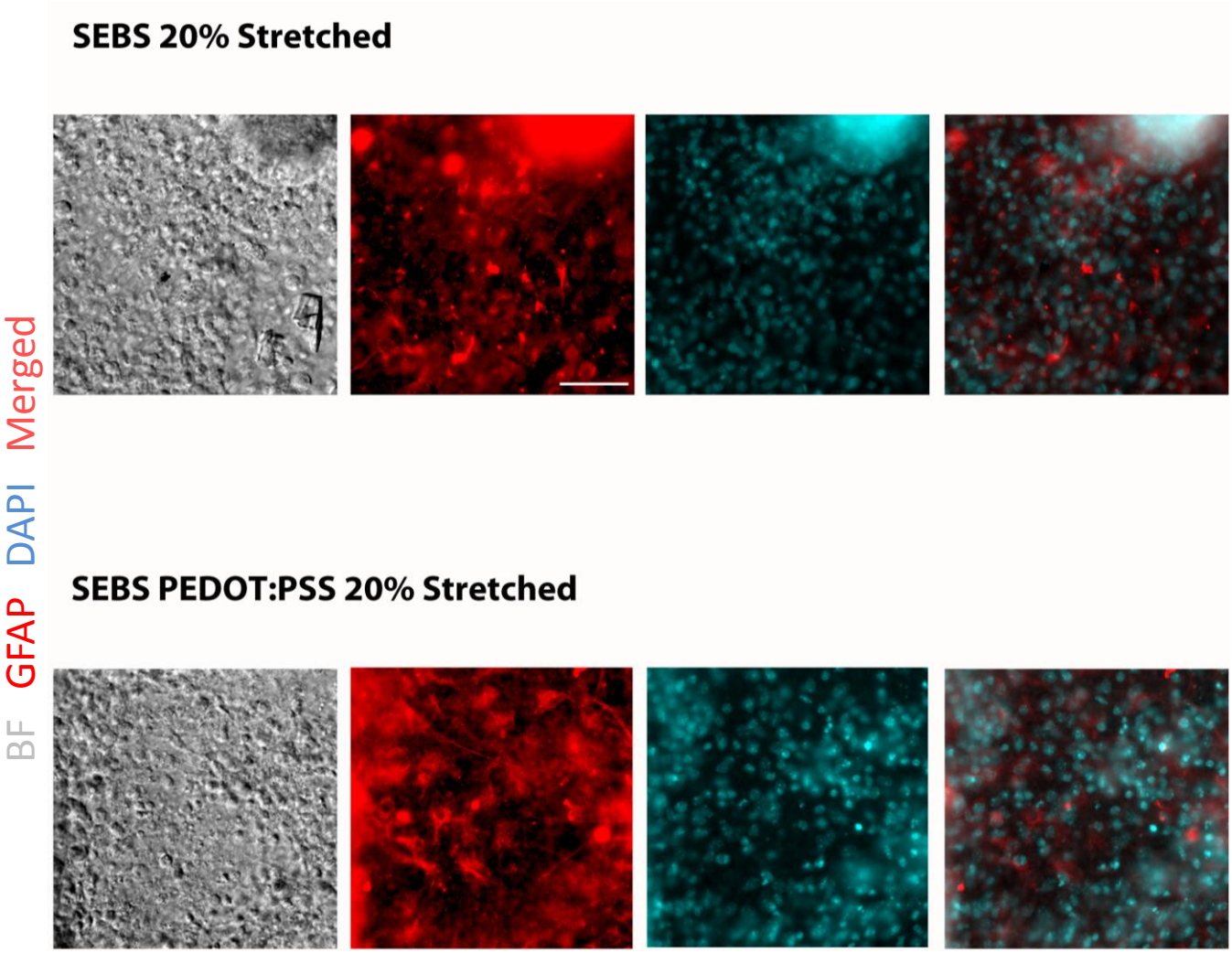

Fig. 3.22- Differentiation of ESNPs into glial cells on strained (20%) SEBS and CP-coated SEBS substrates. The number of glial cells on both the substrates is nearly equal and few glial cells tend to be present within the aggregates on CP-coated substrates. Scale bar 50µm.

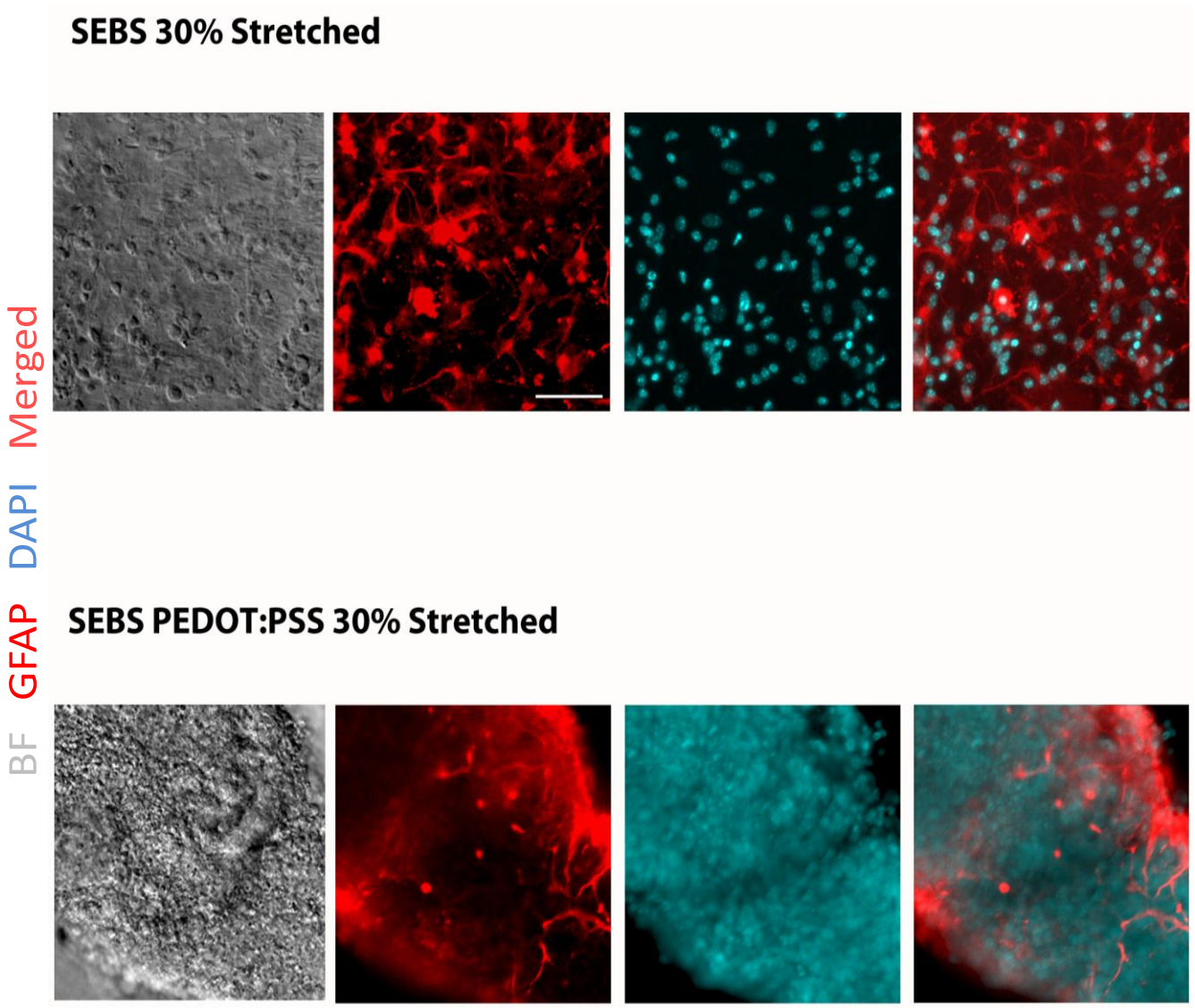

Fig. 3.23- Differentiation of ESNPs into glial cells on strained (30%) SEBS and CP-coated SEBS substrates. The number of glial cells decreases and most of them are present within the aggregates on CP-coated substrates. Scale bar 50µm.

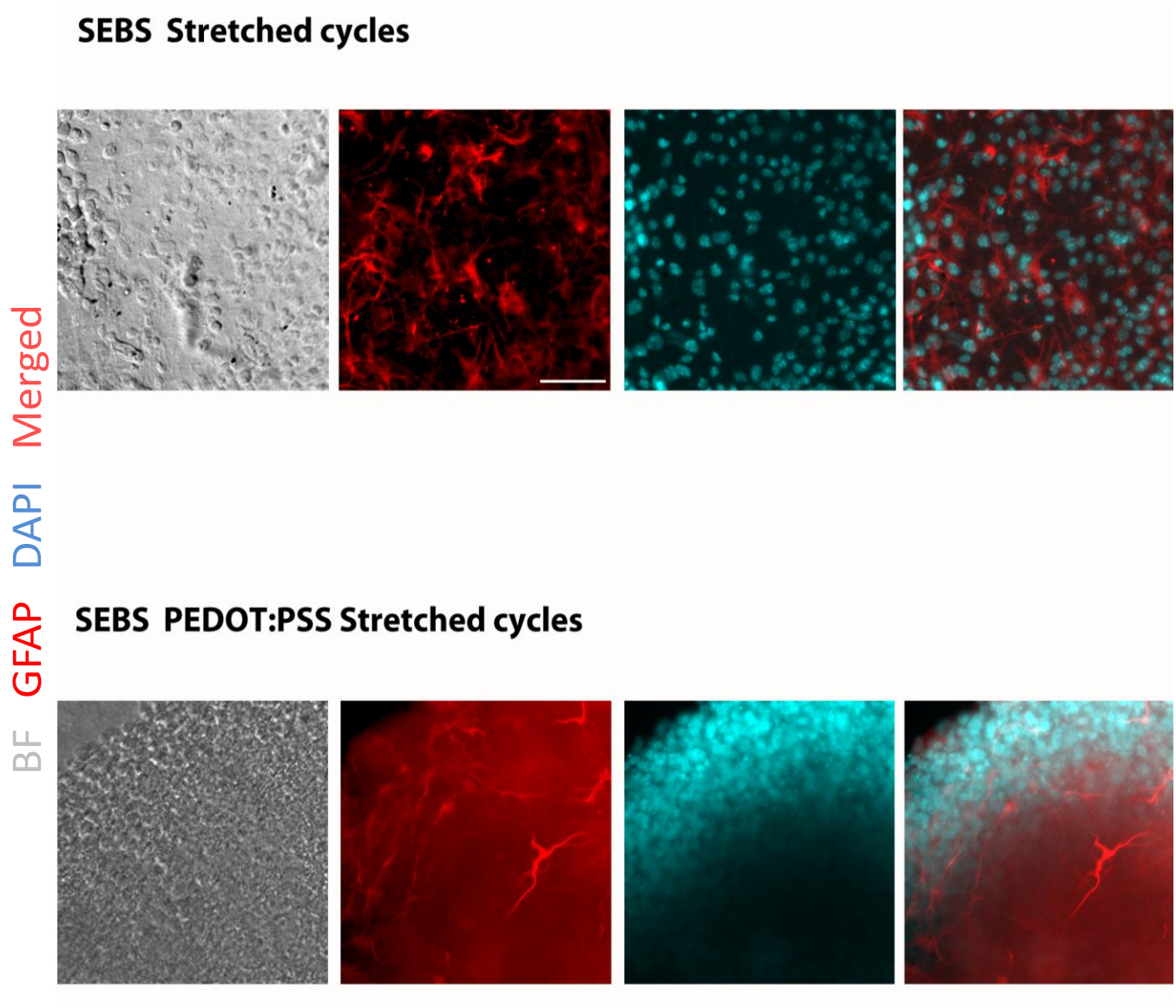

Fig. 3.24- Differentiation of ESNPs into glial cells on strained (cycles) SEBS and CP-coated SEBS substrates. Most of the glial cells are present within the aggregates on CP-coated substrates while on pristine SEBS substrates, they are spread uniformly on the surface. Scale bar 50µm.

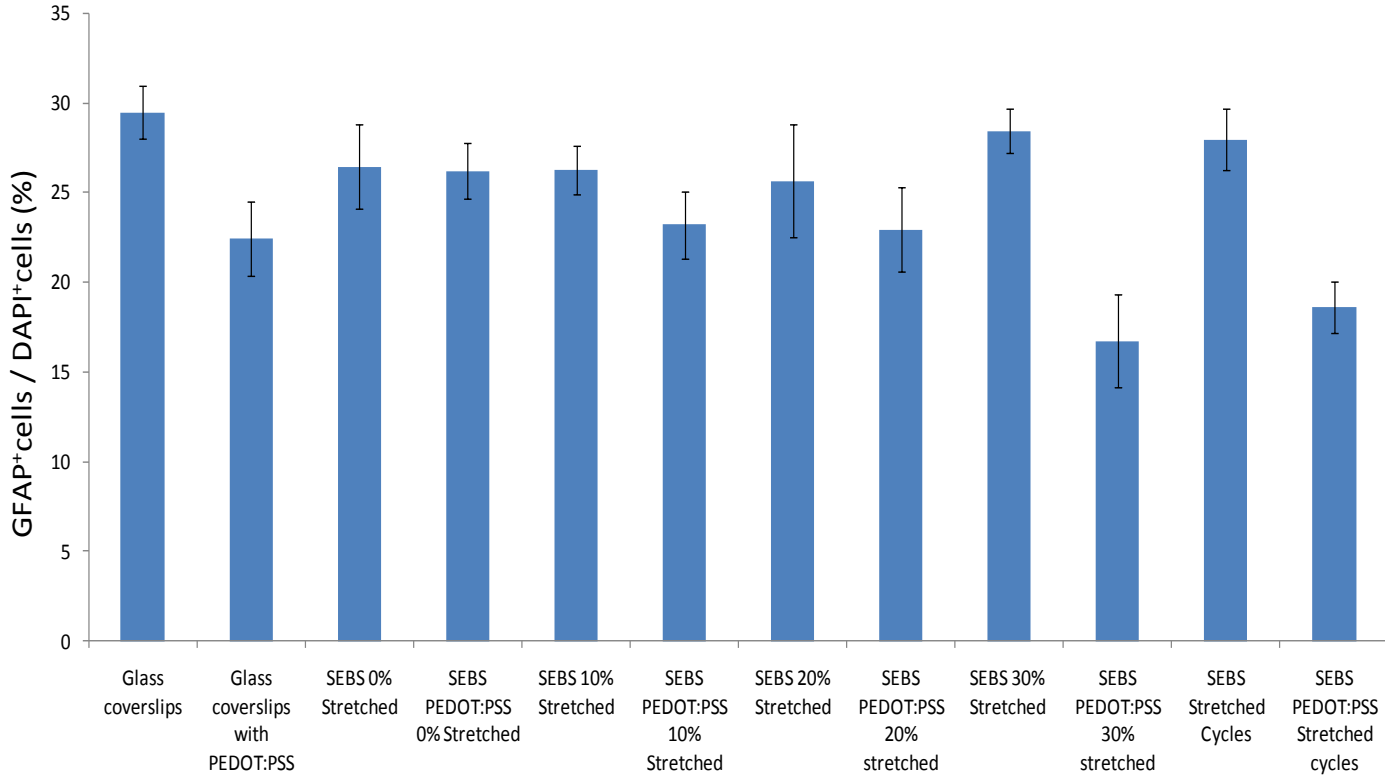

Fig. 3.25- Quantification of percentage of GFAP positive cells on polymeric substrates. Data is represented as mean± SD, (n=3).

3.8 Conclusion

ES-NPs were seeded on all the substrates and a combination of soluble factors and guidance cues from the substrate promoted their differentiation into neurons. But, a variation in neuronal differentiation is observed on the conducting CP substrates and non-conducting pristine SEBS-substrates. This variation further enhanced upon the application of strain on the corresponding substrates. Most of the neuronal differentiation on CP substrates occurred within the aggregateswhich resulted in a decrease in the neuronal differentiation and neurite length. The non-conducting pristine SEBS substrates, in contrast, promoted spreading of the neurons on the surface with an increase in the number of neurons and the corresponding length of neurites.

The shorter length of neurites on the strained CP substrates is attributed to the presence of neurons in the aggregates which reduced the distance between the adjacent neurons, leaving a limited space to spread and extend neurites. The neurite retraction from the adjoining areas may also have taken place during initial stages of differentiation leading to the aggregate formation and shortened neurites on these strained substrates. Confocal scanning of the cellular aggregates on CP showed that the differentiation occurred in all the strata of the aggregates but the morphology of neurons spread on the substratum was quite different from these neurons. Neurons present inside the aggregates were comparatively less matured and extended shorter neurites which is believed to be due to the non-availability of the growth factors to the cells present in the interior of these aggregates. Significant number of ES-NPs differentiated into neurons at the aggregate-polymer interface than at the top of aggregates. This suggesteda role of the polymeric substrate for providing physical guidance during the differentiation of ES cells.

All the substrates used in the study supported glial differentiation and a significant population was present on all the substrates. The glial differentiation of ES-NPs was not affected significantly by the conducting polymer component or application of strain as observed with neurons. But, an increased tendency of aggregation was observed on 30% strained CP-coated substrates. The difference in the pattern of neuronal and glial differentiation might stem from the fact that the glial cells are much more rigid in comparison to the pliant neuronal cells.

Hence, they resist the changes in the cytoskeletal framework of the cells caused by the underlying substrate.

The directional guidance was provided to the growing cell aggregates on highly strained CP substrates. It was observed that most of these aggregates were aligned along the local defects generated on the highly strained CP-substrates. Meanwhile, a sharp decrease in the directional alignment of the aggregates was observed with the diminishing value of the applied strain. The PEDOT:PSS layer over the underlying SEBS substrates yielded easily upon the application of strain which resulted in the generation of these cracks. SEBS surface in comparison maintains its texture and the defects arise only on the application of larger strain levels. The changes in the neuronal differentiation on CP substrates especially on straining point out towards a role played by the guidance cues provided by the substrate.

Chapter 4

Actin cytoskeleton rearrangement

4.1 Introduction

Most cells are specific to the requirement of a solid substrate to attach and proliferate. These cells are not viable in suspension cultures even in presence of soluble proteins which can engage cell adhesion molecules (like integrin binding RGD peptide)[215]. Adherent cells and extracellular matrix (ECM) together contribute to establish an elastic microenvironment in our body. The elasticity is clearly evident on macro scale by the ability of the solid tissue to rapidly regain its shape upon application of mild force.

At the cellular scale, cells probe elasticity as they anchor and pull on their surroundings. These processes are dependent on actin-myosin based contractile apparatus and transcellular adhesion mediated by integrins, cadherins, catenin and vinculin[216-217]. Normal tissues not only apply forces but also respond to it through cytoskeletal organization which redistributes the forces sensed by cells. The application of forces by the adherent cells (traction forces) was first observed on soft gels and thin films [218-221]. The intracellular forces generated by the contractile apparatus act on surrounding cells as well and its importance has been demonstrated in tissue morphogenesis and embryo development [222-231]. This contractile force is necessary for a number of biological processes like cell migration, mitosis, stem cell differentiation and self-renewal[5, 13, 232-238]. Cell migration and mitosis is directly related to intra- and intercellular forces, while the role of forces in genetic responses such as cell proliferation and differentiation is similar to cytokines.

Epithelial cells and fibroblasts perceive and respond distinctly to stiffness of ligand-coated substrates[4, 6]. Physical guidance by the underlying substrate plays a major role in modulating

stem cell differentiation and affects its lineage specificity [13].Nanotopography, surface hydrophobicity, density and spacing between the ligands affect a broad range of cellular properties ranging from morphology of embryonic cells and tissues to behavior of tumor cells and disease progression[239-244].

These studies clearly show the role played by ECM in guiding the stem cells towards lineage commitment. Cells are not passive elements but are dynamic entities constantly scouting and using the signals from ECM to tune their mechanical properties by dynamically remodeling cytoskeletal networks. Thus, cellular responses to mechanical perturbations are not only a function of input stimuli but are also determined by the coupling of these stimuli to mechanosensititve changes in the cytoskeletal organization, interaction with ECM and cellular force production.

Biochemical characteristics of the substrate as well as its rigidity and spatial organization are recognized by cells through differential signaling from integrin-based molecular complexes known as focal adhesion complexes (FA) [3-4, 241]. These complexes are also involved in the sensing and processing of external mechanical stimuli such as substrate stretching and fluid shear flow. The insight into the molecular complexity of these adhesion sensing units is important to understand how cells sense and respond to the changes in the physical environment. A brief introduction to the focal adhesion complexes, the proteins which play a role in its formation and the associated downstream signaling molecules is mandatory to understand the changes in ES-NP differentiation discussed in the previous chapter.

4.2 Force transducing machinery at Cell-ECM Junctions

The understanding of physical guidance by ECM and environmental sensing by the cells can be divided into two parts:-

1. Studies of cellular structures bear stress or forces.
2. Studies of structures which transduce the transmitted force into biochemical signals.

It should be noted that in all these studies, cells should be in direct contact with ECM and not in isolation. This is because the adhesion of a cell to the matrix results in structural organization of the cell itself. Integrin binding and clustering against ECM ligands lead to changes in cell shape and cytoskeletal architecture, anchoring the actin cytoskeleton to the sites of adhesion. The cytoskeleton is linked to the nuclear envelope and thus the forces experienced or generated by cell-ECM module are transmitted and sensed throughout the module as a coordinated system.

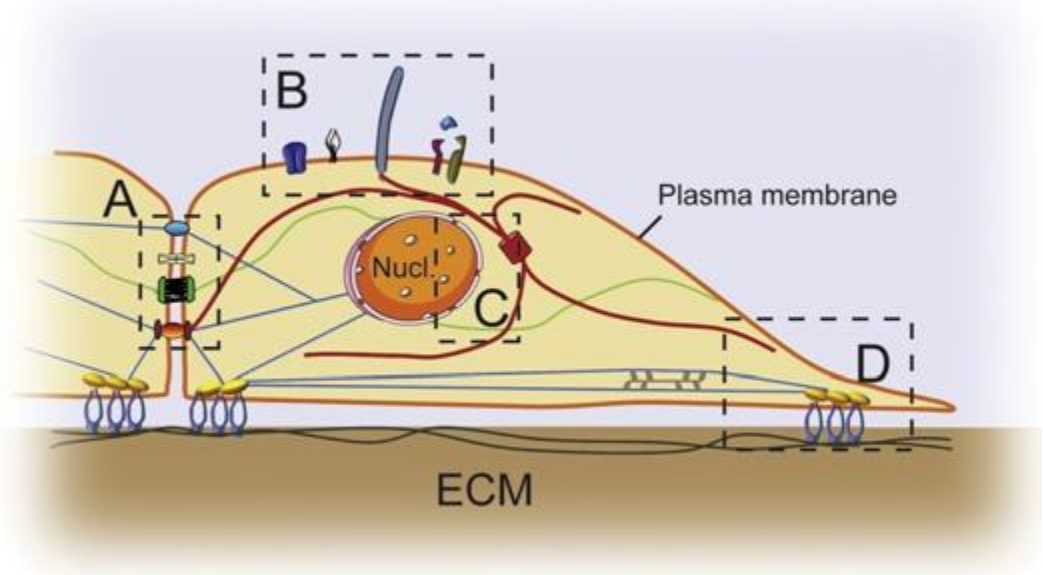

Fig. 4.1-Force sensing and its transduction into biochemical signals is a complex event with many organelles acting individually and also in unison. (A) Cell-Cell contact junctions which mediates intercellular interactions (B) Stretch activated ion channels at cell membrane (C) Mechanotransduction at nucleus (D) Focal adhesion formation at Cell-ECM interface. Adapted from [3] with permission from Elsiever

Stretch activated ion channels are present on the surface of the cell membrane of vascular endothelial cells. Application of stress or force activates these channels which results in the influx of Ca^{2+} ions[245]. These ion channels also mediate the vascular responses to haemodynamic stresses. The presence of these ion channels is also reported in the cells where

physiological response is produced upon the application of stress(fluid flow or weight bearing) [246-249].

The nucleus and other surrounding organelles are connected by the framework of microtubules and intermediate filaments. Nesprins tether the nucleus with actin-myosin cytoskeleton complex. The intricate network of these cytoskeletal components ensure that any change in cell shape upon physical guidance from matrix or change in actin-myosin contractility can alter spatial localization of organelles and induce conformational change in nuclear pores[250-251]. The change in nuclear confirmation directly altersthe genomic structure and accessibility of transcription factors to specific genetic targets. This leads to the changes in the gene transcription levels and induces many physiological changes in the cellular functioning [252-253].

4.2.1 Structural basis of force transmission in cells

Cytoskeleton is the fundamental structure for mediating force transmission in a cell [254].The cytoskeleton is a highly dynamic cellular scaffolding structure composed of filamentous actin (6 nm in diameter), intermediate filaments (10 nm), and microtubules (23 nm)[255]. These three cytoskeletal elements are not single proteins, but consist of many monomers which are able to span large distances within the cell.Actin monomers assemble into filamentous actin (F-actin) and together with myosin filaments, form cytoskeletal contractile apparatus. These cytoskeletal elements are semiflexible wherein they do not form loops or knots but areflexible enough to have significant thermal bending fluctuations[256]. The persistence length of actin filament is around 10 μm and strain stiffening occurs at strain levels as low as 20% [257-259]. Thus, on application of strain, actin filaments stiffen without appreciable increase in molecular weight.At the cell membrane, thesefilaments anchor into clusters of proteins that include focal adhesions(FAs) which link the cytoskeleton through transmembraneintegrin receptors with the ECM. Upon adhesion of cells to ECM, integrin clustering takes place which forms nascent adhesions (NA) which mature to Focal complexes (FX) and focal adhesions, a process controlled by actin-myosin contractility.

Application of force to cell-ECM unit leads to structural deformation and rearrangement of ECM and this force is transmitted through FA to the actin-mysoin contractile apparatus which leads to spatial change in the position of various cell organelles tethered to the actin-mysoin cytoskeleton [260]. This type of signaling is "outside-in" force transmission while in "inside-out" force transmission,the intracellular force generated by the contractile apparatus of the cell imparts force on the ECM [4, 261]. The head domain of myosin-II pulls on actin filaments to generate traction forces which are transmitted to FA and deforms ECM [262].

4.2.2 Mechanosensing at Focal Adhesion Complexes

FAs are one of the most potent sensors and transducers of the physical guidance provided by the ECM. The development of nascent FAs begins with the attachment of cells to the ECM which leads to the clustering of integrins. At cell membrane, the integrin layer is oriented with the head domains connecting to ECM and the cytoplasmic tails binding to Focal Adhesion complex (FAK) and paxillin. This cytoplasmic layer assembles within a stratum containing talin and vinculin and upper-most actin-regulatory sheet consisting of zyxin, vasodilator stimulating phosphoprotein (VASP) and α-actinin which tethers FA to actin-myosin cytoskeleton (fig. 4.2) [263]. Atleast two molecules of talin are involved which connect two α integrin-β integrin dimers with actin filaments [264-265]. Subsequently, binding of vinculin to talin takes place which triggers the clustering of activated integrins and association of these integrins with actin units [266-267].

Structurally, mature focal adhesions are elongated and localized at the termini of stress fibers. Stress fibers are bundles of actin filaments which contain a multitude of proteins such as actin filament cross-linkers like filamin and are linked to myosin filaments especially myosin-II [268]. Myosin confers contractility to this complex such that any change in the mechanical environment is resisted and resulting force is transmitted through FA and integrins to ECM [218, 269-270]. Role of myosin-IIA is especially important in the cells grown on flat, rigid substrates. The nascent adhesions formed in myosin-IIA knockout cells were unable to change into stable and mature FA [271].

Nascent adhesions either turn-over rapidly (~ 60 ms) or mature into large focal complexes (FX) of which some assembled into larger FAs [272-273]. It has been observed that the focal adhesions, which come from micrometer sized focal complexes, usually undergo maturation. The morphogenesis of these adhesions require forces generated by the actin system [274]. It unfolds several protein domains of talin, paxillin and p130 cas exposing binding or phophorylation sites which leads to the stabilization of nascent adhesions into FXs to FA, now tethered to thick actin stress fiber bundles [275-276]. It is also seen that integrin receptor itself switches to a high affinity state in response to force [277].Conversely, inhibition of myosin II or actin assembly with disrupting agents such as cytochalasin-B and reducing cytoskeletaltension leads to disassembly of FAs[278].

Another interesting observation about FAs is that they not only serve as physical anchoring centers but also are biochemical signaling centers. They contain many signaling proteins such as FAK, ERK, JNK, Src, MEK, Ras and Raf which are involved in myriad of pathways such as migration, proliferation and differentiation [279]. The master regulators of essentially every aspect of actin cytoskeleton function are small Rho family GTPases principally Rho and Rac[280]. The activation of Rho GTPases is mediated by guanine nucleotide exchange factors (GEFs), which catalyse the exchange of GDP for GTP. Activation of Rac protein occurs through a GEF which is activated by a pathway that involves the focal adhesion proteins paxillin and p130 cas, both of which respond to mechanical stress.

4.2.3 Focal adhesions and actin assembly

The interaction between integrin-mediated adhesions and actin cytoskeleton is bidirectional: cytoskeletal forces regulate the assembly and maturation of the focal adhesion complexes and the growing adhesion complexes regulate the assembly of the actin system (fig. 4.3). This was observed by plating the cells on micropatterns of varied shapes. On flat, triangular islands the focal adhesions and stress fibers were formed along the edges of the triangles while on semi-circular patterns, a fan-like morphology of actin cytoskeleton was seen [281-282].

Focal adhesions also serve as actin nucleating centers. Actin subunits are predominantly incorporated at the membrane associated ends of actin filaments. It is observed that the stress fibers associated with focal adhesion complexes grow and incorporate new components mainly at stress fiber-focal adhesion interface [283-284]. The molecular mechanism behind the nucleation event is not known completely but the possible protein must play a role in focal complexes as well as in linking actin fiber bundles to these complexes. Zyxin has been postulated as one of the candidates since it is important in force dependent actin polymerization [285].

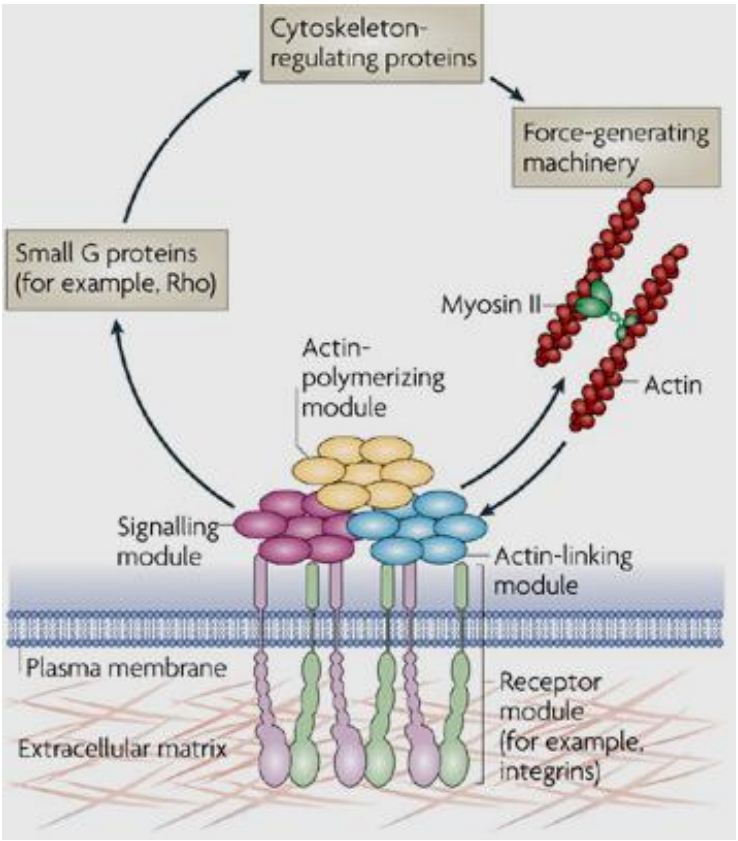

Fig. 4.2- Actin cytoskeleton-focal adhesion interplay. A schematic showing the intricate connection between the actin machinery and integrin-mediated adhesions. Reprinted by permission from Macmillan Publishers limited: Nature Reviews Molecular Cell Biology [3],copyright 2009.

4.2.4 Adhesion complexes, actin assembly and stem cell differentiation

Cells attached to a substrate exert contractile forces due to actin-mysoin network which are intimately connected with the FAs. The presence of myriadof signaling molecules in adhesion complexes, leads to the modulation of cell differentiation by the physical environment of ECM [237]. It was observed that in myoblasts, cultured on collagen strips attached to polymer gels of varying mechanical stiffness, the development of actin/myosin striations appeared only on gels which had properties similar to normal muscles [286]. The stem cell lineage specificity is directly determined by the mechanical properties of the culture substrates. MSCs grown on variably compliant polyacrylamide gels were found to alter their properties in relation to the stiffness of the substrate. Furthermore, the stiffness of the substrate defined the differentiation lineage of the MSCs: softer substrates (< 1 kPa) that mimic the mechanical property of brain cells were found to be neurogenic, intermediate stiffness substrates (8-17 kPa) were myogenic while very stiff substrates (> 25 kPa) promoted osteocyte formation [13].In another study it was seen that in presence of necessary soluble factors in the medium, MSCs adopted the adipogenic or chondrogenic phenotype when cell size was restrictedor contractility was reduced. Conversely, spreading and high contractility promoted osteogenic and myogenic differentiation albeit through different mechanotransduction pathways. The decision between adipo/osteo lineages is driven through RhoA/ ROCK while chondro/myo fate depends on the activation of Rac1. The constitutive RhoA expression shifted cells towards osteogenic lineage and RhoA/ROCK signaling is dependent on the stress generated by the actin/myosin complex[45, 287].

Neural stem cells are also influenced by the substrate stiffness [14]. Cell spreading, self-renewal and differentiation were inhibited on stiffer substrates while the expression of neuronal markers was elevated on more compliant substrates mimicking stiffness range of brain tissue. It was also seen that during differentiation, the mechanical signature of specific cells (cytoskeletal responses and contractility) appeared earlier than the expression of lineage specific genes.

Cells respond to a variety of biochemical, topographical and mechanical cues which is reflected by a change in normal cellular functioning. In the previous chapter, we looked at the effect of various cues provided by the non-conducting/conducting substrates on ES-NP differentiation. These substrates contain various nanotopographical features which are clearly seen in the AFM and KPM images in chapter 2. Application of stress causes the PEDOT domains to elongate and align along the direction of strain hence causing a change in the conductivity of the CP substrate. Apart from that, application of strain leads to the generation of local defect patterns in any viscoelastic/ soft substrate. In conducting substrates, local defect patterns are formed in the direction perpendicular to the application of strain and this leads to the defect patterning of cells. But it is quite intriguing, that physical cues provided by the substrate is assimilated intricately in the developmental pathway and leads to the changes in cell differentiation and spreading. The current chapter shows at the molecular level how the "sensing" takes place which results in the modulation of biochemical signals and produces changes in the ES-NP differentiation. This chapter also tries to draw analogy between the changes responsible for modulation of MSC and neuronal differentiation. The study of the cell-substrate interactions at conducting polymer interface provides an understanding about the role played by the surface potential, nanotopography and local defects in soft polymers and nano-dimensional charged moieties during cell development.

4.3 Actin cytoskeleton rearrangement

Arrangement of actin cytoskeleton was observed in differentiated ES-NPs by immunostaining with Alexa Fluor 488 conjugatedPhalloidin. Phalloidin binds specifically at the interface between F-actin subunits, locking adjacent subunits together. It is a bicyclic heptapeptide which binds actin filaments much more tightly than corresponding monomeric units. This leads to a decrease in the rate constant of the dissociated actin subunits from filament ends, which essentially stabilizes actin filaments through the prevention of filament depolymerization. Moreover, phalloidin is found to inhibit the ATP hydrolysis activity of F-actin.Thus, it traps actin monomers in a conformation distinct from G-actin and stabilizes the

structure of F-actin by greatly reducing the rate constant for monomer dissociation, an event which is associated with the trapping of ADP.

There is no change in the cytoskeletal arrangement of differentiated cells due to phalloidin since immunostaining was done on post-fixed cells. This is of particular importance since any change in the cytoskeletal arrangement of cells may contribute to the change in focal adhesion assembly which may then be transmitted to adjoining ECM surface. Phalloidinimmunostaining was done as explained earlier in chapter 2. The cells were also immunostained with β-III tubulin and co-localized images were used to indicate the cytoskeletal network of neurons specifically amongst the heterogeneous population of cells produced by the differentiation of ES-NPs.

4.3.1 Actin cytoskeleton arrangement on glass coverslips

Glass coverslips were used as controls in the experiment to compare with the results obtained on non-conducting prisitne SEBS and conducting PEDOT:PSS coated SEBS substrates. ES-NPs were differentiated on glass coverslips pretreated with poly-D lysine and laminin.

Cells were fixed for immunocytochemical staining analysis post ES-NP differentiation period of 8 days. Immunostaining was performed by-

3. β-III tubulin which specifically binds the immature neurons differentiated from ES cells. The secondary antibody used in this case is cy-3(red).
4. Alexa Fluor-488 conjugatedPhalloidin which specifically binds F-actin in all the cells. Alexa Fluor 488(green) helps in visualization of Phalloidin upon binding.
5. DAPI to stain the nuclei of the cells.

Post immunocytochemical analysis, confocal imaging was performed using Nikon confocal microscope. The actin filaments of differentiated cells on glass coverslips were clearly seen in figure 4.3. Heterogeneous populations of cells differentiated from ES-NPs posed several problems in visualizing the cytoskeletal arrangement in an individual neuron. Neurons do not

form thick actin stress fiber bundles since they are usually present in soft tissues (modulus of rigidity of brain is < 500 Pa) [288]. In the adjoining images, regular network of actin stress fiber bundles were seen in fibroblasts. The merged image provided an insight into the arrangement of actin fibers of differentiated neurons on glass coverslips. The thin actin fibers of various neurons were arranged in an orderly manner which showed that the neurons were able to attach well to the substrates which is a pre-requisite for the formation of a stable FA.

Glass coverslips

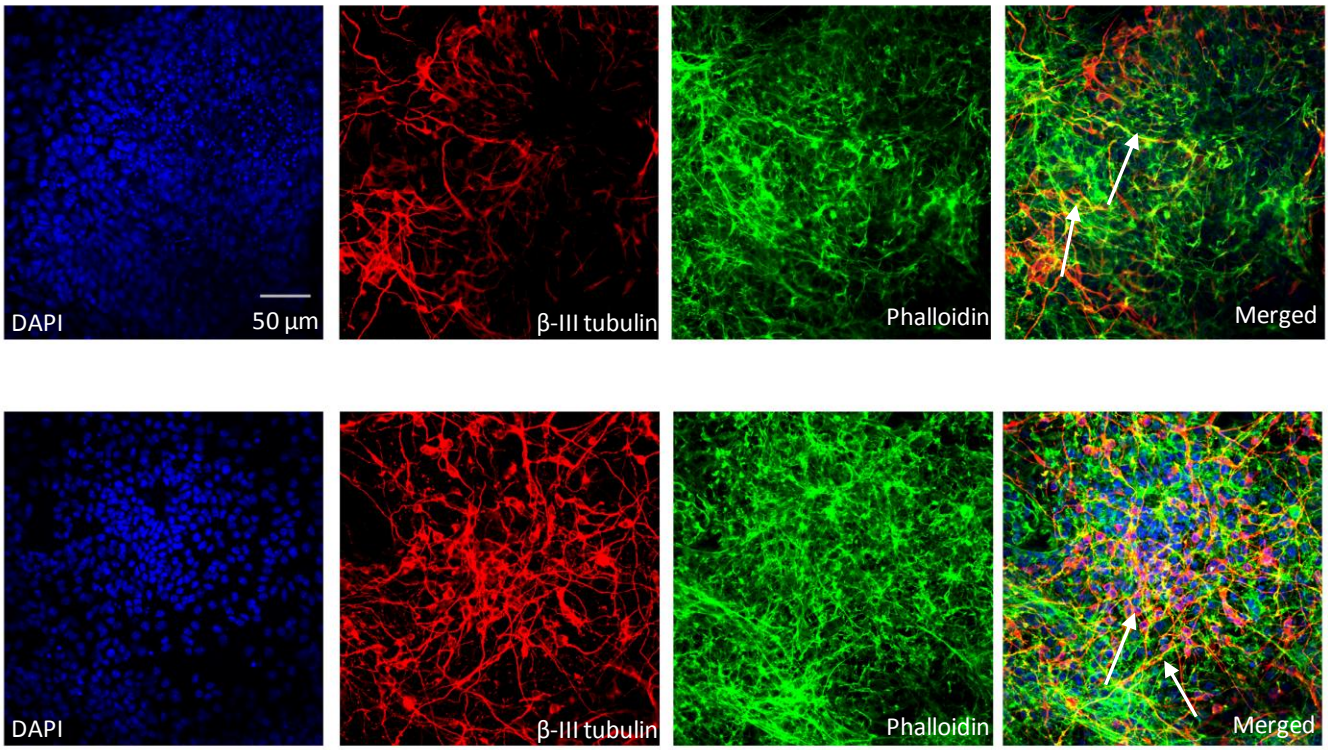

Fig 4.3- Arrangement of actin fibers in neurons differentiated from ES-NPs on glass coverslips. The arrows in the merged image shows the actin fibers of neurons (yellow) arranged in an orderly manner.

The formation of stable FAs enabled neurons to spread out uniformly on the glass coverslips which mimic their properties in natural environment since neurons are adherent cells and tend to spread throughout the substrate forming interconnections with each other.

4.3.2 Actin cytoskeleton arrangement on Glass coverslips coated with conducting polymer PEDOT: PSS

Glass coverslips coated with conducting polymer PEDOT: PSS were used to compare and highlight the role of CP in stem cell differentiation. This provided a better system to gauge the relative importance of elasticity and electrical features on the differentiation potential of ES-NPs. ESNPs were differentiated as described earlier on CP coated glass coverslips, fixed and immunostained with β-III tubulin, Phalloidin and DAPI.

Confocal images of the cells revealed a stark change in the cytoskeletal organization of the cells on the CP-coated coverslips in comparison to their uncoated counterparts. The actin fibers circularized on these substrates leading to the rounding of cells. This tendency was present in the majority of the cells and only a small percentage of cells had well organized actin fibers. Disruption of actin fibers on the CP-coated glass coverslips was akin to cytochalasin treatment on cells which resulted in the loss of contractility of the cells. The disruption of actin fibers lead to the changes in the focal adhesion assembly, preventing it from forming stable FAs and further downstream signaling components of FA play a major role in modulating ES-NP differentiation on these substrates. The disrupted cytoskeletal network also provided an answer to the aggregation tendency of the neurons on CP-coated conducting substrates.The differentiated neurons were not able to spread out on the surface of the substratum and hence tended to aggregate together and proliferate over each other. As seen in row 2 and 3 of fig. 4.4, the disruption of actin fibers was much more in the cells present on top of the aggregate. The neurons had comparatively less disrupted cytoskeleton at aggregate-polymer interface, while cytoskeletal fibers formed round or circular patterns at the top of the aggregates.

Glass coverslips with PEDOT:PSS

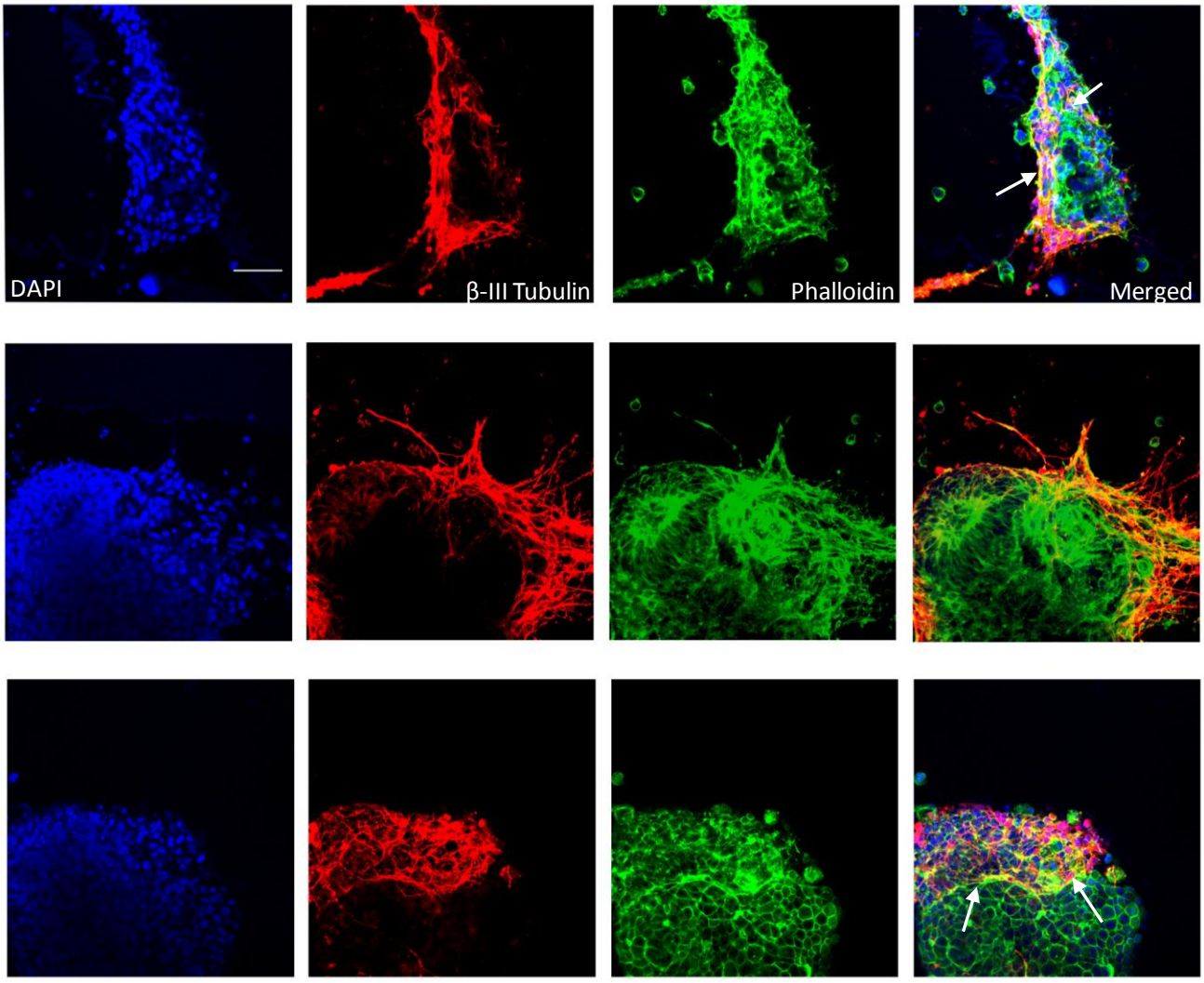

Fig 4.4- Arrangement of actin fibers in neurons differentiated from ES-NPs on glass coverslips coated with PEDOT: PSS. The arrows in the merged image show the disruption in actin fibers of neurons (yellow).Row 2 and 3 show a typical actin fiber arrangement at polymer-aggregate interface and at top of the aggregate respectively. Scale bar, 50µm.

Neurons are too soft to provide a proper anchorage to the layer of cells above them and do not prefer to grow over each other thus preferring a solid substrate to adhere. This lead to a two-fold decrease in the traction forces observed by the cells which further disrupted the actin fiber pattern and hence, lesser differentiation was observed in the aggregates away from the cell-substrate interface.

4.3.3 Actin cytoskeleton arrangement on non-conducting elastomer SEBS and conducting polymer PEDOT: PSS coated SEBS

In the previous chapter, we looked at the differentiation of ES cells on non-conducting elastomer SEBS and conducting polymer PEDOT: PSS coated SEBS substrates. We observed a distinct role played by the surface of each polymeric substrate in guiding the differentiation of cells. Since differentiation of stem cells is intricately connected with the changes in the focal adhesion complex and cytoskeletal arrangement, we investigated these factors to explain the observations of cells on various substrates.

A patterned substrate was used to study the actin fiber arrangement on non-conducting elastomer SEBS and conducting polymer PEDOT: PSS coated SEBS substrates. The substrates were patterned in a manner such that one half of the substrate was coated with PEDOT: PSS while the other half consisted of pristine SEBS. Thus, there were two variable regions on the substrates in terms of conductivity and nanodimensional features. The region coated with PEDOT: PSS provided a conducting surface for cell growth while the other region provided an non-conducting region, thus allowing us to compare the organization of cytoskeletal component of cells on two contrasting substrates in the same field of observation. ES-NPs were differentiated as described earlier on the patterned substrates, fixed and immunostained with β-III tubulin, phalloidin and DAPI. The merged images of β-III tubulin and phalloidin were observed to study the actin fiber arrangement on the substrates.

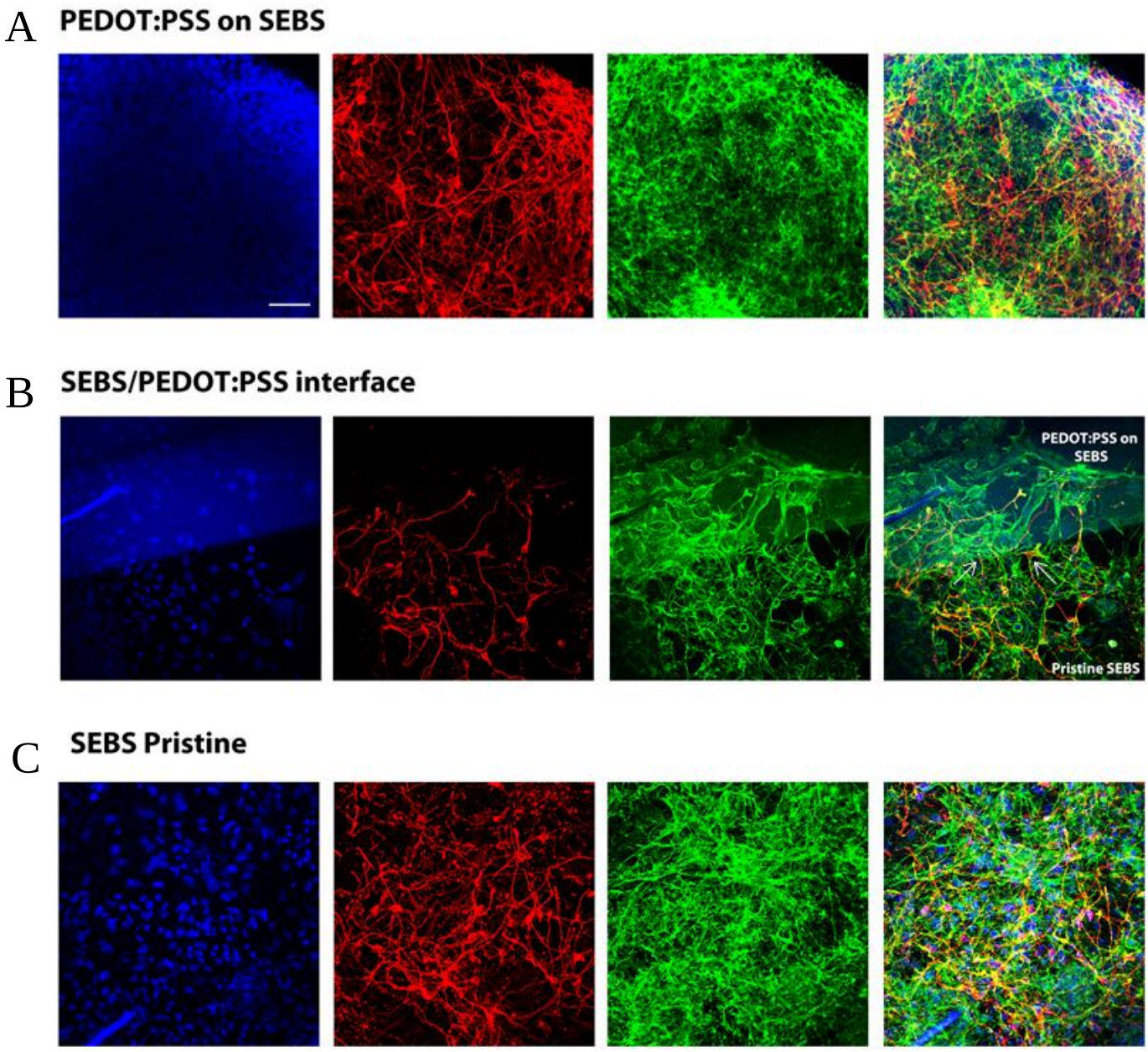

Fig 4.5- Arrangement of actin fibers in neurons differentiated from ES-NPs on SEBS/PEDOT: PSS coated SEBS substrates. The arrangement of actin fibers is distinct on both the substrates. At SEBS/PEDOT: PSS interface, the disruption is quite evident on the conducting substrate with the cells rounding up and the arrowheads show the neurite endings at the interface. Scale bar, 50µm.

Fig. 4.5 depicts the actin arrangement of the differentiated cells on patterned substrates which consist of a conducting and a non-conducting region. The disruption in the cytoskeletal arrangement lead to a more rounded morphology of cells on PEDOT: PSS substrates. Actin fiber pattern in neurons aggregated on conducting polymer was quite distinct from a well spread-out network of neurons on SEBS substrate. The cells adopted a more rounded morphology due to the disruption of their cytoskeletal system which impeded the spreading on the conducting substrates. The arrangement of actin fibers on SEBS substrates was in an orderly manner which helped in generation of stable FA which translated into better differentiation potential of ES-NPs and neuronal spreading. The cells extended out longer neurites on these substrates and only few cells aggregated together.

Fig. 4.5 (B), depicts the actin fiber arrangement on the patterned substrates which further corroborated the observations on the pristine SEBS and CP-coated substrates. Neuronal differentiation and spreading were better on pristine SEBS side of these substrates. The arrows in the figure point out the neurites which abruptly terminated near the interface of both the substrates. These neurites might be retracted by the neurons on the SEBS side, thus preventing them from spreading on the conducting substrates. It was also observed from this image that alongwith neurons, other cell types like fibroblasts, which differentiated from ES-NP cells, also showed disruption of cytoskeletal actin fibers and had tendency to circularize. Fibroblasts generally have a well-developed network of actin stress fibers on SEBS substrates which disrupted on the conducting polymer scaffold. Such stark difference in the arrangement of the actin fibers on the patterned substrate accounted for the change in the neuronal differentiation potential of ES-NPs and cell spreading on conducting CP-coated and non-conducting SEBS substrates.

Actin fiber arrangement on pristine SEBS, CP-coated SEBS and control substrates, helped us to draw a judicious comparison between the physical guidance provided by different substrates. An ordered pattern of actin fiber was seen on Glass coverslips and SEBS compared to the disrupted arrangement in actin fibers on conducting substrates. Cells on CP exhibited disrupted cytoskeleton which showed the role played by the conducting polymer in modulating the cellular behavior. The changes in the cytoskeletal arrangement of cells were transmitted to the adhesion complexes which modulated the traction forces and affected the down-stream

signaling components. These changes resulted in the variability in expression of genes involved in developmental pathways and hence overall neuronal differentiation and cell spreading was affected.

4.4 Discussion

In the previous chapter, effect of various cues provided by the non-conducting elastomeric SEBS and conducting PEDOT: PSS coated SEBS substrates on neuronal differentiation of ES-NPs was seen. The resulting observations were compared with the results obtained on the controls: glass coverslips and PEDOT: PSS coated glass coverslips.

Both, conducting PEDOT: PSS coated SEBS substrates and non-conducting pristine SEBS substrates along with the controls supported neuronal differentiation of ES-NPs. The immature neurons, differentiated from ES-NPs, were identified by β-III tubulin staining while the nucleus of the cell was stained with DAPI. But, the differentiation pattern on the conducting and non-conducting substrates differed vividly. The number of ES-NPs which differentiated into neurons was more on non-conducting SEBS substrates in comparison to their conducting counterparts coated with PEDOT: PSS. Neurons extended longer neurites and spread throughout the substrates on SEBS while on PEDOT: PSS coated substrates neurons tend to stay in aggregates. The spreading and length of neurites was markedly reduced on straining the CP-substrates while an opposite trend was observed on strained SEBS substrates. An increase in the number of differentiated neurons was observed on these substrates which extended even longer neurites. The length of the neurites is directly related to the neuronal spreading and since most of the neurons were present in aggregates or in close proximity, it resulted in the formation of shorter neurites on the conducting substrate in comparison to the non-conducting ones. Increase in the neurite arbor was also observed on the strained non-conducting SEBS substrates.

The aggregates tend to be fewer in number but with a larger surface area on more strained conducting substrates while much smaller and well dispersed aggregates were present on the pristine SEBS substrates. The neurons, within an aggregate, formed inter-linking networks with

the other neurons confined in the neighboring aggregates. The tendency of neurons to remain within the aggregate also attenuated on strained CP-substrates.

Confocal scanning of the aggregates revealed the insights about the differentiation of neurons in these 3-d aggregates. Neuronal differentiation occurred in all the strata of the aggregates but the morphology of these neurons was quite different from the ones which were spread on the surface. Neurons, present inside the aggregates, were comparatively less matured and extended shorter neurites. The neuronal differentiation of ES-NPs was influenced by thestacking of neurons over each other in the aggregates and their distance from the surface. Hence, a decrease in the neuronal differentiation was observed at the top of aggregates in comparison to the aggregate-polymer interface.

ES-NPs also differentiated into glial cells alongwith the neuronal population in a mixed culture. Glial fibrillary acidic protein (GFAP) is a common marker for glial cells and was used to identify them in the culture. It was observed that the glial differentiation was not affected considerably in contrast to the observations with the neuronal population.

Applications of strain on the substrates lead to the generation of local defects in the polymer film. These local defects were able to guide the cell aggregation and "defect patterning" was observed on highly strained PEDOT: PSS substrates. The influence of these defects was more on the conducting substrates as compared to the non-conducting ones since PEDOT:PSS film is more pliable. Defect patterning of cells decreased significantly with the decrease in the strain of substrates and the physical guidance by the local defects was absent on less strained pristine SEBS substrates.

These observations of "environmental sensing" by ES-NPs and physical guidance by the substrate pointed out towards a mechano-transductive type of changes in the cells. The arrangement ofactin cytoskeleton of differentiated ES-NPs on conducting and non-conducting polymeric substrates was investigated.It was observed that the actin cytoskeleton of the cells on conducting substrates was highly disrupted in comparison to its ordered arrangement on non-conducting SEBS substrates and glass coverslips. Heterogeneous population of cells were differentiated from ES-NPs and the differentiated fibroblasts, which secrete neurotrophic factors, had well developed stress fiber bundles of actin filaments on SEBS substrates but on

PEDOT: PSS coated substrates they exhibited prominent disruption in their actin organization. These results are in complete conjunction with the role of cytoskeletal tension in modulating the differentiation, movement and growth of cells. The disruption in the actin fiber arrangement resulted in a loss of cytoskeletal tension in the cells. Stable focal adhesion assemblies are required to support the traction forces applied on the ECM by the cells and any change in the traction forces will lead to further cytoskeletal rearrangement. These changes in actin fibers and their rearrangement are transmitted to all the organelles since they form the basic framework of the cells. As discussed earlier, various signaling molecules like JNK, Src, MEK, Ras and Raf are integral components of the focal adhesion assembly and the loss of stable assembly may lead to changes in the expression level of these signaling molecules. These signaling molecules are involved in various cellular activities like cell migration, proliferation and differentiation and variation in their activity may lead to change in the cellular activities.Cell migration also depends on the formation of stable adhesion complex since it involves active propulsion of cell which can be maintained only after a stable adhesion complexes are generated to bear the weight.

Rho-A and ROCK signaling modulates the stress generated by actin-myosin complex and their role has been implicated in regulating the MSC differentiation into osteoblasts and chondrocytes[289]. Cell shape affected the expression of RhoA which acted as molecular switch between the committment of cells towards adipo/osteo lineages. RhoA effector ROCK lies further downstream of the cell shape requirements and it affects the myosin generated cytoskeletal tension which leads the cells towards osteocyte lineage. The role of substrate stiffness in directing the differentiation of stem cells has shown similar changes in cytoskeletal system [290-291]. When the cells receive adequate traction forces from ECM such that the stable focal adhesion assemblies are formed, it maintains the integrity of cytoskeletal system of the cells. This leads to proper lineage commitment depending on the cell type differentiated. The maturation of focal adhesion complexes is mediated by integrin clustering which recruits other down-stream signaling molecules and this process is controlled by actin-myosin contractility[231].

Thus, it can be clearly seen that mechanotransductive machinery modulates the differentiation of ES-NPs. The role played by cytoskeletal element actin in controlling neuronal differentiation

and spreading is analogous to its effect on cellular behavior on substrates of variable stiffness. But an intriguing question still remains as to how these changes take place in the arrangement of actin fibers and what possible role does surface and inherent property of polymers play in this context.

The initial events leading to cell adhesion on any substrate is accompanied by seeding of extra-cellular matrix proteins to which the surface receptors of the cells bind. The conformation, orientation and quantity of proteins adsorbed are influenced by the surface features, roughness and conductivity of the polymers [292-293]. Polymer oxidation state and surface charge on polymers also modulate the adsorption of DNA and proteins on the surface. It has been reported that Polypyrrole (PPy) adsorbs proteins more easily in its oxidized state than its neutral counterpart [292]. Nanotopographical features influence the stem cell differentiation especially maintenance of its multipotency. The cells interact with the nanopatterned substrates in a manner similar to their interaction with ECM at the nanoscale. Nanoscaled topography mimics the *in vivo* surroundings of the cell which leads to the assimilation of its influence in the biochemical and developmental signaling pathways. It was observed that the upstream changes in the cell adhesion are mediated only in the presence of serum [294]. This means that in the absence of serum there is no change in the cell adhesion which implies constant ECM protein concentration on the surface of the substratum. The orientation and conformation of proteins adsorbed on the surface is crucial for integrins to recognize the specific sites on the adsorbed protein which is a pre-requisite for the initiation of adhesion mediated signaling events. Surface nanotopography also induces certain changes in the geometrical packing of proteins [295].

The substrates used in the experiment contain different nanotopographical features especially the conducting polymer PEDOT: PSS. KPM images of PEDOT: PSS substrates clearly show the presence of PEDOT rich domains in the PSS matrix. PEDOT clusters typically have pan-cake shaped morphology with a domain size in the range of 150-200 nm. When stress is applied on these substrates, it tends to elongate the domains and circular domains become more elliptical. The alignment of PEDOT domains in the matrix of PSS and the generation of local defect patterns result in the formation of regions showing variability in the surface potential and conductivity which modulates the amount of ECM proteins adsorbed on these substrates. Cell adhesion proteins preferentially bind to the PEDOT domains and the variation in the adsorption

of ECM proteins due to conductivity of the substrates modulates the cell adhesion on strained conducting substrates. The elongation of ellipsoidal PEDOT domains results in the development of distinct islands of PEDOT interspersed within PSS matrix and the cell adhesion takes place at these islands. This leads to aggregate formation interspersed throughout the substrates and the modulation of cell adhesion in this mannerresults in the change of actin cytoskeletal arrangement. This further leads to the variation in traction forces which the cells obtain from the substrate. Initial cell adhesion events are dependent upon the favorable surface potential regions but the aggregate formation and cell spreading is influenced strongly by the underlying macroscopic film quality. On highly strained conducting substrates, the distribution of surface potential is more prominent leading to the confinement of cells and presence of larger defect patterns influences the cell spreading which leads to the formation of cellular aggregates. The absence of a CP leads to a uniform distribution of surface potentialon non-conducting pristine SEBS substrateswhich results in a different pattern of cell differentiation. Loss of contractility due to disruption of actin fibers also explains the cell spreading on different substrates. Highly strained conducting substrates lead to unstable adhesion assemblies which results in loss of cell spreading on these substrates. The decrease in the neurite length is observed on these substrates due to aggregation of cells. Inside the aggregates, neurons grow over each other and are not able to provide necessary traction forces since they are very soft. This further leads to the disruption of the actin fiber arrangement and thus, the neuronal differentiation decrease further as we move up along various strata of the aggregate.

AFM images of the conducting and non-conducting substrates show distinct nanotopographical features. The application of strain planarises the substrates and there is a significant decrease in the surface roughness of pristine SEBS substrates. This may influence the differentiation of ES cellsand lead to increase in the number of neuronal cells formed.

The adsorption of extra-cellular matrix proteins on the surface of the substratum is modulated by the bulk hydrophobicity of the substrates[296]. We assessed the role of this form of physical guidance by the substrate and found that the surface hydrophobicity of the conducting PEDOT:PSScoated SEBS and non-conducting SEBS substrates remained constant upon application of strain which ruled out its contribution in affecting the attachment of cells.

The modulus of elasticity of SEBS is in the range of 2 MPa and a thin CP coating does not influence the mechanical property of SEBS considerably. Strain hardening of the polymers upon application of strain leads to further increase in the stiffness of the substrates. The surface of elastomeric polymer SEBS is quite stiff in comparison to the natural environment in which neurons grow and henceit does not contributes appreciably to the changes in cell spreading and differentiation. This clearly shows the role of surface charges, domain alignment of the PEDOT, conductivity of the substrate and local defect patterns in modulating the differentiation of ES cells and subsequently neuronal spreading.

4.5 Conclusion

Electrically conducting polymers are prospective candidates as active substrates for the development of neuroprosthetic devices. The utility of these substrates for promoting differentiation of Embryonic Stem cells paves viable routes for regenerative medicine. In this work the role of conductivity and microstructure of the conducting polymer (CP) surface for stem cell differentiation and development was shown. The electrical and mechanical cues provided to embryonic stem cells during differentiation were precisely modulated by straining the PEDOT: PSS coated on an elastomeric SEBS substrate. The neural differentiation of embryonic stem cells markedly decreases on straining the conducting substrate and differentiated cells tend to remain aggregated on these substrates with differentiation being more at the aggregate-polymer interface. The pattern of neuronal differentiation on non-conducting SEBS, on the other hand, shows an opposite trend with an increase in the neuronal differentiation and cell spreading. Polymer chains and domains on alignment in strained substrates lead to disruption of actin cytoskeleton of cells which provides a mechano-transductive basis for the observed changes in the differentiation. Local defects were generated in the conducting substrates which guided cells to pattern along them resulting in “defect patterning” of cells. These results demonstrate that along with biochemical and mechanical cues, conductivity of the polymer plays a major role in cellular differentiation thus providing another control feature to modulate the differentiation and proliferation of stem cells.

Chapter 5

Summary and Future Directions

Conducting polymers possess interesting optical and electronic properties. Apart from the field of photovoltaics and optoelectronics, these polymers find increasing relevance in the field of tissue engineering. Neuronal cells are terminally differentiated cells which lose their ability to regenerate upon maturation, thus making the treatment of CNS diseases much more difficult. The ability of these polymers to stimulate the neuronal cells which aids in their development has provided a boon to the area of neural tissue engineering. Stretchable conducting polymer (CP) substrates offer an alternate substrate for neuronal growth which can be used for the development of neuroprosthetic devices. Promotion of neuronal growth on the conducting polymer electrodes enables intricate contact at the cell-electrode interface which provides long term cellular activation and functional recordings. Electrically conducting polymer on a soft elastomeric scaffold provides a rigid support for the differentiation of stem cells. These substrates can be used for the implantation in the injured tissue areas providing mechanical support and spatially arranged cues for the regenerating neurons.

The effect of conducting physical microenvironment of CP was studied on the neuronal differentiation potential of the embryonic stem cells. In this work, the role of conductivity and microstructure of the conducting polymer surface for stem cell differentiation and proliferation was emphasized. The conductivity of the CP coated elastomeric substrates was precisely controlled by the application of strain. This resulted in the alignment of randomly distributed spherical PEDOT domains into ellipsoidal domains within the polyanionic PSS matrix. The surface potential distribution of the CP substrate changed significantly suggesting a control of the distribution of these surface potentials at nanometer length scales by straining. The stiffness of the substrates also increased upon straining the CP-coated SEBS substrates due to strain hardening. AFM images also showed the variation in the surface roughness of the CP-coated and pristine SEBS substrates. The value of surface roughness also changed upon straining these

substrates. Thus, CP-coating and application of strain resulted in a significant change in the surface properties of these polymeric substrates.

The viability of these substrates for stem cell differentiation was then assessed by maintaining the culture of GFP tagged ES cells which clearly showed that these substrates are conducive for the development of neurons. Next, the ES-NPs were cultured on these substrates to study the affect of the physical cues provided by the substrates. The cells were then immunostained with specific neuronal marker β-III tubulin, glial marker GFAP and DAPI to stain the nuclei of cells. Strained CP and elastomeric substrates were used to study the influence of the strained substrates on the neuronal differentiation. It was observed that the conducting substrates affected the cell spreading and induced the formation of cellular aggregates. Neuronal differentiation was markedly reduced and aggregation of cells took place on strained CP substrates with most neurons differentiating within the aggregates thus leading to a decrease in neurite length. In comparison, the neurons differentiated and spread well on the elastomeric substrates and these strained substrates promoted this cellular behavior.

The choice of spatial location on the strained substrate can possibly be explained by the formation of topographical features. Delamination of the CP films takes place on straining the CP-coated elastomeric substrates which resulted in the formation of slip defects orthogonal to the strain direction. It can be interpreted that these defects could lead to 'defect patterning' of cells with cellular aggregates aligning along these defects on highly strained CP substrates.

The cause of the changes in the neuronal differentiation and spreading were investigated further. Actin cytoskeletal arrangement of differentiated neurons was assessed by phalloidinimmunostaining and disruption of actin fiber arrangement was observed on CP substrates. In comparison, the neurons on non-conducting SEBS substrates and glass coverslips exhibited well-arranged actin fibers. This showed that the changes in the cytoskeletal arrangement played a major role in modulating the stem cell activity. We looked into the possible role of the substrate in modulating actin arrangement. The variation in the surface potential modulated the extra-cellular matrix proteins adsorbed on the substrate which affects the initial cell adhesion events. The cellular spreading and aggregate formation of cells is also affected by the underlying macroscopic film quality and the highly strained CP substrates perturb these cellular functions. Non-conducting elastomers, on the other hand, are devoid of

these changes in the surface potential and present a neutral surface where cells adhere and spread evenly throughout and straining these substrates lead to a decrease in surface roughness which may have alleviated the neuronal differentiation and spreading.

Detailed investigation in the role of focal adhesion assembly on the conducting substrates is mandated. The role of Vinculin also needs to be observed to clearly understand the changes in the actin cytoskeleton. The understanding of the molecular events accompanying these changes will help us to engineer the intelligent substrates for desired biomedical applications.*in vivo* studies of these substrates is need to ascertain their cytotoxicity, haemocompatibility and biocompatibility.

References

1. Peppas, N.A., et al., *Hydrogels in biology and medicine: From molecular principles to bionanotechnology.* Advanced Materials, 2006. **18**(11): p. 1345-1360.
2. Collazos-Castro, J.E., et al., *Bioelectrochemical control of neural cell development on conducting polymers.* Biomaterials, 2010. **31**(35): p. 9244-9255.
3. Eyckmans, J., et al., *A hitchhiker's guide to mechanobiology.* Dev Cell, 2011. **21**(1): p. 35-47.
4. Discher, D.E., P. Janmey, and Y.L. Wang, *Tissue cells feel and respond to the stiffness of their substrate.* Science, 2005. **310**(5751): p. 1139-43.
5. Lo, C.M., et al., *Cell movement is guided by the rigidity of the substrate.* Biophysical Journal, 2000. **79**(1): p. 144-152.
6. Pelham, R.J. and Y.L. Wang, *Cell locomotion and focal adhesions are regulated by substrate flexibility.* Proceedings of the National Academy of Sciences of the United States of America, 1997. **94**(25): p. 13661-13665.
7. Flanagan, L.A., et al., *Neurite branching on deformable substrates.* Neuroreport, 2002. **13**(18): p. 2411-2415.
8. Leach, J.B., et al., *Neurite outgrowth and branching of PC12 cells on very soft substrates sharply decreases below a threshold of substrate rigidity.* Journal of Neural Engineering, 2007. **4**(2): p. 26-34.
9. Gunn, J.W., S.D. Turner, and B.K. Mann, *Adhesive and mechanical properties of hydrogels influence neurite extension.* Journal of Biomedical Materials Research Part A, 2005. **72**(1): p. 91-7.
10. Dubey, N., P.C. Letourneau, and R.T. Tranquillo, *Neuronal contact guidance in magnetically aligned fibrin gels: effect of variation in gel mechano-structural properties.* Biomaterials, 2001. **22**(10): p. 1065-75.
11. Thomas, T.W. and P.A. DiMilla, *Spreading and motility of human glioblastoma cells on sheets of silicone rubber depend on substratum compliance.* Med Biol Eng Comput, 2000. **38**(3): p. 360-70.
12. Levental, I., P.C. Georges, and P.A. Janmey, *Soft biological materials and their impact on cell function.* Soft Matter, 2007. **3**(3): p. 299-306.
13. Engler, A.J., et al., *Matrix elasticity directs stem cell lineage specification.* Cell, 2006. **126**(4): p. 677-689.
14. Saha, K., et al., *Substrate Modulus Directs Neural Stem Cell Behavior.* Biophysical Journal, 2008. **95**(9): p. 4426-4438.
15. Yoda, R., *Elastomers for biomedical applications.* J Biomater Sci Polym Ed, 1998. **9**(6): p. 561-626.
16. Irvine, D.J., et al., *Nanoscale clustering of RGD peptides at surfaces using comb polymers. 2. Surface segregation of comb polymers in polylactide.* Biomacromolecules, 2001. **2**(2): p. 545-556.
17. Hubbell, J.A., *Bioactive biomaterials.* Current Opinion in Biotechnology, 1999. **10**(2): p. 123-129.
18. Goddard, J.M. and J.H. Hotchkiss, *Polymer surface modification for the attachment of bioactive compounds.* Progress in Polymer Science, 2007. **32**(7): p. 698-725.

19. Richey, T., et al., *Surface modification of polyethylene balloon catheters for local drug delivery.* Biomaterials, 2000. **21**(10): p. 1057-65.
20. Langer, R., *Drug delivery and targeting.* Nature, 1998. **392**(6679 Suppl): p. 5-10.
21. Moy, V.T., E.L. Florin, and H.E. Gaub, *Intermolecular Forces and Energies between Ligands and Receptors.* Science, 1994. **266**(5183): p. 257-259.
22. Alferiev, I.S., et al., *Surface heparinization of polyurethane via bromoalkylation of hard segment nitrogens.* Biomacromolecules, 2006. **7**(1): p. 317-322.
23. Liu, X.H. and P.X. Ma, *Polymeric scaffolds for bone tissue engineering.* Annals of Biomedical Engineering, 2004. **32**(3): p. 477-486.
24. Kuhl, P.R. and L.G. GriffithCima, *Tethered epidermal growth factor as a paradigm for growth factor-induced stimulation from the solid phase.* Nature Medicine, 1996. **2**(9): p. 1022-1027.
25. Sakiyama-Elbert, S.E., A. Panitch, and J.A. Hubbell, *Development of growth factor fusion proteins for cell-triggered drug delivery.* Faseb Journal, 2001. **15**(7): p. 1300-1302.
26. Zisch, A.H., et al., *Covalently conjugated VEGF-fibrin matrices for endothelialization.* Journal of Controlled Release, 2001. **72**(1-3): p. 101-113.
27. Lutolf, M.R., et al., *Repair of bone defects using synthetic mimetics of collagenous extracellular matrices.* Nature Biotechnology, 2003. **21**(5): p. 513-518.
28. Hubbell, J.A., *Biomaterials in tissue engineering.* Biotechnology (N Y), 1995. **13**(6): p. 565-76.
29. Massia, S.P. and J.A. Hubbell, *Vascular endothelial cell adhesion and spreading promoted by the peptide REDV of the IIICS region of plasma fibronectin is mediated by integrin alpha 4 beta 1.* J Biol Chem, 1992. **267**(20): p. 14019-26.
30. Langer, R. and J.P. Vacanti, *Tissue engineering.* Science, 1993. **260**(5110): p. 920-6.
31. Peppas, N.A. and R. Langer, *New challenges in biomaterials.* Science, 1994. **263**(5154): p. 1715-20.
32. Bischoff, F., *Organic polymer biocompatibility and toxicology.* Clin Chem, 1972. **18**(9): p. 869-94.
33. Braley, S., *The Chemistry and Properties of the Medical-Grade Silicones.* Journal of Macromolecular Science: Part A - Chemistry, 1970. **4**(3): p. 529-544.
34. Tang, Z., et al., *Biomedical Applications of Layer-by-Layer Assembly: From Biomimetics to Tissue Engineering.* Advanced Materials, 2006. **18**(24): p. 3203-3224.
35. Subramanian, A. and H.Y. Lin, *Crosslinked chitosan: its physical properties and the effects of matrix stiffness on chondrocyte cell morphology and proliferation.* Journal of Biomedical Materials Research Part A, 2005. **75**(3): p. 742-53.
36. Hensten-Pettersen, A. and A. Hulterström, *Assessment of in vitro cytotoxicity of four RTV-silicone elastomers used for maxillofacial prostheses.* Acta Odontologica Scandinavica, 1980. **38**(3): p. 163-167.
37. Chauvel-Lebret, D., P. Auroy, and M. Bonnaure-Mallet, *Biocompatibility of Elastomers*, in *Polymeric Biomaterials, Revised and Expanded*. 2001, CRC Press.
38. Kalicharan, D., et al., *Cell-Ingrowth in a Silicone Plombe - Interactions between Biomaterial and Scleral Tissue after 8 Years Insitu - a Sem and Tem Investigation.* Documenta Ophthalmologica, 1991. **78**(3-4): p. 307-315.
39. Silver, J.H., et al., *Surface properties and hemocompatibility of alkyl-siloxane monolayers supported on silicone rubber: effect of alkyl chain length and ionic functionality.* Biomaterials, 1999. **20**(17): p. 1533-1543.
40. Chen, H., M.A. Brook, and H. Sheardown, *Silicone elastomers for reduced protein adsorption.* Biomaterials, 2004. **25**(12): p. 2273-2282.
41. Fujii, T., *PDMS-based microfluidic devices for biomedical applications.* Microelectronic Engineering, 2002. **61-2**: p. 907-914.

42. Abbasi, F., H. Mirzadeh, and A.A. Katbab, *Modification of polysiloxane polymers for biomedical applications: a review.* Polymer International, 2001. **50**(12): p. 1279-1287.
43. Mata, A., A.J. Fleischman, and S. Roy, *Characterization of polydimethylsiloxane (PDMS) properties for biomedical micro/nanosystems.* Biomedical Microdevices, 2005. **7**(4): p. 281-293.
44. Georges, P.C., et al., *Matrices with Compliance Comparable to that of Brain Tissue Select Neuronal over Glial Growth in Mixed Cortical Cultures.* Biophysical Journal, 2006. **90**(8): p. 3012-3018.
45. McBeath, R., et al., *Cell shape, cytoskeletal tension, and RhoA regulate stem cell lineage commitment.* Dev Cell, 2004. **6**(4): p. 483-95.
46. Cooper, S.L. and A.V. Tobolsky, *Properties of linear elastomeric polyurethanes.* Journal of Applied Polymer Science, 1966. **10**(12): p. 1837-1844.
47. Boretos, J.W. and W.S. Pierce, *Segmented Polyurethane: A New Elastomer for Biomedical Applications.* Science, 1967. **158**(3807): p. 1481-1482.
48. Bonart, R., *X-ray investigations concerning the physical structure of cross-linking in segmented urethane elastomers.* Journal of Macromolecular Science, Part B, 1968. **2**(1): p. 115-138.
49. Coury, A.J., et al., *Factors and interactions affecting the performance of polyurethane elastomers in medical devices.* J Biomater Appl, 1988. **3**(2): p. 130-79.
50. Takahara, A., et al., *Effect of soft segment chemistry on the biostability of segmented polyurethanes. I. In vitro oxidation.* J Biomed Mater Res, 1991. **25**(3): p. 341-56.
51. Hergenrother, R.W., X.H. Yu, and S.L. Cooper, *Blood-Contacting Properties of Polydimethylsiloxane Polyurea-Urethanes.* Biomaterials, 1994. **15**(8): p. 635-640.
52. Capone, C.D., *Biostability of a non-ether polyurethane.* J Biomater Appl, 1992. **7**(2): p. 108-29.
53. Lim, F., C.Z. Yang, and S.L. Cooper, *Synthesis, Characterization and Ex-Vivo Evaluation of Polydimethylsiloxane Polyurea-Urethanes.* Biomaterials, 1994. **15**(6): p. 408-416.
54. Pinchuk, L., *A review of the biostability and carcinogenicity of polyurethanes in medicine and the new generation of 'biostable' polyurethanes.* J Biomater Sci Polym Ed, 1994. **6**(3): p. 225-67.
55. Bakker, D., et al., *Biocompatibility of six elastomers in vitro.* J Biomed Mater Res, 1988. **22**(5): p. 423-39.
56. Bschorer, R., et al., *Experimental Improvement of Microvascular Allografts with the New Material Polyurethane and Microvessel Endothelial-Cell Seeding.* International Journal of Oral and Maxillofacial Surgery, 1994. **23**(6): p. 389-392.
57. Bakker, D., et al., *Biocompatibility of a Polyether Urethane, Polypropylene Oxide, and a Polyether Polyester Copolymer - a Qualitative and Quantitative Study of 3 Alloplastic Tympanic Membrane Materials in the Rat Middle-Ear.* Journal of Biomedical Materials Research, 1990. **24**(4): p. 489-515.
58. Sigot-Luizard, M.F., et al., *A novel microporous polyurethane blood conduit: biocompatibility assessment of the UTA arterial prosthesis by an organo-typic culture technique.* J Invest Surg, 1993. **6**(3): p. 251-71.
59. Huang, B., et al., *Cellular reaction to the Vascugraft polyesterurethane vascular prosthesis: in vivo studies in rats.* Biomaterials, 1992. **13**(4): p. 209-16.
60. Collier, T., et al., *Biocompatibility of poly(etherurethane urea) containing dehydroepiandrosterone.* J Biomed Mater Res, 1998. **41**(2): p. 192-201.
61. Saad, B., et al., *Interactions of osteoblasts and macrophages with biodegradable and highly porous polyesterurethane foam and its degradation products.* Journal of Biomedical Materials Research, 1996. **32**(3): p. 355-366.
62. Saad, B., et al., *Development of degradable polyesterurethanes for medical applications: in vitro and in vivo evaluations.* J Biomed Mater Res, 1997. **36**(1): p. 65-74.

63. Nakamura, A., et al., *Correlations among Chemical-Constituents, Cytotoxicities and Tissue Responses - in the Case of Natural-Rubber Latex Materials.* Biomaterials, 1990. **11**: p. 92-94.
64. Razzak, M.T., et al., *Modification of Natural-Rubber Tubes for Biomaterials .1. Radiation-Induced Grafting of N,N-Dimethyl Acrylamide onto Natural-Rubber Tubes.* Journal of Applied Polymer Science, 1988. **36**(3): p. 645-653.
65. Tucci, M.G., et al., *Structural features of latex gloves in dental practice.* Biomaterials, 1996. **17**(5): p. 517-522.
66. Lendlein, A. and R. Langer, *Biodegradable, elastic shape-memory polymers for potential biomedical applications.* Science, 2002. **296**(5573): p. 1673-1676.
67. de Las Heras Alarcon, C., S. Pennadam, and C. Alexander, *Stimuli responsive polymers for biomedical applications.* Chem Soc Rev, 2005. **34**(3): p. 276-85.
68. Chow, D., et al., *Peptide-based biopolymers in biomedicine and biotechnology.* Materials Science & Engineering R-Reports, 2008. **62**(4): p. 125-155.
69. Langer, R. and N.A. Peppas, *Advances in biomaterials, drug delivery, and bionanotechnology.* Aiche Journal, 2003. **49**(12): p. 2990-3006.
70. Lin, C.C. and K.S. Anseth, *PEG Hydrogels for the Controlled Release of Biomolecules in Regenerative Medicine.* Pharmaceutical Research, 2009. **26**(3): p. 631-643.
71. Merrill, E.W., et al., *Platelet-compatible hydrophilic segmented polyurethanes from polyethylene glycols and cyclohexane diisocyanate.* Trans Am Soc Artif Intern Organs, 1982. **28**: p. 482-7.
72. Ratner, B.D., et al., *Biomaterials Science - An Introduction to Materials in Medicine (2nd Edition)*, Elsevier.
73. West, J.L. and J.A. Hubbell, *Photopolymerized Hydrogel Materials for Drug-Delivery Applications.* Reactive Polymers, 1995. **25**(2-3): p. 139-147.
74. Hern, D.L. and J.A. Hubbell, *Incorporation of adhesion peptides into nonadhesive hydrogels useful for tissue resurfacing.* Journal of Biomedical Materials Research, 1998. **39**(2): p. 266-276.
75. Kidane, A., J.M. Szabocsik, and K. Park, *Accelerated study on lysozyme deposition on poly(HEMA) contact lenses.* Biomaterials, 1998. **19**(22): p. 2051-2055.
76. Lu, S.X. and K.S. Anseth, *Photopolymerization of multilaminated poly(HEMA) hydrogels for controlled release.* Journal of Controlled Release, 1999. **57**(3): p. 291-300.
77. Meyvis, T.K.L., et al., *Influence of the degradation mechanism of hydrogels on their elastic and swelling properties during degradation.* Macromolecules, 2000. **33**(13): p. 4717-4725.
78. Sefton, M.V., et al., *Making microencapsulation work: conformal coating, immobilization gels and in vivo performance.* Journal of Controlled Release, 2000. **65**(1-2): p. 173-186.
79. Hassan, C.M. and N.A. Peppas, *Structure and Morphology of Freeze/Thawed PVA Hydrogels.* Macromolecules, 2000. **33**(7): p. 2472-2479.
80. Nuttelman, C.R., et al., *Attachment of fibronectin to poly(vinyl alcohol) hydrogels promotes NIH3T3 cell adhesion, proliferation, and migration.* J Biomed Mater Res, 2001. **57**(2): p. 217-23.
81. Peppas, N.A. and E.W. Merrill, *Development of semicrystalline poly(vinyl alcohol) hydrogels for biomedical applications.* J Biomed Mater Res, 1977. **11**(3): p. 423-34.
82. Martens, P.J., S.J. Bryant, and K.S. Anseth, *Tailoring the degradation of hydrogels formed from multivinyl poly(ethylene glycol) and poly(vinyl alcohol) macromers for cartilage tissue engineering.* Biomacromolecules, 2003. **4**(2): p. 283-92.
83. Schmedlen, R.H., K.S. Masters, and J.L. West, *Photocrosslinkable polyvinyl alcohol hydrogels that can be modified with cell adhesion peptides for use in tissue engineering.* Biomaterials, 2002. **23**(22): p. 4325-32.
84. Khare, A.R. and N.A. Peppas, *Release behavior of bioactive agents from pH-sensitive hydrogels.* J Biomater Sci Polym Ed, 1993. **4**(3): p. 275-89.

85. Podual, K. and N.A. Peppas, *Relaxational behavior and swelling-pH master curves of poly[(diethylaminoethyl methacrylate)-graft-(ethylene glycol)] hydrogels.* Polymer International, 2005. **54**(3): p. 581-593.
86. Sershen, S. and J. West, *Implantable, polymeric systems for modulated drug delivery (vol 54, pg 1225, 2002).* Advanced Drug Delivery Reviews, 2003. **55**(3): p. 439-439.
87. Lee, K.Y. and D.J. Mooney, *Hydrogels for tissue engineering.* Chemical Reviews, 2001. **101**(7): p. 1869-1879.
88. Lee, C.R., A.J. Grodzinsky, and M. Spector, *The effects of cross-linking of collagen-glycosaminoglycan scaffolds on compressive stiffness, chondrocyte-mediated contraction, proliferation and biosynthesis.* Biomaterials, 2001. **22**(23): p. 3145-3154.
89. Lee, C.R., A.J. Grodzinsky, and M. Spector, *Modulation of the contractile and Biosynthetic activity of chondrocytes seeded in collagen-glycosaminoglycan matrices.* Tissue Engineering, 2003. **9**(1): p. 27-36.
90. Schoof, H., et al., *Control of pore structure and size in freeze-dried collagen sponges.* Journal of Biomedical Materials Research, 2001. **58**(4): p. 352-357.
91. Vercruysse, K.P., et al., *Synthesis and in vitro degradation of new polyvalent hydrazide cross-linked hydrogels of hyaluronic acid.* Bioconjugate Chemistry, 1997. **8**(5): p. 686-694.
92. Burdick, J.A., et al., *Controlled degradation and mechanical behavior of photopolymerized hyaluronic acid networks.* Biomacromolecules, 2005. **6**(1): p. 386-391.
93. Kuo, C.K. and P.X. Ma, *Ionically crosslinked alginate hydrogels as scaffolds for tissue engineering: Part 1. Structure, gelation rate and mechanical properties.* Biomaterials, 2001. **22**(6): p. 511-521.
94. Drury, J.L., R.G. Dennis, and D.J. Mooney, *The tensile properties of alginate hydrogels.* Biomaterials, 2004. **25**(16): p. 3187-3199.
95. Suh, J.K.F. and H.W.T. Matthew, *Application of chitosan-based polysaccharide biomaterials in cartilage tissue engineering: a review.* Biomaterials, 2000. **21**(24): p. 2589-2598.
96. Ishihara, M., et al., *Photocrosslinkable chitosan as a dressing for wound occlusion and accelerator in healing process.* Biomaterials, 2002. **23**(3): p. 833-840.
97. Lee, K.Y., W.S. Ha, and W.H. Park, *Blood Compatibility and Biodegradability of Partially N-Acylated Chitosan Derivatives.* Biomaterials, 1995. **16**(16): p. 1211-1216.
98. Li, J. and Z. Xu, *Physical characterization of a chitosan-based hydrogel delivery system.* J Pharm Sci, 2002. **91**(7): p. 1669-77.
99. Gil, E.S. and S.M. Hudson, *Stimuli-reponsive polymers and their bioconjugates.* Progress in Polymer Science, 2004. **29**(12): p. 1173-1222.
100. Burdick, J.A., A. Khademhosseini, and R. Langer, *Fabrication of gradient hydrogels using a microfluidics/photopolymerization process.* Langmuir, 2004. **20**(13): p. 5153-6.
101. Burdick, J.A. and K.S. Anseth, *Photoencapsulation of osteoblasts in injectable RGD-modified PEG hydrogels for bone tissue engineering.* Biomaterials, 2002. **23**(22): p. 4315-23.
102. Kobayashi, H. and Y. Ikada, *Covalent immobilization of proteins on to the surface of poly(vinyl alcohol) hydrogel.* Biomaterials, 1991. **12**(8): p. 747-51.
103. Mann, B.K., R.H. Schmedlen, and J.L. West, *Tethered-TGF-beta increases extracellular matrix production of vascular smooth muscle cells.* Biomaterials, 2001. **22**(5): p. 439-44.
104. Suzuki, Y., et al., *Alginate hydrogel linked with synthetic oligopeptide derived from BMP-2 allows ectopic osteoinduction in vivo.* J Biomed Mater Res, 2000. **50**(3): p. 405-9.
105. Lahooti, S. and M.V. Sefton, *Agarose enhances the viability of intraperitoneally implanted microencapsulated L929 fibroblasts.* Cell Transplantation, 2000. **9**(6): p. 785-796.
106. Lahooti, S. and M.V. Sefton, *Effect of an immobilization matrix and capsule membrane permeability on the viability of encapsulated HEK cells.* Biomaterials, 2000. **21**(10): p. 987-995.

107. Lim, F. and A.M. Sun, *Microencapsulated islets as bioartificial endocrine pancreas.* Science, 1980. **210**(4472): p. 908-10.
108. Sershen, S.R., et al., *Independent optical control of microfluidic valves formed from optomechanically responsive nanocomposite hydrogels.* Advanced Materials, 2005. **17**(11): p. 1366-+.
109. Morrison, S.J., N.M. Shah, and D.J. Anderson, *Regulatory mechanisms in stem cell biology.* Cell, 1997. **88**(3): p. 287-98.
110. Zipori, D., *The stem state: plasticity is essential, whereas self-renewal and hierarchy are optional.* Stem Cells, 2005. **23**(6): p. 719-26.
111. Ogawa, M., *Differentiation and proliferation of hematopoietic stem cells.* Blood, 1993. **81**(11): p. 2844-53.
112. Bain, G., et al., *Embryonic stem cells express neuronal properties in vitro.* Dev Biol, 1995. **168**(2): p. 342-57.
113. Bradley, A., et al., *Formation of germ-line chimaeras from embryo-derived teratocarcinoma cell lines.* Nature, 1984. **309**(5965): p. 255-6.
114. Thomson, J.A., et al., *Embryonic stem cell lines derived from human blastocysts.* Science, 1998. **282**(5391): p. 1145-7.
115. Smith, A.G., et al., *Inhibition of pluripotential embryonic stem cell differentiation by purified polypeptides.* Nature, 1988. **336**(6200): p. 688-90.
116. Xu, C., et al., *Feeder-free growth of undifferentiated human embryonic stem cells.* Nature Biotechnology, 2001. **19**(10): p. 971-4.
117. Martin, M.J., et al., *Human embryonic stem cells express an immunogenic nonhuman sialic acid.* Nat Med, 2005. **11**(2): p. 228-32.
118. Gage, F.H., *Mammalian neural stem cells.* Science, 2000. **287**(5457): p. 1433-1438.
119. Novak, U. and A.H. Kaye, *Extracellular matrix and the brain: components and function.* Journal of Clinical Neuroscience, 2000. **7**(4): p. 280-290.
120. Steindler, D.A., et al., *Boundaries during normal and abnormal brain development: In vivo and in vitro studies of glia and glycoconjugates.* Experimental Neurology, 1990. **109**(1): p. 35-56.
121. Steindler, D.A., *Glial boundaries in the developing nervous system.* Annu Rev Neurosci, 1993. **16**: p. 445-70.
122. Steindler, D.A., et al., *Boundaries Defined by Adhesion Molecules during Development of the Cerebral-Cortex - the J1/Tenascin Glycoprotein in the Mouse Somatosensory Cortical Barrel Field.* Developmental Biology, 1989. **131**(1): p. 243-260.
123. Laywell, E.D., et al., *Enhanced expression of the developmentally regulated extracellular matrix molecule tenascin following adult brain injury.* Proc Natl Acad Sci U S A, 1992. **89**(7): p. 2634-8.
124. Kearns, S.M., et al., *Extracellular matrix effects on neurosphere cell motility.* Exp Neurol, 2003. **182**(1): p. 240-4.
125. George, E.L., et al., *Defects in mesoderm, neural tube and vascular development in mouse embryos lacking fibronectin.* Development, 1993. **119**(4): p. 1079-91.
126. Pons, S., et al., *Vitronectin regulates Sonic hedgehog activity during cerebellum development through CREB phosphorylation.* Development, 2001. **128**(9): p. 1481-1492.
127. Kearns, S.M., et al., *Extracellular matrix effects on neurosphere cell motility.* Experimental Neurology, 2003. **182**(1): p. 240-244.
128. Rogers, S.L., et al., *Neurite extension by peripheral and central nervous system neurons in response to substratum-bound fibronectin and laminin.* Dev Biol, 1983. **98**(1): p. 212-20.
129. Grimpe, B., et al., *The critical role of basement membrane-independent laminin gamma 1 chain during axon regeneration in the CNS.* J Neurosci, 2002. **22**(8): p. 3144-60.

130. Dunnett, S.B., D.C. Rogers, and S.J. Richards, *Nigrostriatal reconstruction after 6-OHDA lesions in rats: combination of dopamine-rich nigral grafts and nigrostriatal "bridge" grafts.* Exp Brain Res, 1989. **75**(3): p. 523-35.
131. Metallo, C.M., et al., *Engineering the stem cell microenvironment.* Biotechnol Prog, 2007. **23**(1): p. 18-23.
132. Williams, C.A. and E.B. Lavik, *Engineering the CNS stem cell microenvironment.* Regen Med, 2009. **4**(6): p. 865-77.
133. Manasek, F.J., M.B. Burnside, and R.E. Waterman, *Myocardial cell shape change as a mechanism of embryonic heart looping.* Developmental Biology, 1972. **29**(4): p. 349-371.
134. Folkman, J. and A. Moscona, *Role of cell shape in growth control.* Nature, 1978. **273**(5661): p. 345-9.
135. Holtzer, H., et al., *The Loss of Phenotypic Traits by Differentiated Cells in Vitro, I. Dedifferentiation of Cartilage Cells.* Proc Natl Acad Sci U S A, 1960. **46**(12): p. 1533-42.
136. Abbott, J. and H. Holtzer, *The loss of phenotypic traits by differentiated cells. 3. The reversible behavior of chondrocytes in primary cultures.* J Cell Biol, 1966. **28**(3): p. 473-87.
137. Benya, P.D. and J.D. Shaffer, *Dedifferentiated chondrocytes reexpress the differentiated collagen phenotype when cultured in agarose gels.* Cell, 1982. **30**(1): p. 215-24.
138. Chen, C.S., et al., *Micropatterned surfaces for control of cell shape, position, and function.* Biotechnol Prog, 1998. **14**(3): p. 356-63.
139. Chen, C.S., et al., *Cell shape provides global control of focal adhesion assembly.* Biochem Biophys Res Commun, 2003. **307**(2): p. 355-61.
140. Ingber, D.E., *The mechanochemical basis of cell and tissue regulation.* Mech Chem Biosyst, 2004. **1**(1): p. 53-68.
141. Hadjipanayi, E., V. Mudera, and R.A. Brown, *Close dependence of fibroblast proliferation on collagen scaffold matrix stiffness.* J Tissue Eng Regen Med, 2009. **3**(2): p. 77-84.
142. Guo, W.H., et al., *Substrate rigidity regulates the formation and maintenance of tissues.* Biophysical Journal, 2006. **90**(6): p. 2213-20.
143. Pelham, R.J. and Y.L. Wang, *Cell locomotion and focal adhesions are regulated by substrate flexibility (vol 94, pg 13661, 1997).* Proceedings of the National Academy of Sciences of the United States of America, 1998. **95**(20): p. 12070-12070.
144. Wang, H.-B., M. Dembo, and Y.-L. Wang, *Substrate flexibility regulates growth and apoptosis of normal but not transformed cells.* American Journal of Physiology - Cell Physiology, 2000. **279**(5): p. C1345-C1350.
145. Deroanne, C.F., C.M. Lapiere, and B.V. Nusgens, *In vitro tubulogenesis of endothelial cells by relaxation of the coupling extracellular matrix-cytoskeleton.* Cardiovasc Res, 2001. **49**(3): p. 647-58.
146. Hayman, M.W., et al., *Growth of human stem cell-derived neurons on solid three-dimensional polymers.* J Biochem Biophys Methods, 2005. **62**(3): p. 231-40.
147. Recknor, J.B., D.S. Sakaguchi, and S.K. Mallapragada, *Directed growth and selective differentiation of neural progenitor cells on micropatterned polymer substrates.* Biomaterials, 2006. **27**(22): p. 4098-108.
148. Yim, E.K.F., S.W. Pang, and K.W. Leong, *Synthetic nanostructures inducing differentiation of human mesenchymal stem cells into neuronal lineage.* Experimental Cell Research, 2007. **313**(9): p. 1820-1829.
149. Christopherson, G.T., H. Song, and H.Q. Mao, *The influence of fiber diameter of electrospun substrates on neural stem cell differentiation and proliferation.* Biomaterials, 2009. **30**(4): p. 556-564.
150. Arnold, M., et al., *Activation of integrin function by nanopatterned adhesive interfaces.* Chemphyschem, 2004. **5**(3): p. 383-388.

151. Kolind, K., et al., *Guidance of stem cell fate on 2D patterned surfaces.* Biomaterials, 2012. **33**(28): p. 6626-33.
152. Freijlarsson, C., et al., *Effects of a Polymeric Additive in a Biomedical Poly(Ether Urethaneurea).* Journal of Applied Polymer Science, 1993. **49**(5): p. 815-821.
153. Bacakova, L., et al., *Adhesion and proliferation of cultured human aortic smooth muscle cells on polystyrene implanted with N+, F+ and Ar+ ions: Correlation with polymer surface polarity and carbonization.* Biomaterials, 1996. **17**(11): p. 1121-1126.
154. Shirakawa, H., et al., *Synthesis of electrically conducting organic polymers: halogen derivatives of polyacetylene, (CH).* Journal of the Chemical Society, Chemical Communications, 1977(16): p. 578-580.
155. Heeger, A.J., *Semiconducting and Metallic Polymers: The Fourth Generation of Polymeric Materials (Nobel Lecture) Copyright(c) The Nobel Foundation 2001. We thank the Nobel Foundation, Stockholm, for permission to print this lecture.* Angew Chem Int Ed Engl, 2001. **40**(14): p. 2591-2611.
156. Aleshin, A.N., S.R. Williams, and A.J. Heeger, *Transport properties of poly(3,4-ethylenedioxythiophene)/poly(styrenesulfonate).* Synthetic Metals, 1998. **94**(2): p. 173-177.
157. George, P.M., et al., *Fabrication and biocompatibility of polypyrrole implants suitable for neural prosthetics.* Biomaterials, 2005. **26**(17): p. 3511-3519.
158. Guimard, N.K., N. Gomez, and C.E. Schmidt, *Conducting polymers in biomedical engineering.* Progress in Polymer Science, 2007. **32**(8-9): p. 876-921.
159. Schmidt, C.E., et al., *Stimulation of neurite outgrowth using an electrically conducting polymer.* Proceedings of the National Academy of Sciences of the United States of America, 1997. **94**(17): p. 8948-8953.
160. Pettersson, L.A.A., et al., *Spectroscopic ellipsometry studies of the optical properties of doped poly(3,4-ethylenedioxythiophene): An anisotropic metal.* Thin Solid Films, 1998. **313**: p. 356-361.
161. Groenendaal, B.L., et al., *Poly(3,4-ethylenedioxythiophene) and its derivatives: Past, present, and future.* Advanced Materials, 2000. **12**(7): p. 481-494.
162. Heywang, G. and F. Jonas, *Poly(Alkylenedioxythiophene)S - New, Very Stable Conducting Polymers.* Advanced Materials, 1992. **4**(2): p. 116-118.
163. Crispin, X., et al., *Conductivity, morphology, interfacial chemistry, and stability of poly(3,4-ethylene dioxythiophene)–poly(styrene sulfonate): A photoelectron spectroscopy study.* Journal of Polymer Science Part B: Polymer Physics, 2003. **41**(21): p. 2561-2583.
164. Lefebvre, M., et al., *Chemical synthesis, characterization, and electrochemical studies of poly(3,4-ethylenedioxythiophene)/poly(styrene-4-sulfonate) composites.* Chemistry of Materials, 1999. **11**(2): p. 262-268.
165. Ghosh, S. and O. Inganas, *Conducting polymer hydrogels as 3D electrodes: Applications for supercapacitors.* Advanced Materials, 1999. **11**(14): p. 1214-1218.
166. Kudoh, Y., K. Akami, and Y. Matsuya, *Solid electrolytic capacitor with highly stable conducting polymer as a counter electrode.* Synthetic Metals, 1999. **102**(1-3): p. 973-974.
167. Ghosh, S. and O. Inganas, *Electrochemical characterization of poly(3,4-ethylene dioxythiophene) based conducting hydrogel networks.* Journal of the Electrochemical Society, 2000. **147**(5): p. 1872-1877.
168. Karg, S., et al., *Increased brightness and lifetime of polymer light-emitting diodes with polyaniline anodes.* Synthetic Metals, 1996. **80**(2): p. 111-117.
169. Carter, J.C., et al., *Operating stability of light-emitting polymer diodes based on poly(p-phenylene vinylene).* Applied Physics Letters, 1997. **71**(1): p. 34-36.
170. Pei, Q.B., et al., *Electrochromic and Highly Stable Poly(3,4-Ethylenedioxythiophene) Switches between Opaque Blue-Black and Transparent Sky Blue.* Polymer, 1994. **35**(7): p. 1347-1351.

171. Jonas, F. and J.T. Morrison, *3,4-polyethylenedioxythiophene (PEDT): Conductive coatings technical applications and properties.* Synthetic Metals, 1997. **85**(1-3): p. 1397-1398.
172. Jönsson, S.K.M., et al., *The effects of solvents on the morphology and sheet resistance in poly(3,4-ethylenedioxythiophene)–polystyrenesulfonic acid (PEDOT–PSS) films.* Synthetic Metals, 2003. **139**(1): p. 1-10.
173. Foulds, N.C. and C.R. Lowe, *Enzyme entrapment in electrically conducting polymers. Immobilisation of glucose oxidase in polypyrrole and its application in amperometric glucose sensors.* Journal of the Chemical Society, Faraday Transactions 1: Physical Chemistry in Condensed Phases, 1986. **82**(4): p. 1259-1264.
174. Umana, M. and J. Waller, *Protein-modified electrodes. The glucose oxidase/polypyrrole system.* Analytical Chemistry, 1986. **58**(14): p. 2979-2983.
175. Aebischer, P., et al., *Piezoelectric guidance channels enhance regeneration in the mouse sciatic nerve after axotomy.* Brain Research, 1987. **436**(1): p. 165-168.
176. Valentini, R.F., et al., *Polymer electret guidance channels enhance peripheral nerve regeneration in mice.* Brain Research, 1989. **480**(1–2): p. 300-304.
177. Cosnier, S., *Biomolecule immobilization on electrode surfaces by entrapment or attachment to electrochemically polymerized films. A review.* Biosensors and Bioelectronics, 1999. **14**(5): p. 443-456.
178. Gerard, M., A. Chaubey, and B.D. Malhotra, *Application of conducting polymers to biosensors.* Biosensors & Bioelectronics, 2002. **17**(5): p. 345-359.
179. Çete, S., A. Yaşar, and F. Arslan, *An Amperometric Biosensor for Uric Acid Determination Prepared from Uricase Immobilized in Polypyrrole Film.* Artificial Cells, Blood Substitutes and Biotechnology, 2006. **34**(3): p. 367-380.
180. Giaever, I. and C.R. Keese, *Monitoring fibroblast behavior in tissue culture with an applied electric field.* Proc Natl Acad Sci U S A, 1984. **81**(12): p. 3761-4.
181. Ateh, D.D., P. Vadgama, and H.A. Navsaria, *Culture of human keratinocytes on polypyrrole-based conducting polymers.* Tissue Engineering, 2006. **12**(4): p. 645-655.
182. Castano, H., et al., *Polypyrrole thin films formed by admicellar polymerization support the osteogenic differentiation of mesenchymal stem cells.* Macromol Biosci, 2004. **4**(8): p. 785-94.
183. Kim, D.H., M. Abidian, and D.C. Martin, *Conducting polymers grown in hydrogel scaffolds coated on neural prosthetic devices.* Journal of Biomedical Materials Research Part A, 2004. **71A**(4): p. 577-585.
184. Yamato, H., M. Ohwa, and W. Wernet, *Stability of Polypyrrole and Poly(3,4-Ethylenedioxythiophene) for Biosensor Application.* Journal of Electroanalytical Chemistry, 1995. **397**(1-2): p. 163-170.
185. Cui, X.Y. and D.C. Martin, *Electrochemical deposition and characterization of poly(3,4-ethylenedioxythiophene) on neural microelectrode arrays.* Sensors and Actuators B-Chemical, 2003. **89**(1-2): p. 92-102.
186. Ludwig, K.A., et al., *Chronic neural recordings using silicon microelectrode arrays electrochemically deposited with a poly(3,4-ethylenedioxythiophene) (PEDOT) film.* Journal of Neural Engineering, 2006. **3**(1): p. 59-70.
187. Vijay, V., A.D. Rao, and K.S. Narayan, *In situ studies of strain dependent transport properties of conducting polymers on elastomeric substrates.* Journal of Applied Physics, 2011. **109**(8).
188. Nardes, A.M., et al., *Microscopic understanding of the anisotropic conductivity of PEDOT : PSS thin films.* Advanced Materials, 2007. **19**(9): p. 1196-+.
189. Reubinoff, B.E., et al., *Neural progenitors from human embryonic stem cells.* Nature Biotechnology, 2001. **19**(12): p. 1134-40.
190. Reubinoff, B.E., et al., *Embryonic stem cell lines from human blastocysts: somatic differentiation in vitro.* Nature Biotechnology, 2000. **18**(4): p. 399-404.

191. Pera, M.F., B. Reubinoff, and A. Trounson, *Human embryonic stem cells.* J Cell Sci, 2000. **113 (Pt 1)**: p. 5-10.
192. Bain, G., et al., *Embryonic Stem Cells Express Neuronal Properties in Vitro.* Developmental Biology, 1995. **168**(2): p. 342-357.
193. Muotri, A.R., et al., *Development of functional human embryonic stem cell-derived neurons in mouse brain.* Proc Natl Acad Sci U S A, 2005. **102**(51): p. 18644-8.
194. Perrier, A.L., et al., *Derivation of midbrain dopamine neurons from human embryonic stem cells.* Proc Natl Acad Sci U S A, 2004. **101**(34): p. 12543-8.
195. Tabar, V., et al., *Migration and differentiation of neural precursors derived from human embryonic stem cells in the rat brain.* Nature Biotechnology, 2005. **23**(5): p. 601-6.
196. Zhang, S.C., et al., *In vitro differentiation of transplantable neural precursors from human embryonic stem cells.* Nature Biotechnology, 2001. **19**(12): p. 1129-33.
197. Carpenter, M.K., et al., *Enrichment of neurons and neural precursors from human embryonic stem cells.* Exp Neurol, 2001. **172**(2): p. 383-97.
198. Schuldiner, M., et al., *Induced neuronal differentiation of human embryonic stem cells.* Brain Res, 2001. **913**(2): p. 201-5.
199. Sanalkumar, R., et al., *Neuronal vs. glial fate of embryonic stem cell-derived neural progenitors (ES-NPs) is determined by FGF2/EGF during proliferation.* J Mol Neurosci, 2010. **42**(1): p. 17-27.
200. Longair, M.H., D.A. Baker, and J.D. Armstrong, *Simple Neurite Tracer: open source software for reconstruction, visualization and analysis of neuronal processes.* Bioinformatics, 2011. **27**(17): p. 2453-4.
201. Abramoff, M.D., P.J. Magelhaes, and S.J. Ram, *{Image processing with ImageJ}.* Biophotonics Int, 2004. **11**(7): p. 36-42.
202. Schneider, C.A., W.S. Rasband, and K.W. Eliceiri, *NIH Image to ImageJ: 25 years of image analysis.* Nat Meth, 2012. **9**(7): p. 671-675.
203. Evans, N.D., E. Gentleman, and J.M. Polak, *Scaffolds for stem cells.* Materials Today, 2006. **9**(12): p. 26-33.
204. Li, Y., et al., *Culturing and differentiation of murine embryonic stem cells in a three-dimensional fibrous matrix.* Cytotechnology, 2003. **41**(1): p. 23-35.
205. Mitjavila-Garcia, M.T., C. Simonin, and M. Peschanski, *Embryonic stem cells: Meeting the needs for cell therapy.* Advanced Drug Delivery Reviews, 2005. **57**(13): p. 1935-1943.
206. Chai, C. and K.W. Leong, *Biomaterials approach to expand and direct differentiation of stem cells.* Mol Ther, 2007. **15**(3): p. 467-80.
207. Vacanti, J.P. and R. Langer, *Tissue engineering: the design and fabrication of living replacement devices for surgical reconstruction and transplantation.* The Lancet, 1999. **354**: p. S32-S34.
208. Pittenger, M.F., et al., *Multilineage potential of adult human mesenchymal stem cells.* Science, 1999. **284**(5411): p. 143-7.
209. Garreta, E., et al., *Osteogenic differentiation of mouse embryonic stem cells and mouse embryonic fibroblasts in a three-dimensional self-assembling peptide scaffold.* Tissue Eng, 2006. **12**(8): p. 2215-27.
210. Gage, F.H., *Mammalian neural stem cells.* Science, 2000. **287**(5457): p. 1433-8.
211. Bibel, M., et al., *Differentiation of mouse embryonic stem cells into a defined neuronal lineage.* Nature Neuroscience, 2004. **7**(9): p. 1003-1009.
212. Kim, D.H., et al., *Effect of immobilized nerve growth factor on conductive polymers: Electrical properties and cellular response.* Advanced Functional Materials, 2007. **17**(1): p. 79-86.
213. Shimomura, O., F.H. Johnson, and Y. Saiga, *Extraction, purification and properties of aequorin, a bioluminescent protein from the luminous hydromedusan, Aequorea.* J Cell Comp Physiol, 1962. **59**: p. 223-39.

214. Adams, L.D., et al., *Double lox targeting for neural cell transgenesis.* Brain Res Mol Brain Res, 2003. **110**(2): p. 220-33.
215. Ruoslahti, E. and M.D. Pierschbacher, *New perspectives in cell adhesion: RGD and integrins.* Science, 1987. **238**(4826): p. 491-7.
216. Hartsock, A. and W.J. Nelson, *Adherens and tight junctions: structure, function and connections to the actin cytoskeleton.* Biochim Biophys Acta, 2008. **1778**(3): p. 660-9.
217. Tsukita, S., et al., *Molecular linkage between cadherins and actin filaments in cell—cell adherens junctions.* Current Opinion in Cell Biology, 1992. **4**(5): p. 834-839.
218. Balaban, N.Q., et al., *Force and focal adhesion assembly: a close relationship studied using elastic micropatterned substrates.* Nature Cell Biology, 2001. **3**(5): p. 466-472.
219. Harris, A.K., P. Wild, and D. Stopak, *Silicone rubber substrata: a new wrinkle in the study of cell locomotion.* Science, 1980. **208**(4440): p. 177-9.
220. Dembo, M. and Y.L. Wang, *Stresses at the cell-to-substrate interface during locomotion of fibroblasts.* Biophysical Journal, 1999. **76**(4): p. 2307-2316.
221. Tan, J.L., et al., *Cells lying on a bed of microneedles: An approach to isolate mechanical force.* Proceedings of the National Academy of Sciences of the United States of America, 2003. **100**(4): p. 1484-1489.
222. Hutson, M.S., et al., *Forces for morphogenesis investigated with laser microsurgery and quantitative modeling.* Science, 2003. **300**(5616): p. 145-9.
223. Adams, D.S., R. Keller, and M.A. Koehl, *The mechanics of notochord elongation, straightening and stiffening in the embryo of Xenopus laevis.* Development, 1990. **110**(1): p. 115-30.
224. von Dassow, M. and L.A. Davidson, *Natural variation in embryo mechanics: gastrulation in Xenopus laevis is highly robust to variation in tissue stiffness.* Dev Dyn, 2009. **238**(1): p. 2-18.
225. Hove, J.R., et al., *Intracardiac fluid forces are an essential epigenetic factor for embryonic cardiogenesis.* Nature, 2003. **421**(6919): p. 172-7.
226. Davidson, L. and R. Keller, *Measuring mechanical properties of embryos and embryonic tissues.* Methods Cell Biol, 2007. **83**: p. 425-39.
227. Nelson, C.M., et al., *Emergent patterns of growth controlled by multicellular form and mechanics.* Proc Natl Acad Sci U S A, 2005. **102**(33): p. 11594-9.
228. Shraiman, B.I., *Mechanical feedback as a possible regulator of tissue growth.* Proceedings of the National Academy of Sciences of the United States of America, 2005. **102**(9): p. 3318-3323.
229. Toyama, Y., et al., *Apoptotic force and tissue dynamics during Drosophila embryogenesis.* Science, 2008. **321**(5896): p. 1683-1686.
230. Farge, E., *Mechanotransduction in Development.* Forces and Tension in Development, 2011. **95**: p. 243-265.
231. Eyckmans, J., et al., *A Hitchhiker's Guide to Mechanobiology.* Developmental Cell, 2011. **21**(1): p. 35-47.
232. Chen, C.S., et al., *Geometric control of cell life and death.* Science, 1997. **276**(5317): p. 1425-1428.
233. Wozniak, M.A. and C.S. Chen, *Mechanotransduction in development: a growing role for contractility.* Nature Reviews Molecular Cell Biology, 2009. **10**(1): p. 34-43.
234. Wingate, K., et al., *Compressive elasticity of three-dimensional nanofiber matrix directs mesenchymal stem cell differentiation to vascular cells with endothelial or smooth muscle cell markers.* Acta Biomaterialia, 2012. **8**(4): p. 1440-1449.
235. Rehfeldt, F., A.J. Engler, and D.E. Discher, *Biomechanics of adult stem cell differentiation guided by matrix elasticity.* Biophysical Journal, 2007: p. 636a-636a.
236. Yeung, T., et al., *Effects of substrate stiffness on cell morphology, cytoskeletal structure, and adhesion.* Cell Motility and the Cytoskeleton, 2005. **60**(1): p. 24-34.

237. Guilak, F., et al., *Control of Stem Cell Fate by Physical Interactions with the Extracellular Matrix.* Cell Stem Cell, 2009. **5**(1): p. 17-26.
238. Vogel, V. and M. Sheetz, *Local force and geometry sensing regulate cell functions.* Nature Reviews Molecular Cell Biology, 2006. **7**(4): p. 265-275.
239. Cavalcanti-Adam, E.A., et al., *Cell spreading and focal adhesion dynamics are regulated by spacing of integrin ligands.* Biophysical Journal, 2007. **92**(8): p. 2964-2974.
240. Arnold, M., et al., *Induction of cell polarization and migration by a gradient of nanoscale variations in adhesive ligand spacing.* Nano Letters, 2008. **8**(7): p. 2063-2069.
241. Geiger, B., J.P. Spatz, and A.D. Bershadsky, *Environmental sensing through focal adhesions.* Nature Reviews Molecular Cell Biology, 2009. **10**(1): p. 21-33.
242. Paszek, M.J., et al., *Tensional homeostasis and the malignant phenotype.* Cancer Cell, 2005. **8**(3): p. 241-254.
243. Ayala, R., et al., *Engineering the cell-material interface for controlling stem cell adhesion, migration, and differentiation.* Biomaterials, 2011. **32**(15): p. 3700-11.
244. Stetler-Stevenson, W.G., S. Aznavoorian, and L.A. Liotta, *Tumor cell interactions with the extracellular matrix during invasion and metastasis.* Annu Rev Cell Biol, 1993. **9**: p. 541-73.
245. Lansman, J.B., T.J. Hallam, and T.J. Rink, *Single stretch-activated ion channels in vascular endothelial cells as mechanotransducers?* Nature, 1987. **325**(6107): p. 811-3.
246. Formigli, L., et al., *Sphingosine 1-phosphate induces cytoskeletal reorganization in C2C12 myoblasts: physiological relevance for stress fibres in the modulation of ion current through stretch-activated channels.* J Cell Sci, 2005. **118**(Pt 6): p. 1161-71.
247. McMahon, L.A., V.A. Campbell, and P.J. Prendergast, *Involvement of stretch-activated ion channels in strain-regulated glycosaminoglycan synthesis in mesenchymal stem cell-seeded 3D scaffolds.* J Biomech, 2008. **41**(9): p. 2055-9.
248. Ostrow, L.W., T.M. Suchyna, and F. Sachs, *Stretch induced endothelin-1 secretion by adult rat astrocytes involves calcium influx via stretch-activated ion channels (SACs).* Biochem Biophys Res Commun, 2011. **410**(1): p. 81-6.
249. Sachs, F., *Stretch-activated ion channels: what are they?* Physiology (Bethesda), 2010. **25**(1): p. 50-6.
250. Anno, T., N. Sakamoto, and M. Sato, *Role of nesprin-1 in nuclear deformation in endothelial cells under static and uniaxial stretching conditions.* Biochem Biophys Res Commun, 2012.
251. Chancellor, T.J., et al., *Actomyosin tension exerted on the nucleus through nesprin-1 connections influences endothelial cell adhesion, migration, and cyclic strain-induced reorientation.* Biophysical Journal, 2010. **99**(1): p. 115-23.
252. Lammerding, J., et al., *Lamin A/C deficiency causes defective nuclear mechanics and mechanotransduction.* J Clin Invest, 2004. **113**(3): p. 370-8.
253. Rosette, C. and M. Karin, *Cytoskeletal control of gene expression: depolymerization of microtubules activates NF-kappa B.* J Cell Biol, 1995. **128**(6): p. 1111-9.
254. Wang, N., J.P. Butler, and D.E. Ingber, *Mechanotransduction across the Cell-Surface and through the Cytoskeleton.* Science, 1993. **260**(5111): p. 1124-1127.
255. Schliwa, M. and J. van Blerkom, *Structural interaction of cytoskeletal components.* J Cell Biol, 1981. **90**(1): p. 222-35.
256. Storm, C., et al., *Nonlinear elasticity in biological gels.* Nature, 2005. **435**(7039): p. 191-4.
257. Xu, J., Y. Tseng, and D. Wirtz, *Strain hardening of actin filament networks. Regulation by the dynamic cross-linking protein alpha-actinin.* J Biol Chem, 2000. **275**(46): p. 35886-92.
258. Janmey, P.A., et al., *The mechanical properties of actin gels. Elastic modulus and filament motions.* J Biol Chem, 1994. **269**(51): p. 32503-13.
259. Janmey, P.A., *Mechanical properties of cytoskeletal polymers.* Curr Opin Cell Biol, 1991. **3**(1): p. 4-11.

260. Sims, J.R., S. Karp, and D.E. Ingber, *Altering the cellular mechanical force balance results in integrated changes in cell, cytoskeletal and nuclear shape.* J Cell Sci, 1992. **103 (Pt 4)**: p. 1215-22.
261. Throm Quinlan, A.M., et al., *Combining dynamic stretch and tunable stiffness to probe cell mechanobiology in vitro.* PLoS One, 2011. **6**(8): p. e23272.
262. Vicente-Manzanares, M., et al., *Non-muscle myosin II takes centre stage in cell adhesion and migration.* Nat Rev Mol Cell Biol, 2009. **10**(11): p. 778-90.
263. Kanchanawong, P., et al., *Nanoscale architecture of integrin-based cell adhesions.* Nature, 2010. **468**(7323): p. 580-U262.
264. Tanentzapf, G., et al., *Multiple factors contribute to integrin-talin interactions in vivo.* Journal of Cell Science, 2006. **119**(8): p. 1632-1644.
265. Smith, S.J. and R. McCann, *A C-terminal dimerization motif is required for focal adhesion targeting of Talin 1 and the interaction of the Talin 1 I/LWEQ module with F-actin.* Biochemistry, 2007. **46**(38): p. 10886-10898.
266. Humphries, J.D., et al., *Vinculin controls focal adhesion formation by direct interactions with talin and actin.* Journal of Cell Biology, 2007. **179**(5): p. 1043-1057.
267. Galbraith, C.G., K.M. Yamada, and M.P. Sheetz, *The relationship between force and focal complex development.* Journal of Cell Biology, 2002. **159**(4): p. 695-705.
268. Pellegrin, S. and H. Mellor, *Actin stress fibres.* Journal of Cell Science, 2007. **120**(20): p. 3491-3499.
269. Bershadsky, A.D., N.Q. Balaban, and B. Geiger, *Adhesion-dependent cell mechanosensitivity.* Annual Review of Cell and Developmental Biology, 2003. **19**: p. 677-695.
270. Peterson, L.J., et al., *Simultaneous stretching and contraction of stress fibers in vivo.* Molecular Biology of the Cell, 2004. **15**(7): p. 3497-3508.
271. Even-Ram, S., et al., *Myosin IIA regulates cell motility and actomyosin microtubule crosstalk.* Nature Cell Biology, 2007. **9**(3): p. 299-U104.
272. Zimerman, B., T. Volberg, and B. Geiger, *Early molecular events in the assembly of the focal adhesion-stress fiber complex during fibroblast spreading.* Cell Motil Cytoskeleton, 2004. **58**(3): p. 143-59.
273. Choi, C.K., et al., *Actin and alpha-actinin orchestrate the assembly and maturation of nascent adhesions in a myosin II motor-independent manner.* Nature Cell Biology, 2008. **10**(9): p. 1039-50.
274. Parsons, J.T., A.R. Horwitz, and M.A. Schwartz, *Cell adhesion: integrating cytoskeletal dynamics and cellular tension.* Nat Rev Mol Cell Biol, 2010. **11**(9): p. 633-43.
275. Zaidel-Bar, R., et al., *A paxillin tyrosine phosphorylation switch regulates the assembly and form of cell-matrix adhesions.* J Cell Sci, 2007. **120**(Pt 1): p. 137-48.
276. Sawada, Y., et al., *Force sensing by mechanical extension of the Src family kinase substrate p130Cas.* Cell, 2006. **127**(5): p. 1015-26.
277. Friedland, J.C., M.H. Lee, and D. Boettiger, *Mechanically activated integrin switch controls alpha5beta1 function.* Science, 2009. **323**(5914): p. 642-4.
278. Kirfel, G., et al., *Cell migration: mechanisms of rear detachment and the formation of migration tracks.* Eur J Cell Biol, 2004. **83**(11-12): p. 717-24.
279. Miyamoto, S., et al., *Integrin function: molecular hierarchies of cytoskeletal and signaling molecules.* J Cell Biol, 1995. **131**(3): p. 791-805.
280. Burridge, K. and K. Wennerberg, *Rho and Rac take center stage.* Cell, 2004. **116**(2): p. 167-79.
281. Thery, M., et al., *Anisotropy of cell adhesive microenvironment governs cell internal organization and orientation of polarity.* Proceedings of the National Academy of Sciences of the United States of America, 2006. **103**(52): p. 19771-19776.

282. Thery, M., et al., *Cell distribution of stress fibres in response to the geometry of the adhesive environment.* Cell Motility and the Cytoskeleton, 2006. **63**(6): p. 341-355.
283. Endlich, N., et al., *Movement of stress fibers away from focal adhesions identifies focal adhesions as sites of stress fiber assembly in stationary cells.* Cell Motil Cytoskeleton, 2007. **64**(12): p. 966-76.
284. Hotulainen, P. and P. Lappalainen, *Stress fibers are generated by two distinct actin assembly mechanisms in motile cells.* J Cell Biol, 2006. **173**(3): p. 383-94.
285. Lele, T.P., et al., *Mechanical forces alter zyxin unbinding kinetics within focal adhesions of living cells.* Journal of Cellular Physiology, 2006. **207**(1): p. 187-194.
286. Engler, A.J., et al., *Myotubes differentiate optimally on substrates with tissue-like stiffness: pathological implications for soft or stiff microenvironments.* J Cell Biol, 2004. **166**(6): p. 877-87.
287. Bhadriraju, K., et al., *Activation of ROCK by RhoA is regulated by cell adhesion, shape, and cytoskeletal tension.* Exp Cell Res, 2007. **313**(16): p. 3616-23.
288. Elkin, B.S., et al., *Mechanical heterogeneity of the rat hippocampus measured by atomic force microscope indentation.* Journal of Neurotrauma, 2007. **24**(5): p. 812-822.
289. McBeath, R., et al., *Cell Shape, Cytoskeletal Tension, and RhoA Regulate Stem Cell Lineage Commitment.* Developmental Cell, 2004. **6**(4): p. 483-495.
290. Georges, P.C., et al., *Matrices with compliance comparable to that of brain tissue select neuronal over glial growth in mixed cortical cultures*, in *Biophysical Journal*. 2006. p. 3012-3018.
291. Discher, D.E., P. Janmey, and Y.L. Wang, *Tissue cells feel and respond to the stiffness of their substrate.* Science, 2005. **310**(5751): p. 1139-1143.
292. Lord, M.S., M. Foss, and F. Besenbacher, *Influence of nanoscale surface topography on protein adsorption and cellular response.* Nano Today, 2010. **5**(1): p. 66-78.
293. Wong, J.Y., R. Langer, and D.E. Ingber, *Electrically conducting polymers can noninvasively control the shape and growth of mammalian cells.* Proceedings of the National Academy of Sciences, 1994. **91**(8): p. 3201-3204.
294. Lim, J.Y., et al., *Human foetal osteoblastic cell response to polymer-demixed nanotopographic interfaces.* Journal of the Royal Society Interface, 2005. **2**(2): p. 97-108.
295. Rechendorff, K., et al., *Enhancement of Protein Adsorption Induced by Surface Roughness.* Langmuir, 2006. **22**(26): p. 10885-10888.
296. Ayala, R., et al., *Engineering the cell–material interface for controlling stem cell adhesion, migration, and differentiation*, in *Biomaterials*. 2011. p. 3700-3711.

ADDENDUM

1) Pg. 69, “Electrode arrays coated with…..six weeks without illiciting any adverse reaction….” is replaced by “Electrode arrays coated with…..six weeks without eliciting any adverse reaction….”.

2) Pg. 71, “The pristine SEBS substrates were prepared in the similar manner…” is replaced by “The pristine SEBS substrates were prepared in similar manner…”.